SELF-ALIGNED MICROCHIP DEVICE FOR AUTOMATED MEASUREMENT OF QUANTAL EXOCYTOSIS

A Dissertation

presented to

the Faculty of the Graduate school

University of Missouri-Columbia

In Partial Fulfillment

of the Requirements for the degree

Doctor of Philosophy

---

by

SYED BARIZUDDIN

Drs. Shubhra Gangopadhyay & Kevin Gillis, Co- advisors

May 2010

The undersigned, appointed by the Dean of the Graduate School have, examined the dissertation titled

SELF-ALIGNED MICROCHIP DEVICE FOR AUTOMATED MEASUREMENT OF QUANTAL EXOCYTOSIS

presented by Syed Barizuddin,

a candidate for the degree of Doctor of Philosophy,

and hereby certify that in their opinion is worthy of acceptance

_____

Professor Shubhra Gangopadhyay

_____

Professor Kevin Gillis

_____

Professor Satish Nair

_____

Professor Naz Islam

To My Family

ACKNOWLEMENTS

During the course of this work, I had been fortunate to have met and worked with some very smart and amazing people, professors and colleagues alike. Looking back, it is surprising to see how small bits and pieces of information from so many different people at different times could contribute to ones understanding and knowledge over the long term.

In this endeavor I have been immensely lucky to have been co-advised by Professors Shubhra Gangopadhyay and Kevin Gillis.

I have known and worked for Dr. Gangopadhyay for many years now. She has helped me at important times during the course of my academic career when I needed help for which I am immensely grateful and thankful. Her advice over the course of the years has not only helped me complete my degrees, but has helped me to acquire detailed understanding of my research. Being a part of her group, who work in many different fields has contributed to my understanding of different types of research in different fields of science and engineering. Her amazing labs have given me an opportunity to work on so many diverse and expensive equipments, which I believe would not be possible in a regular course of a graduate study.

I have worked with Dr. Gillis all through my Ph.D. His knowledge and understanding of the field of biology, physiology and electrical engineering, and

his ability to correlate the interface between them is amazing. He imparts this knowledge to students like me, with such ease and clarity that it really makes understanding difficult topics easy. His easy demeanor is very helpful in the general intense atmosphere of the graduate study. I would like to express my sincere thanks and gratitude for his guidance that helped me during the research.

Besides my advisors, I would like to thank the other members of my dissertation committee, Prof. Satish Nair and Prof. Naz Islam for their advice, encouragement and help whenever I needed it.

My sincere thanks are also due to Drs. Xin Liu, Joseph Mathai and Maruf Hossain, who have worked with me on one aspect or the other of the project over a period of time.

I would also like to appreciate my colleagues Drs. Xiaohui Chen, Korampally Venumadhav and Yuanfang Gao, some of whom I still see and meet, and others who have left for bigger and better things, for being able to discuss with them parts of the research and their thoughtful comments.

Atanu Sen, who worked with me during his M.S is one who I would like to thank for his dedication and assistance whenever I need it.

Other colleagues, who I worked closely for different amounts of time, some long, some short, but all very valuable and who I need to thank are Jia Yao, Jaya Ghosh, Sangho Bok and Dr. Sneghdamai Praharaj.

Thanks to Dr. Louis Polo Parada who was kind enough to let me use the imaging equipment in his lab.

It is very possible that I may have inadvertently missed somebody to thank by name, but nevertheless I would like to thank all those people who may have contributed in any way during the course of this work.

SELF-ALIGNED MICROCHIP DEVICE FOR AUTOMATED MEASUREMENT OF QUANTAL EXOCYTOSIS

Table of Contents

CHAPTER 2

CHAPTER 3

CHAPTER 4

CHAPTER 5

CHAPTER 6

INCORPORATING Pt NANOPARTICLES ON ELECTRODES IN ORDER TO IMPROVE SENSITIVITY TO DETECTING THE RELEASE OF CATECHOLAMAINE OR OTHER ELECTROACTIVE ANALYTES FROM CELLS

List of Figures

CHAPTER 1

CHAPTER 2

CHAPTER 3

CHAPTER 4

CHAPTER 5

CHAPTER 6

LIST OF TABLES

CHAPTER 2

CHAPTER 3

CHAPTER 5

CHAPTER 6

SELF-ALIGNED MICROCHIP DEVICE FOR AUTOMATED MEASUREMENT OF QUANTAL EXOCYTOSIS

Syed Barizuddin.

Drs. Shubhra Gangopadhyay & Kevin Gillis, Dissertation supervisors

ABSTRACT

The nature of the cells is such that they adhere well to some surfaces and not as well to others. This premise is of the utmost importance in fabricating these devices, and our work involves modifying substrate surface with lithographic techniques to meet this end. This adherence property of cells with respect to materials, when used with the process of microfabrication can be used to target, sort or study many single cells in parallel. Here we describe a protocol to fabricate a multi channel high throughput microchip device for measurement of hormone and neurotransmitter secretions from individual cells. These measurements are usually carried out using probes, which are manually manipulated to the cell's surface while observing under the microscope. These approaches are extremely time consuming, labor intensive and require sophisticated equipment. We have developed a microchip device platform that performs single-cell assays of hormonal/neurotransmitter secretion through self-aligning of cells on electrochemical microelectrodes. The device is fabricated in such a way that single cell sized docking sites on the biocomptible and cell friendly electrochemical electrodes are exposed to the surface such that single cells can adhere to them, whereas all other areas are covered with a thin film, with properties that inhibit cell adhesion. This thin film also provides electrical isolation between the microelectrodes.We believe that development of this approach will provide much more efficiencient and faster means than the current technologies used today for similar applications.

Key words: automatic cell positioning, quantal exocytosis, amperometric detection.

CHAPTER 1

INTRODUCTION

1-1 Background and Motivation

MEMS (micro electro-mechanical systems) is an important technology that has blossomed over the last few decades (Bao and Wang 1996; Ho and Tai 1996; Hynes, Ashraf et al. 1999; Sarro 2000). MEMS technology has provided the means to fabricate devices with micron-sized features. The micron sized features are especially useful for probing living organisms at the cellular level. Devices used in biological applications are referred to as Bio-MEMS (Kotzar, Freas et al. 2002; Shawgo, Richards Grayson et al. 2002; Hilt, Gupta et al. 2003; Park and Shuler 2003; Voskerician, Shive et al. 2003; Bashir 2004; Ziaie, Baldi et al. 2004). An important goal in Bio-MEMS is to study individual cells, which usually requires patterning individual cells to specific locations on a microchip (Spegel, Heiskanen et al. 2008).

Bio-MEMS use techniques like micro-patterning (Britland, Perez-Arnaud et al. 1992; Tadanaga, Morinaga et al. 2000; Lehnert, Wehrle-Haller et al. 2004; Falconnet, Csucs et al. 2006), micro-fluidics (Becker and Gärtner 2000; McDonald, Duffy et al. 2000; Beebe, Mensing et al. 2002; Andersson and van den Berg 2003; Andersson and van den Berg 2004; Squires and Quake 2005; Dittrich and Manz 2006), microfabricated transducers (Kopp, Crabtree et al. 1997; Pizziconi and Page 1997; Tasche, Meyhofer et al. 1999; Tanaka, Sato et al. 2007), micro-nozzles (Andersson and van den Berg 2003; Andersson and van

den Berg 2004), cell sorters (Fu, Chou et al. 2002; Andersson and Berg 2004), electroporation (Huang and Rubinsky 2001; Huang and Rubinsky 2003; El-Ali, Sorger et al. 2006; Fox, Esveld et al. 2006), laminar flow patterning (McDonald and Whitesides 2002) and micro-gripper (Yi, Li et al. 2006) etc. which can be used to study biological processes. Techniques like these are used to study single biological cells or cells in small clusters. An important challenge for most of these techniques is to target single cells and hold them in place without damage.

Dielectrophoresis, can be used for single cell studies, but the strong electrical fields can affect and damage the cells (Lafon and Pohl 1981; Marks, Huang et al. 1994; Markx, Dyda et al. 1996; Pethig and Markx 1997; Fiedler, Shirley et al. 1998; Beebe, Mensing et al. 2002; Cummings and Singh 2003; Das, Becker et al. 2005; Hu, Bessette et al. 2005; Lin, Ho et al. 2006). In addition, the setup requires a complicated electrode layout.

The goal of this research was to fabricate a bio-mems device that is capable of automated positioning of single cells on electrochemical electrodes to achieve high-throughput measurement of quantal exocytosis. In this study we report the microfabrication of a device that exploits material properties to achieve very specific targeting of single cell to electrodes. This device was fabricated using materials which were receptive (cytophilic) or inhibitory (cytophobic) to cell adhesion (Corey, Brunette et al. 1997; Chang, Brewer et al. 2000; Bai, Shao et al. 2009; Sen, Barizuddin et al. 2009; Varma, McLachlan et al. 2010). In this study we demonstrated the suitability of different electrode materials for promoting cell adhesion together with cell viability. In the same work we

demonstrated the cytophobic nature of the insulating material teflon and cytophilic material DLC:N (n-doped diamond like carbon), which is a carbon based material (Ferrari ; Robertson 1993; Lettington 1998; Allen, Myer et al. 2001; Grill 2003; Sen, Barizuddin et al. 2009) with properties that promotes cell adhesion. Since DLC:N can be batch fabricated and has properties very similar to the carbon fiber electrode, it can be a very succesful replacement for carbon fiber elctrode in electrochemical measurements.

Electrochemical detection of exocytosis requires that the contents released by stimulation of cells be oxidized on the surface of the electrode (Pihel, Hsieh et al. 1995; Michael and Wightman 1999; Sarada, Rao et al. 2000), and although DLC:N by itself has a high resistivity, a thin layer of ITO (indium tin oxide) (Joshi, Singh et al. 1995; Tak, Kim et al. 2002) sputtered below the DLC:N film provides a charge transfer path (Gao, Chen et al. 2008) . ITO is a highly transparent and conducting material widely used. DLC is doped with small amounts of nitrogen while sputtering, which creates additional energy states within the material (Robertson 1993; Robertson 2002), and thus reduces resistance (Ferreira, Silva et al. 2002).

A high-throughput microfabricated device that combines electrode properties that are suitable for electrochemical detection and provide single cell targeting would significantly enhance the pace of basic neuroscience research which requires large amounts of data. In this study we report the fabrication of such a device. This device is easy to fabricate, is reusable, and can potentially be used for higher-throughput experimentation. A potential application of the device is to

discover or test drugs to treat disorders associated with exocytosis such as Parkinson's disease and type II diabetes.

1-2Thesis overview

Chapter 2 Materials & characterization

The choice of materials is generally a very important aspect of any device, especially if it involves being used for biological and physiological applications. Issues like biocompatibility, toxicity and adhesion become a vital part in the material choice. Carbon and gold are better than platinum or indium-tin-oxide as electrode materials in terms of promoting cell adhesion, but platinum provides a catalytic surface, whereas indium tin oxide is the most transparant . This chapter covers in detail all the materials that were used or considered for use in the microdevices. A series of electrochemical, electrical and material property tests are presented in this chapter.

Chapter 3 Device microfabrication

Chapter 3 details all aspects of fabrication - from process flow to the final design. This process evolved over a period of time. The process of micro-fabrication involves the steps of cleaning, material deposition, spin coating, alligning and etching.

Chapter 4 Cell culture, imaging and quantification

For this project we used two types of cells, primary cells and cell lines. Chromaffin cells were isolated every week from fresh bovine adrenal glands, and the cell lines used were immortal dividing insulin-1 (INS-1) cells. Chapter 4 details the steps from harvesting these cells, to passing and preparing them for the tests. Imaging the cells under the microscope is vital because it indicates the cells health, viability and location.

Chapter 5 Amperometry and data analysis

Exocytosis is measured using an electrochemical electrode in very close promity (usually in the nano to micron range) to the cell surface to oxidize the catecholamine released from the surface of the cell. During amperometric measurements the catecholamines are stored in small vesicle packets or “Quanta”, and are released from these vesicles to produce amperometric spikes of current. The shape of this electrochemical current spike gives information on the number of the molecules released in each “quanta”, and time course of release. We have studied many single cells, and in chapter 5 we analyze all this data from the single cells individually and cumulatively and infer results.

Chapter 6

This chapter presents preliminary tests incorporating Pt nano-particles on electrodes in order to potentially improve the sensitivity to detecting the release of catecholamine or other electroactive analytes from cells

Nanoparticles, as the name suggests, have dimensions in the nano scale. At this scale the properties, especially of metal particles, are very different than at larger scales (Manna, Imae et al. 2001; Park, Xie et al. 2002; Jain, Lee et al. 2006). A lot of research is being done to not only find the exact properties of these particles but also to apply them to make practical devices. For example, the mere size of these particles makes them undetectable by the immune system of the body, hence they could be used as vehicles of drug delivery (Müller, Mäder et al. 2000; Gelperina, Kisich et al. 2005). These particles can be used for charge storage (Yun, Muller et al. 2009), and also to increase the catalytic property without the need for a thin film (Paul, Pearson et al. 2003; Subramanian, Wolf et al. 2003; Sugimoto, Yokoshima et al. 2006). Metals, polymer and other type of nanoparticles are being evaluated for specific applications such as drug delivery (Brannon-Peppas 1995; Hans and Lowman 2002; Panyam and Labhasetwar 2003; Paciotti, Kingston et al. 2006; Han, Ghosh et al. 2007). The “size” of the nanoparticle is key to its properties, for example a nanoparticle with a size of 0.8 nm behaves very differently compared with a nanoparticle with a size of 3 nm (Yun, Muller et al. 2009). In this chapter we have tried to incorporate and exploit the catalytic properties of platinum nanoparticles (Matson, Langlais et al. 1984; Cooper, Foreman et al. 1995; Koh and Bellen 2003) to create a more sensitive sensor that would potentially detect reactive species released from biological cells such as reactive oxygen species (ROS) and reactive nitrogen species (RNS) (Smith, Kapoor et al. 1999; Hensley, Robinson et al. 2000; Reiter, Tan et

al. 2001; Fubini and Hubbard 2003) in addition to the catacholamines from the cells .

To the best of my knowledge this is the first successful attempt towards using microfabricated devices to detect ROS and RNS species from chromaffin cells. We believe the utility of this type of sensor is potentially of immense value in understanding physiological conditions like “oxidative stress”, (Coyle and Puttfarcken 1993; Markesbery 1997; Sies 1997; Mittler 2002; Amatore, Arbault et al. 2008) and NO signaling.

1-3 Introduction

Transmitters are signaling molecules that are packaged inside small vesicles within cells. Transmitter is released from cells as vesicles fuse with the plasma membrane and release their contents to the outside of the cell in the process of exocytosis as shown in figure 1-1. In excitable cells, the principle stimulus for exocytosis of transmitter is the elevation of the cytosolic Ca^{2+} concentration ([Ca^{2+}]i) that results from Ca influx through voltage-gated Ca^{2+} channels (Rettig and Neher 2002). Release of the contents of individual vesicles (quantal exocytosis) can be measured using electrochemical microelectrodes placed immediately adjacent to the cell surface (Wightman, Jankowski et al. 1991). In particular, carbon-fiber amperometry has been used to detect the spike of current that results from oxidation of biogenic amines released from an individual vesicle that fuses near the surface of the electrode (Travis and Wightman 1998; Borges, Camacho et al. 2008). Amperometric spikes are analyzed to determine the

amount of transmitter released from each vesicle, the kinetics of release and the flux of transmitter through a nanometer-sized fusion pore that often proceeds the full fusion reaction (Chow, von Ruden et al. 1992; Lindau and Alvarez de Toledo 2003).

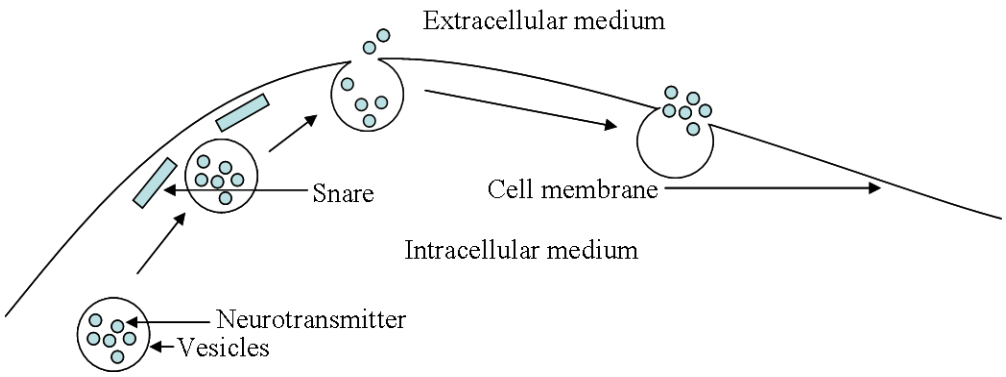

Figure1-1 Exocytosis from a single vesicle “quantum”.

The process of exocytosis leads to chemical communication between neurons and endocrine cells (Neher 1992; Chen, Gavin et al. 1995; Carmignoto 2000; Archer, Graham et al. 2002; Machado, Alonso et al. 2002; Malacombe, Bader et al. 2006) and a powerful method for studying exocytosis of individual vesicles (quantal exocytosis) is carbon-fiber amperometry as shown in figure 1-2. Carbon fiber amperometry is an analytical technique used for monitoring the oxidation of electroactive neurotransmitter molecules at the surface of the electrochemical electrode (Wightman, Jankowski et al. 1991; Ciolkowski, Maness

et al. 1994; Wightman, Schroeder et al. 1995; Sun and Gillis 2006), in which a spike of current is produced as the contents of the vesicles are oxidized on the electrode surface. This technique can be used to measure the frequency of vesicle exocytosis as well as the amount of transmitter released from individual vesicles, and the dynamics of release from each vesicle. Amperometry has a millisecond temporal resolution and can detect zeptomole quantities of transmitter (Wightman, Jankowski et al. 1991; Thompson, Porter et al. 1993; Zhou, Misler et al. 1996; Galli, Blakely et al. 1998; Hochstetler, Puopolo et al. 1999).

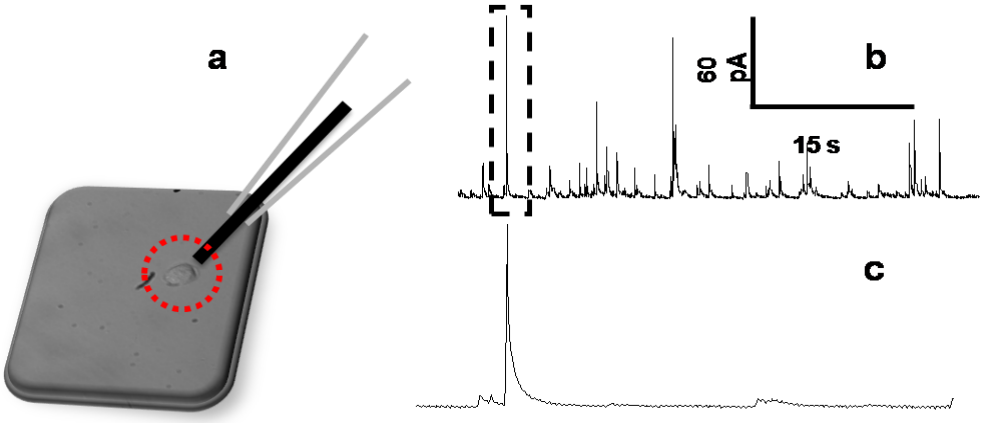

Figure 1-2 Measurement of amperometry with a carbon fiber electrode. A) a single cell in close proximity to the carbon fiber, b) amperometric current spikes and c) expanded single spike.

With amperometry, only those cells with contents that are readily oxidizable can be measured. The most extensively studied substances are

catecholamines like dopamine, epinephrine and nor-epinephrine (Hernández, Sánchez et al. 1998; Bruns 2004; Chicharro, Sánchez et al. 2004). Though a variety of cells can be used (Douglas. 1968); (Finnegan, Pihel et al. 1996), chromaffin cells are particularly popular because they have large dense core vesicles which packages large quantities of neurotransmitter and thus give current spikes with large amplitudes and frequent occurance (Ashery, Varoqueaux et al. 2000; Gil, Rueda et al. 2000; Graham, Fisher et al. 2000; Sun and Gillis 2006). Hence these cells are a natural choice for the study of exocytosis. Analysis of these amperometric spikes (Angleson and Betz 1997; Mosharov and Sulzer 2005; Amatore, Arbault et al. 2009) provides information on content and frequency of the neurotransmitter release from the vesicles. In addition, the initial slow phase of release through a nanometer-scale “fusion” pore can be detected as a “foot signal” which preceeds the amperometric spike (Albillos, Dernick et al. 1997; Xu and Tse 1999; Lindau and Alvarez de Toledo 2003; Sombers, Hanchar et al. 2004; Jackson 2007).

Carbon-fiber amperometry with other biophysical techniques such as patch-clamp has greatly contributed to the understanding of quantal exocytosis, especially kinetic processes like “kiss and run” (Ales, Tabares et al. 1999; Stevens and Williams 2000; Tsuboi, McMahon et al. 2004), whereby a partial, reversible fusion of the vesicle with the membrane forms a transient aqueous pore through which the neurotransmitter molecules are released (Ceccarelli, Hurlbut et al. 1973; Heuser and Reese 1973).

Use of carbon-fiber amperometry together with pharmacological agents or genetic perturbations has greatly contributed to our understanding of the molecular mechanisms of exocytosis. For example, amperometric measurements have shown that the drug LDOPA provides symptomatic relief for Parkinson's disease by increasing the amount of dopamine packaged into individual vesicles (Gong, Hafez et al. 2003; Fang, Berberian et al. 2008). On the other hand, Botulinum Toxin A which is used for treatment of cervical dystonia in addition to its use as a cosmetic, inhibits exocytosis in part by disturbing the structure of the fusion pore and delaying fusion pore expansion (Fang, Berberian et al. 2008). However, routine use of the technique for probing the mechanisms whereby drugs and toxins modulate exocytosis has been hampered by the labor-intensive nature of performing experiments using carbon-fiber electrodes.

Microchip technology offers potential for cheaper, higher throughput experiments which can be used for discovering drugs that target exocytosis, can accelerate the pace of basic biological experiments to understand molecular mechanisms regulating exocytosis and can potentially be used as cell-based sensors for neurotoxins which target exocytosis.

Electrochemical electrodes on microchips have recently been used as an alternative to carbon-fiber microelectrodes to record quantal exocytosis (Hafez, Kisler et al. 2005; Sun and Gillis 2006; Spégel, Heiskanen et al. 2007; Gao, Chen et al. 2008; Yuanfang and et al. 2009). Micro fabricated devices offer the

potential for higher throughput and massively parallel recordings and can be batch fabricated to reduce costs. A new challenge with these devices is that, rather than bringing the microelectrode to the cell with a micropositioner, one must bring the cell to the microchip electrode. In addition, the electrode must be very small (cell sized) in order to have an acceptably small level of current noise. Random seeding of cells on microchip electrode arrays is not ideal because some electrodes do not have an adjacent cell and others have many cells so that there is a low probability of recording release events from a single cell.

Three recent reports describe microfluidic approaches to automatically target cells to electrochemical electrodes (Spegel, Heiskanen et al. 2008; Yuanfang and et al. 2009). Spegel et al. used solution flow through a small aperture on a chip to bring cells to the working electrode. In another study, one group trapped cells over an electrode using a constriction in a microfluidic channel Dittami, G. M., and Rabbitt, R. D. (2010). Our group has used multiple microfluidic cell traps etched in silicon to move cells to electrodes. A drawback of microfluidic approaches is that a balance must be achieved between using a pressure gradient sufficiently large to bring the cell to the electrode yet be gentle enough to avoid cell damage or induce unintended effects on exocytosis, which is sensitive to membrane tension (Monck, Oberhauser et al. 1995).

There are many reports of patterning individual cells using “cytophilic” islands containing extracellular matrix proteins surrounded by “cytophobic” regions

containing materials which resist protein adsorption (Whitesides, Ostuni et al. 2001) most commonly poly(ethylene glycol. Directly patterning cytophilic and cytophobic materials using photolithography is challenging because the solvents used to process photoresists can damage sensitive biomolecule films (Thomas, Lhoest et al. 1999). Therefore the most common approach to pattern adherent cells is to use “microcontact printing” whereby cytophilic materials are stamped onto a substrate (Whitesides, Ostuni et al. 2001). The stamp is usually fabricated from the flexible polymer poly (dimethysiloxane) which is molded onto a thick photoresist that is patterned using photolithography. For our application use of microcontact printing would be challenging because it would require aligning the flexible stamp with the microchip substrate with μm resolution in order to stamp the cytophilic material precisely in register with the electrochemical electrode (James, C. D., Spence, A. J. et al 2004).

Here we describe a simple “self-aligning” approach for targeting individual cells to microelectrodes using differential surface chemistry created with conventional photolithographic methods as shown in figure 1-3. We previously have shown that nitrogen-doped diamond-like carbon (DLC:N) is well suited as an electrochemical electrode material for amperometric measurement of quantal exocytosis (Gao, Chen et al. 2008) and also promotes adhesion of neuroendocrine cells (Kelly, Regan et al. 2008; Sen, Barizuddin et al. 2009). In contrast, Teflon AF inhibits cell attachment (Sen, Barizuddin et al. 2009) and is also an excellent electrical insulator as shown in figure 1-3. Therefore we use a Teflon AF film both to insulate conductive DLC:N films and to block cell

attachment. Cell-sized holes etched through the Teflon AF film define both the working area of the DLC:N electrode and cell docking sites. In addition to presenting the method for fabricating this device we demonstrate selective targeting of cells to the electrodes and high-resolution sample recordings of quantal exocytosis on the device.

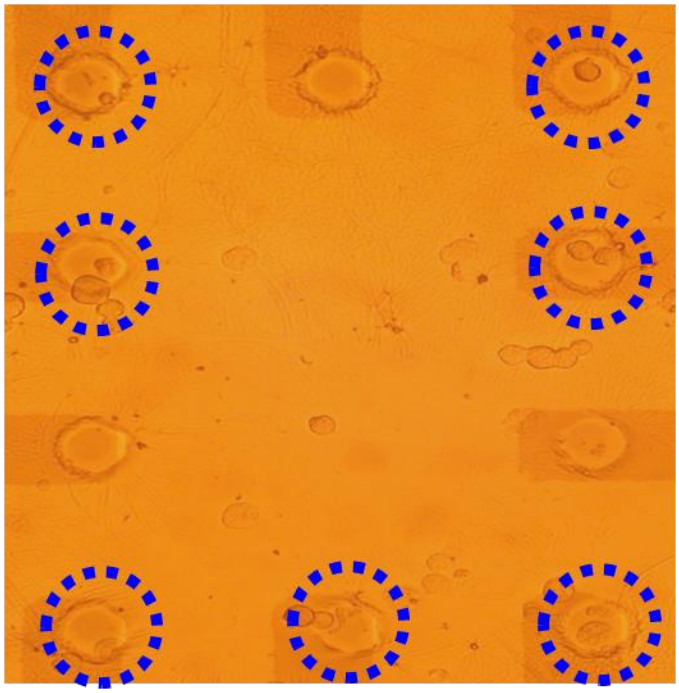

Figure 1-3 Photolithographic patterning of Teflon AF on DLC:N leads for selective attachment of chromaffin cells to electrode. Teflon AF was deposited on top of DLC:N and etched in the region delineated by the dashed lines to expose the underlying DLC:N. The width of the docking sites is approximately 20 µm.

This study is a step towards fabricating a high throuput device. For our application DLC:N (n-doped diamond like carbon) on ITO (Indium tin oxide) is a very favorable combination of an electrode material that is transparant, reasonably conductive, electrochemically active and that also promotes cell adhesion. This electrochemical electrode can be integrated in a batch process. Metallic microelectrodes which are also frequently used for similar applications were also incorporated on some of the devices in lieu of the described carbon based electrode as a means to compare both types of electrodes. A gold microelectrode coated with a mono-layer of poly-lysine improves cell adhesion (Manos, Pancrazio et al. 1999; Jun, Hynd et al. 2007) significantly and can be a very effective material in the adhesion of primary cells.

We have used these devices to record quantal exocytosis from cells using several electrode materials and noted differences between spike characteristics. For example, spike amplitude (I max) from the gold microelectrode is significantly higher than DLC:N on ITO microelectrode. Conversly DLC:N on ITO has smaller offset currents compared with gold or platinum electrode.

1-4 Micro-fabricated high throughput device

Below are the images of micro-fabricated bio-chip prototype with electrochemical electrodes that are capable of oxidizing catecholamine's on its surface in the high-throughput study of vesicular exocytosis and also a customized chip holder that allows easy visualization of cells sitting on top of the transparent electrodes.

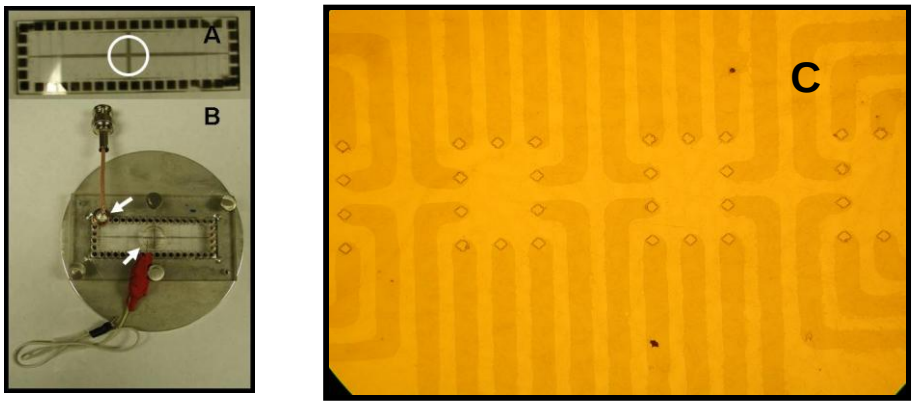

Figure 1-4 Show a microfabricated device with 40 electrodes / cell docking sites. Once the cells are placed on the device, the connection pin is moved from one connecting pad to select each electrode to be recorded. a) a microfabricated bio-chip, b) custom chip holder for use on a microscope, (c) a micrograph of the area in the white circle which indicates the single cell docking sites. The bio-chip has been designed such that all the docking sites are in a single field of view of the microscope when using a 40X objective lens.

References

Albillos, A., G. Dernick, et al. (1997). "The exocytotic event in chromaffin cells revealed by patch amperometry." Nature **389**(6650): 509-512.

Ales, E., L. Tabares, et al. (1999). "High calcium concentrations shift the mode of exocytosis to the kiss-and-run mechanism." Nat Cell Biol **1**(1): 40-44.

Amatore, C., S. Arbault, et al. (2009). "Quantitative investigations of amperometric spike feet suggest different controlling factors of the fusion pore in exocytosis at chromaffin cells." Biophys Chem **143**(3): 124-131.

Amatore, C., S. Arbault, et al. (2008). "Electrochemical monitoring of single cell secretion: vesicular exocytosis and oxidative stress." Chem Rev **108**(7): 2585-2621.

Andersson, H. and A. v. d. Berg (2004). Microfluidic devices for cellomics**:** 1-22.

Andersson, H. and A. van den Berg (2003). "Microfluidic devices for cellomics: a review." Sensors and Actuators B: Chemical **92**(3): 315-325.

Andersson, H. and A. van den Berg (2004). "Microfabrication and microfluidics for tissue engineering: state of the art and future opportunities." Lab Chip **4**(2): 98-103.

Andersson, H. and A. van den Berg (2004). "Microtechnologies and nanotechnologies for single-cell analysis." Current Opinion in Biotechnology **15**(1): 44-49.

Angleson, J. K. and W. J. Betz (1997). "Monitoring secretion in real time: capacitance, amperometry and fluorescence compared." Trends Neurosci **20**(7): 281-287.

Archer, D. A., M. E. Graham, et al. (2002). "Complexin regulates the closure of the fusion pore during regulated vesicle exocytosis." J Biol Chem **277**(21): 18249-18252.

Ashery, U., F. Varoqueaux, et al. (2000). "Munc13-1 acts as a priming factor for large dense-core vesicles in bovine chromaffin cells." EMBO J **19**(14): 3586-3596.

Bai, H.-J., M.-L. Shao, et al. (2009). "Patterned Au/Poly(dimethylsiloxane) Substrate Fabricated by Chemical Plating Coupled with Electrochemical Etching for Cell Patterning." Langmuir **25**(17): 10402-10407.

Bao, M. and W. Wang (1996). "Future of microelectromechanical systems (MEMS)." Sensors and Actuators A: Physical **56**(1-2): 135-141.

Bashir, R. (2004). "BioMEMS: state-of-the-art in detection, opportunities and prospects." Advanced Drug Delivery Reviews **56**(11): 1565-1586.

Becker, H. and C. Gärtner (2000). "Polymer microfabrication methods for microfluidic analytical applications." Electrophoresis **21**(1): 12-26.

Beebe, D. J., G. A. Mensing, et al. (2002). "PHYSICS AND APPLICATIONS OF MICROFLUIDICS IN BIOLOGY." Annual Review of Biomedical Engineering **4**(1): 261-286.

Borges, R., M. Camacho, et al. (2008). "Measuring secretion in chromaffin cells using electrophysiological and electrochemical methods." Acta Physiologica **192**(2): 173-184.

Brannon-Peppas, L. (1995). "Recent advances on the use of biodegradable microparticles and nanoparticles in controlled drug delivery." International Journal of Pharmaceutics **116**(1): 1-9.

Britland, S., E. Perez-Arnaud, et al. (1992). "Micropatterning proteins and synthetic peptides on solid supports: a novel application for microelectronics fabrication technology." Biotechnol Prog **8**(2): 155-160.

Bruns, D. (2004). "Detection of transmitter release with carbon fiber electrodes." Methods **33**(4): 312-321.

Carmignoto, G. (2000). "Reciprocal communication systems between astrocytes and neurones." Progress in Neurobiology **62**(6): 561-581.

Ceccarelli, B., W. P. Hurlbut, et al. (1973). "TURNOVER OF TRANSMITTER AND SYNAPTIC VESICLES AT THE FROG NEUROMUSCULAR JUNCTION." J. Cell Biol. **57**(2): 499-524.

Chang, J. C., G. J. Brewer, et al. (2000). "Microelectrode Array Recordings of Patterned Hippocampal Neurons for Four Weeks." Biomedical Microdevices **2**(4): 245-253.

Chen, G., P. Gavin, et al. (1995). "Observation and quantitation of exocytosis from the cell body of a fully developed neuron in Planorbis corneus." J. Neurosci. **15**(11): 7747-7755.

Chicharro, M., A. Sánchez, et al. (2004). "Capillary electrophoresis of neurotransmitters with amperometric detection at melanin-type polymer-modified carbon electrodes." Analytica Chimica Acta **523**(2): 185-191.

Chow, R. H., L. von Ruden, et al. (1992). "Delay in vesicle fusion revealed by electrochemical monitoring of single secretory events in adrenal chromaffin cells." Nature **356**(6364): 60-63.

Ciolkowski, E. L., K. M. Maness, et al. (1994). "Disproportionation During Electrooxidation of Catecholamines at Carbon-Fiber Microelectrodes." Analytical Chemistry **66**(21): 3611-3617.

Cooper, J. M., P. L. Foreman, et al. (1995). "Glutamate oxidase enzyme electrodes: microsensors for neurotransmitter determination using electrochemically polymerized permselective films." Journal of Electroanalytical Chemistry **388**(1-2): 143-149.

Corey, J. M., A. L. Brunette, et al. (1997). "Differentiated B104 neuroblastoma cells are a high-resolution assay for micropatterned substrates." Journal of Neuroscience Methods **75**(1): 91-97.

Coyle, J. and P. Puttfarcken (1993). "Oxidative stress, glutamate, and neurodegenerative disorders." Science **262**(5134): 689-695.

Cummings, E. B. and A. K. Singh (2003). "Dielectrophoresis in Microchips Containing Arrays of Insulating Posts:â€‰ Theoretical and Experimental Results." Analytical Chemistry **75**(18): 4724-4731.

Das, C. M., F. Becker, et al. (2005). "Dielectrophoretic Segregation of Different Human Cell Types on Microscope Slides." Analytical Chemistry **77**(9): 2708-2719.

Dittrich, P. S. and A. Manz (2006). "Lab-on-a-chip: microfluidics in drug discovery." Nat Rev Drug Discov **5**(3): 210-218.

El-Ali, J., P. K. Sorger, et al. (2006). "Cells on chips." Nature **442**(7101): 403-411.

Falconnet, D., G. Csucs, et al. (2006). "Surface engineering approaches to micropattern surfaces for cell-based assays." Biomaterials **27**(16): 3044-3063.

Fang, Q., K. Berberian, et al. (2008). "The role of the C terminus of the SNARE protein SNAP-25 in fusion pore opening and a model for fusion pore mechanics." Proceedings of the National Academy of Sciences **105**(40): 15388-15392.

Ferreira, N. G., L. L. G. Silva, et al. (2002). "Kinetics study of diamond electrodes at different levels of boron doping as quasi-reversible systems." Diamond and Related Materials **11**(8): 1523-1531.

Fiedler, S., S. G. Shirley, et al. (1998). "Dielectrophoretic Sorting of Particles and Cells in a Microsystem." Analytical Chemistry **70**(9): 1909-1915.

Finnegan, J. M., K. Pihel, et al. (1996). "Vesicular Quantal Size Measured by Amperometry at Chromaffin, Mast, Pheochromocytoma, and Pancreatic β-Cells." Journal of Neurochemistry **66**(5): 1914-1923.

Fox, M., D. Esveld, et al. (2006). "Electroporation of cells in microfluidic devices: a review." Analytical and Bioanalytical Chemistry **385**(3): 474-485.

Fu, A. Y., H.-P. Chou, et al. (2002). "An Integrated Microfabricated Cell Sorter." Analytical Chemistry **74**(11): 2451-2457.

Fubini, B. and A. Hubbard (2003). "Reactive oxygen species (ROS) and reactive nitrogen species (RNS) generation by silica in inflammation and fibrosis." Free Radical Biology and Medicine **34**(12): 1507-1516.

Galli, A., R. D. Blakely, et al. (1998). "Patch-clamp and amperometric recordings from norepinephrine transporters: Channel activity and voltage-dependent uptake." Proceedings of the National Academy of Sciences of the United States of America **95**(22): 13260-13265.

Gao, Y., X. Chen, et al. (2008). "Magnetron sputtered diamond-like carbon microelectrodes for on-chip measurement of quantal catecholamine release from cells." Biomed Microdevices **10**(5): 623-629.

Gelperina, S., K. Kisich, et al. (2005). "The Potential Advantages of Nanoparticle Drug Delivery Systems in Chemotherapy of Tuberculosis." Am. J. Respir. Crit. Care Med. **172**(12): 1487-1490.

Gil, A., J. Rueda, et al. (2000). "The F-actin cytoskeleton modulates slow secretory components rather than readily releasable vesicle pools in bovine chromaffin cells." Neuroscience **98**(3): 605-614.

Gong, L.-W., I. Hafez, et al. (2003). "Secretory Vesicles Membrane Area Is Regulated in Tandem with Quantal Size in Chromaffin Cells." J. Neurosci. **23**(21): 7917-7921.

Graham, M. E., R. J. Fisher, et al. (2000). "Measurement of exocytosis by amperometry in adrenal chromaffin cells: Effects of clostridial neurotoxins and activation of protein kinase C on fusion pore kinetics." Biochimie **82**(5): 469-479.

Hafez, I., K. Kisler, et al. (2005). "Electrochemical imaging of fusion pore openings by electrochemical detector arrays." Proceedings of the National Academy of Sciences of the United States of America **102**(39): 13879-13884.

Han, G., P. Ghosh, et al. (2007). "Functionalized gold nanoparticles for drug delivery." Nanomedicine **2**(1): 113-123.

Hans, M. L. and A. M. Lowman (2002). "Biodegradable nanoparticles for drug delivery and targeting." Current Opinion in Solid State and Materials Science **6**(4): 319-327.

Hensley, K., K. A. Robinson, et al. (2000). "Reactive oxygen species, cell signaling, and cell injury." Free Radical Biology and Medicine **28**(10): 1456-1462.

Hernández, P., I. Sánchez, et al. (1998). "Cyclic voltammetry determination of epinephrine with a carbon fiber ultramicroelectrode." Talanta **46**(5): 985-991.

Heuser, J. E. and T. S. Reese (1973). "EVIDENCE FOR RECYCLING OF SYNAPTIC VESICLE MEMBRANE DURING TRANSMITTER RELEASE AT THE FROG NEUROMUSCULAR JUNCTION." J. Cell Biol. **57**(2): 315-344.

Hilt, J. Z., A. K. Gupta, et al. (2003). "Ultrasensitive Biomems Sensors Based on Microcantilevers Patterned with Environmentally Responsive Hydrogels." Biomedical Microdevices **5**(3): 177-184.

Ho, C.-M. and Y.-C. Tai (1996). "REVIEW: MEMS and Its Applications for Flow Control." Journal of Fluids Engineering **118**(3): 437-447.

Hochstetler, S. E., M. Puopolo, et al. (1999). "Real-Time Amperometric Measurements of Zeptomole Quantities of Dopamine Released from Neurons." Analytical Chemistry **72**(3): 489-496.

Hu, X., P. H. Bessette, et al. (2005). "Marker-specific sorting of rare cells using dielectrophoresis." Proceedings of the National Academy of Sciences of the United States of America **102**(44): 15757-15761.

Huang, Y. and B. Rubinsky (2001). "Microfabricated electroporation chip for single cell membrane permeabilization." Sensors and Actuators A: Physical **89**(3): 242-249.

Huang, Y. and B. Rubinsky (2003). "Flow-through micro-electroporation chip for high efficiency single-cell genetic manipulation." Sensors and Actuators A: Physical **104**(3): 205-212.

Hynes, A. M., H. Ashraf, et al. (1999). "Recent advances in silicon etching for MEMS using the ASE(TM) process." Sensors and Actuators A: Physical **74**(1-3): 13-17.

Jackson, M. B. (2007). "In search of the fusion pore of exocytosis." Biophysical Chemistry **126**(1-3): 201-208.

Jain, P. K., K. S. Lee, et al. (2006). "Calculated Absorption and Scattering Properties of Gold Nanoparticles of Different Size, Shape, and Composition.

Applications in Biological Imaging and Biomedicine." The Journal of Physical Chemistry B **110**(14): 7238-7248.

Joshi, R. N., V. P. Singh, et al. (1995). "Characteristics of indium tin oxide films deposited by r.f. magnetron sputtering." Thin Solid Films **257**(1): 32-35.

Jun, S. B., M. R. Hynd, et al. (2007). "Low-density neuronal networks cultured using patterned poly-l-lysine on microelectrode arrays." Journal of Neuroscience Methods **160**(2): 317-326.

Kelly, S., E. M. Regan, et al. (2008). "Patterned growth of neuronal cells on modified diamond-like carbon substrates." Biomaterials **29**(17): 2573-2580.
Koh, T.-W. and H. J. Bellen (2003). "Synaptotagmin I, a Ca2+ sensor for neurotransmitter release." Trends in Neurosciences **26**(8): 413-422.

Kopp, M. U., H. J. Crabtree, et al. (1997). "Developments in technology and applications of microsystems." Current Opinion in Chemical Biology **1**(3): 410-419.

Kotzar, G., M. Freas, et al. (2002). "Evaluation of MEMS materials of construction for implantable medical devices." Biomaterials **23**(13): 2737-2750.

Lafon, E. E. and H. A. Pohl (1981). "Critical fields in cell fusion and dielectrophoresis." Journal of Biological Physics **9**(4): 209-217.

Lehnert, D., B. Wehrle-Haller, et al. (2004). "Cell behaviour on micropatterned substrata: limits of extracellular matrix geometry for spreading and adhesion." J Cell Sci **117**(1): 41-52.

Lin, R.-Z., C.-T. Ho, et al. (2006). "Dielectrophoresis based-cell patterning for tissue engineering." Biotechnology Journal **1**(9): 949-957.

Lindau, M. and G. Alvarez de Toledo (2003). "The fusion pore." Biochimica et Biophysica Acta (BBA) - Molecular Cell Research **1641**(2-3): 167-173.

Machado, J. D., C. Alonso, et al. (2002). "Nongenomic regulation of the kinetics of exocytosis by estrogens." J Pharmacol Exp Ther **301**(2): 631-637.

Malacombe, M., M. F. Bader, et al. (2006). "Exocytosis in neuroendocrine cells: new tasks for actin." Biochim Biophys Acta **1763**(11): 1175-1183.

Manna, A., T. Imae, et al. (2001). "Synthesis of Dendrimer-Passivated Noble Metal Nanoparticles in a Polar Medium: Comparison of Size between Silver and Gold Particles." Chemistry of Materials **13**(5): 1674-1681.

Manos, P., J. J. Pancrazio, et al. (1999). "Characterization of rat spinal cord neurons cultured in defined media on microelectrode arrays." Neuroscience Letters **271**(3): 179-182.

Markesbery, W. R. (1997). "Oxidative Stress Hypothesis in Alzheimer's Disease." Free Radical Biology and Medicine **23**(1): 134-147.

Marks, G. H., Y. Huang, et al. (1994). "Dielectrophoretic characterization and separation of micro-organisms." Microbiology **140**(3): 585-591.

Markx, G. H., P. A. Dyda, et al. (1996). "Dielectrophoretic separation of bacteria using a conductivity gradient." Journal of Biotechnology **51**(2): 175-180.

Matson, W., P. Langlais, et al. (1984). "n-Electrode three-dimensional liquid chromatography with electrochemical detection for determination of neurotransmitters." Clin Chem **30**(9): 1477-1488.

McDonald, J. C., D. C. Duffy, et al. (2000). "Fabrication of microfluidic systems in poly(dimethylsiloxane)." Electrophoresis **21**(1): 27-40.

McDonald, J. C. and G. M. Whitesides (2002). "Poly(dimethylsiloxane) as a Material for Fabricating Microfluidic Devices." Accounts of Chemical Research **35**(7): 491-499.

Michael, D. J. and R. M. Wightman (1999). "Electrochemical monitoring of biogenic amine neurotransmission in real time." Journal of Pharmaceutical and Biomedical Analysis **19**(1-2): 33-46.

Mittler, R. (2002). "Oxidative stress, antioxidants and stress tolerance." Trends in Plant Science **7**(9): 405-410.

Monck, J. R., A. F. Oberhauser, et al. (1995). "The exocytotic fusion pore interface: a model of the site of neurotransmitter release." Molecular Membrane Biology **12**(1): 151-156.

Mosharov, E. V. and D. Sulzer (2005). "Analysis of exocytotic events recorded by amperometry." Nat Methods **2**(9): 651-658.

Müller, R. H., K. Mäder, et al. (2000). "Solid lipid nanoparticles (SLN) for controlled drug delivery - a review of the state of the art." European Journal of Pharmaceutics and Biopharmaceutics **50**(1): 161-177.

Neher, E. (1992). "Ion channels for communication between and within cells." Bioscience Reports **12**(1): 1-14.

Paciotti, G. F., D. G. I. Kingston, et al. (2006). "Colloidal gold nanoparticles: a novel nanoparticle platform for developing multifunctional tumor-targeted drug delivery vectors." Drug Development Research **67**(1): 47-54.

Panyam, J. and V. Labhasetwar (2003). "Biodegradable nanoparticles for drug and gene delivery to cells and tissue." Advanced Drug Delivery Reviews **55**(3): 329-347.

Park, S., Y. Xie, et al. (2002). "Electrocatalytic Pathways on Carbon-Supported Platinum Nanoparticles: Comparison of Particle-Size-Dependent Rates of Methanol, Formic Acid, and Formaldehyde Electrooxidation." Langmuir **18**(15): 5792-5798.

Park, T. H. and M. L. Shuler (2003). "Integration of Cell Culture and Microfabrication Technology." Biotechnology Progress **19**(2): 243-253.

Paul, S., C. Pearson, et al. (2003). "Langmuir−Blodgett Film Deposition of Metallic Nanoparticles and Their Application to Electronic Memory Structures." Nano Letters **3**(4): 533-536.

Pethig, R. and G. H. Markx (1997). "Applications of dielectrophoresis in biotechnology." Trends in Biotechnology **15**(10): 426-432.

Pihel, K., S. Hsieh, et al. (1995). "Electrochemical detection of histamine and 5-hydroxytryptamine at isolated mast cells." Analytical Chemistry **67**(24): 4514-4521.

Pizziconi, V. B. and D. L. Page (1997). "A cell-based immunobiosensor with engineered molecular recognition--Part I: design feasibility." Biosensors and Bioelectronics **12**(4): 287-299.

Reiter, R., D.-x. Tan, et al. (2001). "Biochemical reactivity of melatonin with reactive oxygen and nitrogen species." Cell Biochemistry and Biophysics **34**(2): 237-256.

Rettig, J. and E. Neher (2002). "Emerging Roles of Presynaptic Proteins in Ca++-Triggered Exocytosis." Science **298**(5594): 781-785.

Robertson, J. (1993). "Deposition mechanisms for promoting sp3 bonding in diamond-like carbon." Diamond and Related Materials **2**(5-7): 984-989.

Robertson, J. (2002). "Diamond-like amorphous carbon." Materials Science and Engineering: R: Reports **37**(4-6): 129-281.

Sarada, B. V., T. N. Rao, et al. (2000). "Electrochemical Oxidation of Histamine and Serotonin at Highly Boron-Doped Diamond Electrodes." Analytical Chemistry **72**(7): 1632-1638.

Sarro, P. M. (2000). "Silicon carbide as a new MEMS technology." Sensors and Actuators A: Physical **82**(1-3): 210-218.

Sen, A., S. Barizuddin, et al. (2009). "Preferential cell attachment to nitrogen-doped diamond-like carbon (DLC:N) for the measurement of quantal exocytosis." Biomaterials **30**(8): 1604-1612.

Shawgo, R. S., A. C. Richards Grayson, et al. (2002). "BioMEMS for drug delivery." Current Opinion in Solid State and Materials Science **6**(4): 329-334.

Sies, H. (1997). "Oxidative stress: oxidants and antioxidants." Exp Physiol **82**(2): 291-295.

Smith, K. J., R. Kapoor, et al. (1999). "Demyelination: The Role of Reactive Oxygen and Nitrogen Species." Brain Pathology **9**(1): 69-92.

Sombers, L. A., H. J. Hanchar, et al. (2004). "The Effects of Vesicular Volume on Secretion through the Fusion Pore in Exocytotic Release from PC12 Cells." J. Neurosci. **24**(2): 303-309.

Spégel, C., A. Heiskanen, et al. (2007). "On-Chip Determination of Dopamine Exocytosis Using Mercaptopropionic Acid Modified Microelectrodes." Electroanalysis **19**(2-3): 263-271.

Spegel, C., A. Heiskanen, et al. (2008). "Fully automated microchip system for the detection of quantal exocytosis from single and small ensembles of cells." Lab Chip **8**(2): 323-329.

Squires, T. M. and S. R. Quake (2005). "Microfluidics: Fluid physics at the nanoliter scale." Reviews of Modern Physics **77**(3): 977.

Stevens, C. F. and J. H. Williams (2000). "“Kiss and run” exocytosis at hippocampal synapses." Proceedings of the National Academy of Sciences of the United States of America **97**(23): 12828-12833.

Subramanian, V., E. E. Wolf, et al. (2003). "Green Emission to Probe Photoinduced Charging Events in ZnO−Au Nanoparticles. Charge Distribution and Fermi-Level Equilibration†." The Journal of Physical Chemistry B **107**(30): 7479-7485.

Sugimoto, W., K. Yokoshima, et al. (2006). "Charge storage mechanism of nanostructured anhydrous and hydrous ruthenium-based oxides." Electrochimica Acta **52**(4): 1742-1748.

Sun, X. and K. D. Gillis (2006). "On-chip amperometric measurement of quantal catecholamine release using transparent indium tin oxide electrodes." Anal Chem **78**(8): 2521-2525.

Sun, X. and K. D. Gillis (2006). "On-Chip Amperometric Measurement of Quantal Catecholamine Release Using Transparent Indium Tin Oxide Electrodes." Analytical Chemistry **78**(8): 2521-2525.

Tadanaga, K., J. Morinaga, et al. (2000). "Superhydrophobicâˆ'Superhydrophilic Micropatterning on Flowerlike Alumina Coating Film by the Solâˆ'Gel Method." Chemistry of Materials **12**(3): 590-592.

Tak, Y.-H., K.-B. Kim, et al. (2002). "Criteria for ITO (indium-tin-oxide) thin film as the bottom electrode of an organic light emitting diode." Thin Solid Films **411**(1): 12-16.

Tanaka, Y., K. Sato, et al. (2007). "Biological cells on microchips: New technologies and applications." Biosensors and Bioelectronics **23**(4): 449-458.

Tasche, C., E. Meyhofer, et al. (1999). "A force transducer for measuring mechanical properties of single cardiac myocytes." Am J Physiol Heart Circ Physiol **277**(6): H2400-2408.

Thomas, C. H., J.-B. Lhoest, et al. (1999). "Surfaces Designed to Control the Projected Area and Shape of Individual Cells." Journal of Biomechanical Engineering **121**(1): 40-48.

Thompson, R. Q., M. Porter, et al. (1993). "Zeptomole detection limit for alkaline phosphatase using 4-aminophenylphosphate, amperometric detection, and an optimal buffer system." Analytica Chimica Acta **271**(2): 223-229.

Travis, E. R. and R. M. Wightman (1998). "SPATIO-TEMPORAL RESOLUTION OF EXOCYTOSIS FROM INDIVIDUAL CELLS." Annual Review of Biophysics and Biomolecular Structure **27**(1): 77-103.

Tsuboi, T., H. T. McMahon, et al. (2004). "Mechanisms of Dense Core Vesicle Recapture following “Kiss and Run” (“Cavicapture”) Exocytosis in Insulin-secreting Cells." Journal of Biological Chemistry **279**(45): 47115-47124.

Varma, S., J. McLachlan, et al. (2010). "Positionally controlled growth of cells using a cytophobic fluorinated polymer." Analytical and Bioanalytical Chemistry **396**(3): 1159-1165.

Voskerician, G., M. S. Shive, et al. (2003). "Biocompatibility and biofouling of MEMS drug delivery devices." Biomaterials **24**(11): 1959-1967.

Whitesides, G. M., E. Ostuni, et al. (2001). "SOFT LITHOGRAPHY IN BIOLOGY AND BIOCHEMISTRY." Annual Review of Biomedical Engineering **3**(1): 335-373.

Wightman, R. M., J. A. Jankowski, et al. (1991). "Temporally resolved catecholamine spikes correspond to single vesicle release from individual chromaffin cells." Proceedings of the National Academy of Sciences of the United States of America **88**(23): 10754-10758.

Wightman, R. M., T. J. Schroeder, et al. (1995). "Time course of release of catecholamines from individual vesicles during exocytosis at adrenal medullary cells." Biophysical Journal **68**(1): 383-390.

Xu, J. and F. W. Tse (1999). "Brefeldin A Increases the Quantal Size and Alters the Kinetics of Catecholamine Release from Rat Adrenal Chromaffin Cells." Journal of Biological Chemistry **274**(27): 19095-19102.

Yi, C., C.-W. Li, et al. (2006). "Microfluidics technology for manipulation and analysis of biological cells." Analytica Chimica Acta **560**(1-2): 1-23.

Yuanfang, G. and et al. (2009). "A microfluidic cell trap device for automated measurement of quantal catecholamine release from cells." Lab on a Chip **9**(23): 3442.

Zhou, Z., S. Misler, et al. (1996). "Rapid fluctuations in transmitter release from single vesicles in bovine adrenal chromaffin cells." Biophysical Journal **70**(3): 1543-1552.

Ziaie, B., A. Baldi, et al. (2004). "Hard and soft micromachining for BioMEMS: review of techniques and examples of applications in microfluidics and drug delivery." Advanced Drug Delivery Reviews **56**(2): 145-172.

CHAPTER 2

MATERIAL & CHARACTERIZATION

2-1 Deposition of electrode materials

Deposition of conductive materials over a substrate in the form of a thin film can be done by evaporation (Laux, Kaiser et al. 1998; Miyake, Ye et al. 2002), sputtering (Sreenivas, Sayer et al. 1989) and e-beam (Palshin, Meletis et al. 1995) among other methods. The quality of the film varies with different kinds of depositions. E-beam deposited films are better quality than sputtering (de Sande, Afonso et al. 1992; Yang, Babcock et al. 1998). Though all of these deposition techniques are employed for thin film deposition, sputtering is commonly used.

Sputtering of a target by energetic ions is assumed to result from cascades of atomic collisions (Sigmund 1969; Thornton 1974; Williams 1979). Magnetron sputtering has become the process of choice for the deposition of a wide range of coatings that include hard, wear-resistant, low friction, corrosion resistant and coatings with specific optical, or electrical properties (Kelly and Arnell 2000).

DC (Schiller, Beister et al. 1984; May and Strümpfel 1999; Teixeira, Cui et al. 2002), pulsed DC (Arnell and Kelly 1999; Kelly and Arnell 2000; Musil, Lestina et al. 2001), AC (Mailly, Giani et al. 2001; Khanna, Bhat et al. 2006) and RF (Wen-Fa and et al. 1994; Joshi, Singh et al. 1995; Mardare, Tasca et al. 2000)

power supplies are used depending on the target material. The sputtering chamber which is evacuated and maintained at a very low pressure contains an assembly of permanent magnets that are located behind the target acting as the deposition source. The Plasma confinement on the target results from the magnetic field that forms closed-loop annular path acting as an electron trap that reshapes the trajectories of the secondary electrons ejected from target into a cycloidal path, increasing the probability of ionization of the sputtering gas within the confinement zone. Inert gases like argon (Hellgren, Johansson et al. 1999) , are used as sputtering gas since they do not react with target material nor combine with any process gases. Other gases like nitrogen (Kaufman, Metin et al. 1989; Burda, Lou et al. 2003; Lindgren, Mwabora et al. 2003; Gao, Chen et al. 2008), hydrogen (Ruske, Sittinger et al. 2005) and oxygen (Beensh-Marchwicka, Kròl-Stepniewska et al. 1982) are also introduced in the chamber depending on the type and characteristics of a film required. Positively charged argon ions from the plasma are accelerated toward the negatively biased target (cathode), resulting in the material being sputtered from the target surface. These ejected materials are deposited on a substrate placed in their path. The thickness of the film depends on the time the substrate is held in the path way of these materials. The more the time, the thicker is the film.

By varying the parameters like power, pressure and temperature, and the composition of gases, the characteristics of the film can be manipulated significantly. All metals, metal oxides and carbon based materials during this

study were deposited using a magnetron sputtering system (ATC2000, AJA International Inc, North Scituate, MA, USA) as shown in figure 2-1.

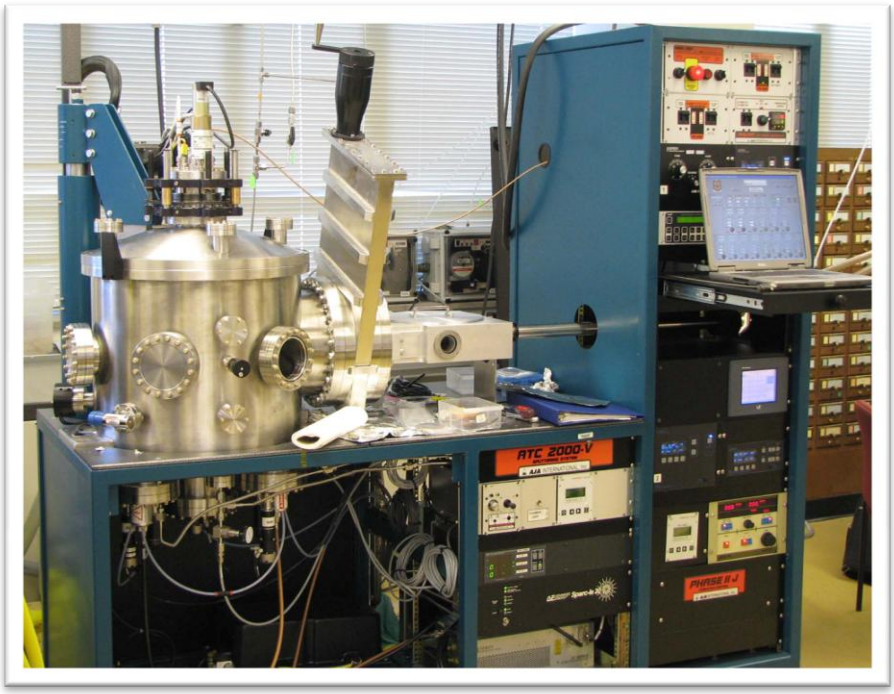

Figure 2-1 Sputtering machine used in this study in Dr. Gangopadhyay's lab.

2-2 Deposition parameters, material properties and characteristics

Before a target material is sputtered on a surface, it is very important that the substrate surface is totally clean and free of any organic and inorganic impurities. For our devices the glass slides (25 mm x 75 mm), (Fisher Scientific Waltham, MA, USA) were used as substrates. These slides were cleaned by soaking in a 4:1 mixture of sulphuric acid and hydrogen peroxide (piranha

solution) for 10 minutes at room temperature. This was followed by rinsing in DI (de-ionized) water (Millipore, Billerica, MA) and then dried with compressed air/ nitrogen stream. The slides were placed on the wafer holder, generally in batches of 6-8 slides with a silicon wafer for control and characterization. Before putting them in the load lock these slides are blown with compressed air to get rid of any particles that might have accumulated on the surface of the substrate during handling. Once the pressure of load lock is below the pressure of the main sputtering chamber as shown, which is maintained at 5×10^{-7} Torr, the partition between the load lock and the chamber is opened and the substrate is inserted in the main chamber.

After the substrate holder is placed firmly and securely in its place, the substrate is heated if the protocol requires deposition above the room temperature, and gas flow is introduced in the chamber. Stabilizing the temperature might take significant amounts of time. The gas in the chamber is controlled by mass flow controllers. Once the gas flow has stabilized, the power is introduced to the electrodes. This ionizes the gas and plasma is formed in the chamber.

Once the plasma is formed the shutters on the target material are automatically or manually moved. This exposes the material target to the accelerated ions of the plasma. When this beam of plasma strikes the surface of the target material, the eroded atoms are ejected from the surface, which are deposited on the surface of the rotating substrate. The substrate is rotated to have a uniformity of the film deposited.

2-2-1 Indium Tin oxide

Indium tin oxide (ITO) was deposited using a (In_2O_3/SnO_2, 10% SnO_2, by weight) (Williams Advanced Materials Inc or Kurt J. Lesker) target, with dimensions of 75 mm diameter, 3 mm thick and 99.99% purity. A radio frequency power supply of 13.56 MHz at a power of 180 W and 20 sccm flow of Ar gas was regulated by a mass-flow controller and maintained at a working pressure of 4 mTorr. The substrate temperature was maintained at 200°C and the deposition time was 20 min resulting in a 100 nm-thick ITO film. In the later part of the research ITO coated slides on glass slides were commercially bought (Sigma-Aldrich, St. Louis, MO).

2-2-1-1 ITO Etching

Etching is a process in which the uppermost layer of the exposed substrate can be removed in the areas that are not protected by photoresist. Etching is divided into two types: wet etch and dry etch. Wet etch processes generally involves the use of liquid chemicals which dissolve the materials of the exposed areas. This type of process is isotropic in nature and has the disadvantage of the undercut. Dry etching techniques like reactive ion etching or deep reactive ion etching give anisotropic patterns and very clean etch. This process does not leave residue that is harmful or toxic which needs to be disposed.

For our process wet chemical etching was found to be suitable as ITO can be readily etched in hydrogen fluoride (HF) solution ($HF:H_2O_2:10H_2O$) and

hydrochloric acid (HCl) solutions of various strengths (Banovec and Kern) , but HCl gave cleaner results, and as it does not have the intense corrosive property as attributed with HF, a 37% HCl concentrate solution was used for wet etching ITO.

2-2-1-2 Etch profile of ITO using 37% HCl Wet etch

Figure 2-2 shows the etch rate of ITO using wet etch method. The patterned substrate was post baked for 3 minutes on a hot plate to give the photoresist extra mechanical strength to withstand a few minutes in the acid. Though HCl is not a very corrosive acid, but it is advisable that the photoresist used is not very thin so as to prevent any inadvertent damage to the film. The etch rate of ITO was found to be 0.31 nm/sec.

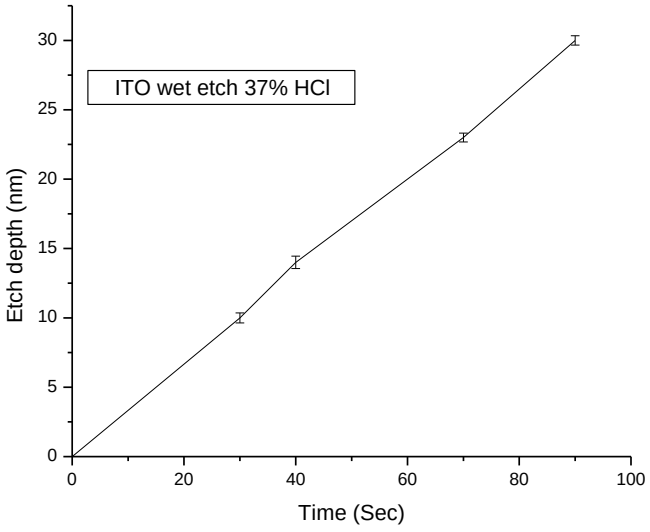

Figure 2-2 Etch profile for etching 60 nm thick ITO (purchased from Sigma-Aldrich, St. Louis, MO).

The undiluted etch solution contained 37% HCl. Figure 2-2 shows the etch rate of ITO on glass substrate etched as a function of time. These reactions were carried out in the class 10,000 clean room with room the temperature of 25°C. The ITO coated glass substrate was patterned using standard photolithography process to enable thickness measurements to be carried out following etching. Photoresist (S 1813) (~ 2.2 µm) was used as the mask for these experiments.

2-2-1-3 RIE Etch profile of DLC:N deposited at 200°C

As mentioned in the earlier sections on etching, reactive ion etching is a form of dry etching in which some plasma components reacts with the material on the surface of the film that needs to be etched. Following is the image of the machine that was used in the etching process.

Figure 2-3 Precision 5000 mark II Applied Materials P-5000 RIE etch set-up in Dr. Gangopadhyay's lab.

The product from the reaction is generally in form of a gas. The optimization of RIE was a necessary step to incorporate it as a micro fabrication compatible material. DLC:N is a very stable and inert material. DLC:N was etched using reactive ion etching (RIE) process with oxygen plasma. This is a dry etch process in which a single or combination of gases are used to etch a material. The protocol used to etch this DLC:N film was, 500 watts of power, 250 milliTorr pressure and an inflow of 50 sccm of oxygen. The rate was found to be 7.86 nm/sec.

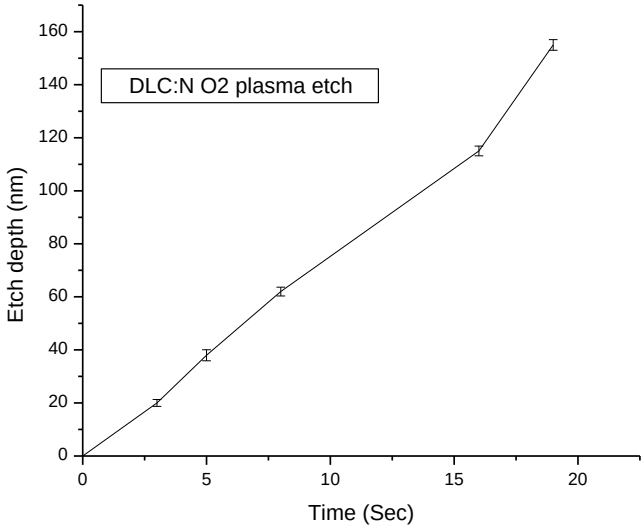

Figure 2-4 Etch rate of DLC:N using RIE dry etch.

2-2-1-4 Etch profile S 1813 photoresist spun at 3000 RPM for 30 sec with acceleration of 1100 and approximate film thickness of 1.6 µm

The photeresist S 1813 was RIE etched with a power of 400 watt, 100 sccm of oxygen and pressure of 250 mTorr. The etch rate is 14 nm/sec.

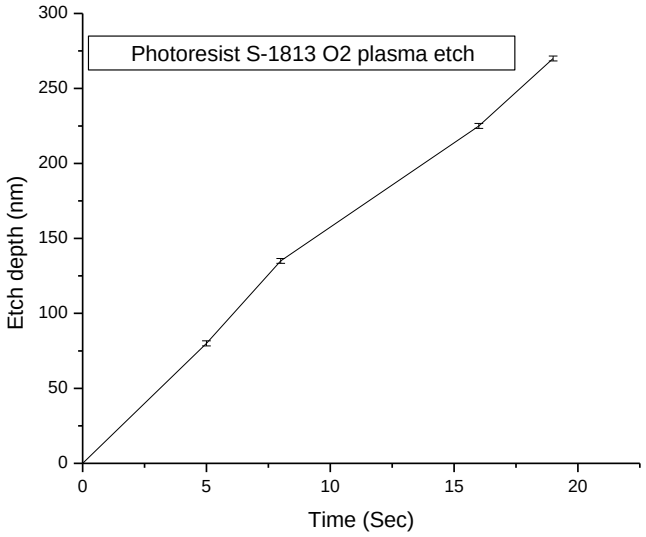

Figure 2-5 RIE etch profile of the positive photoresist S 1813 with approximate thickness of 1.6 µm.

2-2-2 Etch rates of materials

Table 2-1 shows the etch rates of the materials used in the fabrication of this device. Except for ITO, which was wet chemical etched, all the other materials were etched using dry etching.

Material	Etch protocol	Etch rate (nm/sec)
DLC:N	500 watts, 250 milliTorr, 50 sccm O2	7.86
ITO	37% concentrated HCl	0.31
Teflon AF 1600	500 watts, 250 milliTorr, 50 sccm O2	10
Photoresist S1813	400 watts, 250 milliTorr, 100 sccm O2	14.26

Table 2-1 Etch of materials.

2-2-3 Cyclic Voltammetry overview

Cyclic voltammetry (Nicholson 1965; Pihel, Walker et al. 1996) is a process, in which the potential of the working electrode is ramped linearly with respect to time between two limiting potentials as illustrated in figure 2-6. In a three-electrode experiment, the potential is measured between the working electrode and the reference electrode and the current is passed between the working electrode and the counter electrode. The current at the working electrode is plotted versus the applied voltage to give the cyclic voltammogram trace as shown in figure 2-7. Cyclic voltammetry is generally used to study the oxidation and reduction cycle of an electroactive analyte.

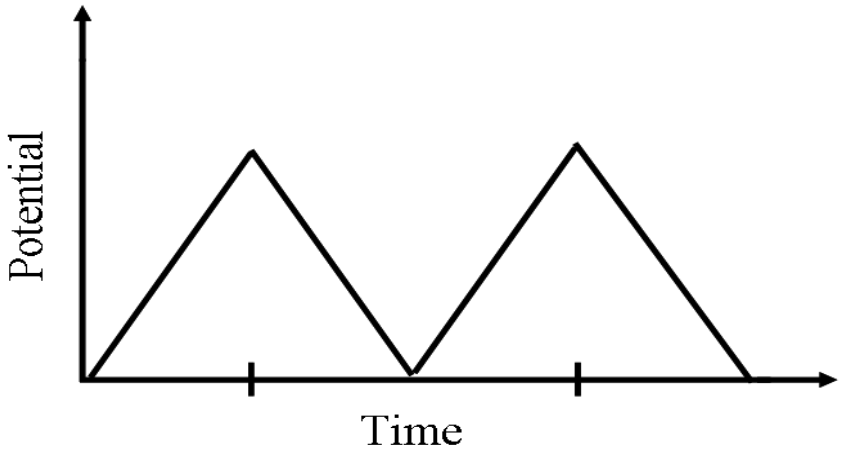

Figure 2-6 Typical triangular waves for cyclic voltammetry.

As the waveform shows, towards the negative (cathodic) potentials, the analyte is reduced on the surface of the electrode to produce the cathodic current. The cathodic peak decays, however, as the concentration of the analyte is depleted near the electrode surface. When the applied potential is ramped to

the positive (anodic) potentials, an oxidative (anodic) current is produced as the analyte is oxidized on the electrode surface. This oxidation peak will usually have a similar shape as the reduction peak. As a result, if the redox reaction is readily reversible (Nagaoka and Yoshino 1986; Ganesh, Pal et al. 2006), information about the redox potential and electrochemical reaction rates of the compounds are obtained.

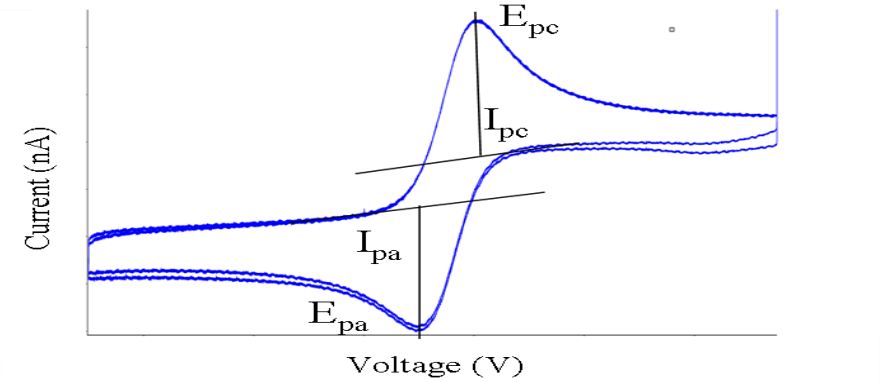

Figure 2-7 Cyclic voltammetry waveform.

If the electronic transfer at the surface is fast and the current is limited by the diffusion of species to the electrode surface, then the current peak will be proportional to the square root of the scan rate. This relationship is described by the Cottrell equation (Hawley and Feldberg 1966; Dayton, Brown et al. 1980) and it is given by

$$I = nFACo(\sqrt{D/\pi t})$$

where I is the flux of electrons at the electrode surface, n is the number of electrons, F is the faraday's constant, A is the area of the electrode, C_o is the concentration, D is the co-efficient and t is the time.

The analyte has to be capable of oxidizing and reducing (Ganesh, Pal et al. 2006) within the potential window of the experiment. Also it is important that the analyte is oxidized in the forward scan and reduced in the reverse scan. The oxidation peak is referred to as Epa (anodic potential) and the reduction peak is referred to as Epc (cathodic potential).

If a redox system remains in equilibrium throughout the potential scan, the redox process is said to be reversible if the surface concentrations of O and R is maintained, and following parameter values are used to characterize the cyclic voltammogram of a reversible process:

1. Peak-to-peak separation $\Delta Ep = Epc - Epa = 59$ mV/n,

   where, n is the number of electrons transferred

2. Peak current ratio $i\,pa / i\,pc = 1$
3. Peak current function = $i\,p / \nu^{1/2}$ where ν is the scan rate

   The peak current $ip = 2.69\times10^5\, n^{3/2}\, ACD^{1/2}\, \nu$ where

   n = number of electrons transferred/molecule

   A = electrode surface area (cm^2)

C = concentration (mol cm^{-3})

D = diffusion coefficient (cm^2 s^{-1})

If the concentration follows the nernstian potential then the concentration of the oxidized form of the species will decrease as the potential becomes negative. Assuming that the electron transfer rate is rapid, the current *i* that is measured as the potential decreases until the reduction on the surface of the electrode is limited by the diffusion rate of the oxidized species to the electrode surface, and it is given by:

$$I_m = 4\,nFDCr,$$

where n is the number of electrons transferred, F is the faraday's constant, D is the diffusion co-efficient, C is the concentration and r is the disk radius.

If variations are observed from these ideal characteristics then the redox reaction is not reversible. The two reasons for a reaction not being reversible are 1) slow electron transfer kinetics, reversibility depends on the relative values of the electron transfer rate constant (k) and the scan rate ν. If the ratio of k/ν is sufficiently small, then the process is said to be *quasi*-reversible (Laviron 1979; O'Dea and Osteryoung 1993; Ferreira, Silva et al. 2002). A quasi-reversible process is characterized by $\Delta Ep > 59/n$ mV, with the value increasing with increasing ν. Increases in ΔEp with increasing ν can also be due to uncompensated solution resistance Rx. 2) chemical reactions of O and R,

equilibrium values of O and R can only be maintained during a cyclic voltammetry experiment if both O and R are stable on the experimental time scale. Therefore, the rate of reduction increases and Epc moves to a more positive value. In addition, ipa/ipc is less than unity (since only a fraction of the molecules that were reduced on the forward scan are available for reoxidation on the reverse scan). The value of the current function can also be affected by chemical reactions following electron transfer.

2-2-3-1 Capacitance and charge on electrode

The electrode-solution interface behaves like a capacitor as shown in figure 2-8,

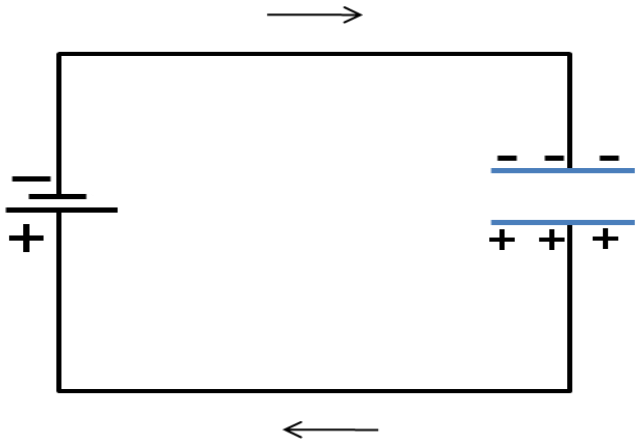

Figure 2-8 Electrical circuit of electrode-solution interface

where charge on the capacitor is given by

$$q/E = C$$

and q is the charge stored on the capacitor, E is the potential across the capacitor and C is the capacitance. When potential is applied, charge accumulates on the parallel plates. During the charging of the capacitor, the current flow is referred to as charging current.

Depending on the polarity of the potential applied at the electrode-electrolyte interface the charges separate as shown in figure 2-9 . At a given potential a charge of qM and qs exist at the electrode and the solution and are given by

$$qM = - qs$$

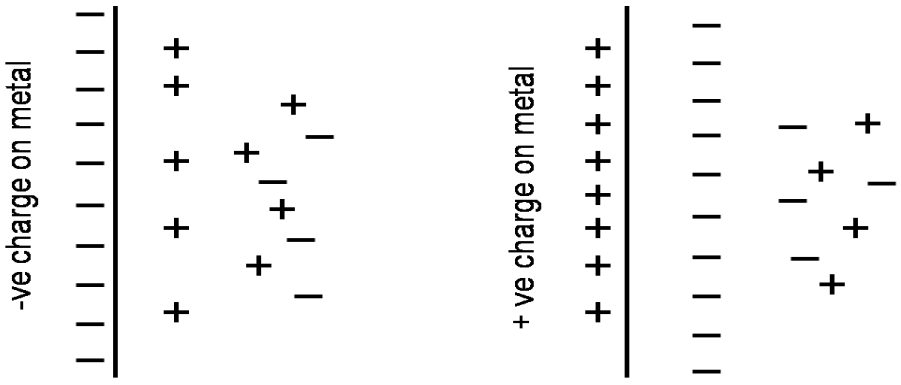

Figure 2-9 Alligning of charge depending on the potential polarity on the electrode.

The charge on the metal qM, represenst an excess or deficiency of electrons that reside ina very thin film (< 0.1°A) on the electrode surface. The charge in the solution qs is made up of ions , which are close to the electrode surface. The charges qM and qs are divided by the electrode area and expressed as charge densities by:

$$\sigma M = -qs = \mu C/cm^2$$

Alligned charged species and oriented dipoles existing at the electrode-electrolyte interface is reffered to as electrical double layer. At a given potential, this interface is charcaterized by a double layer capacitance which is typically in the range of 10-40 $\mu C/cm^2$.

Description of electrical double layer:

The double layer interface between the electrode and the electrolyte is represented as shown in the figure 2-10 .

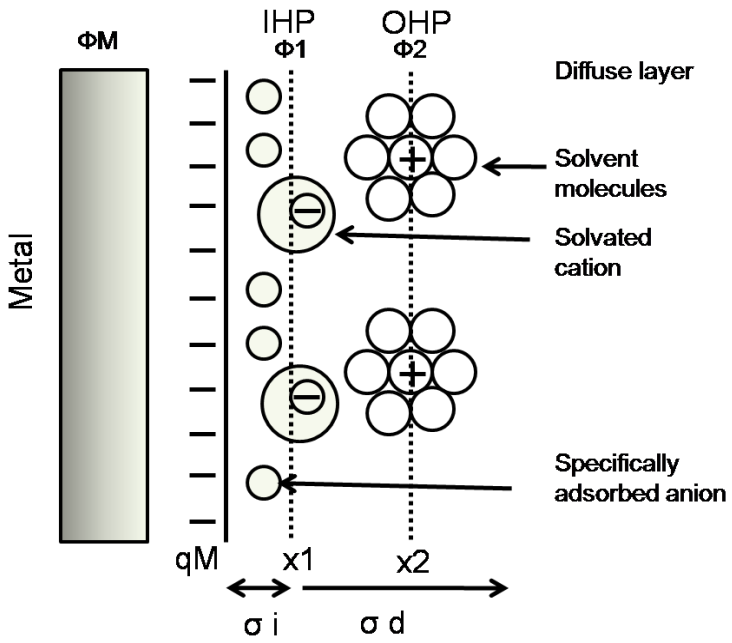

Figure 2-10 Model of double layer of the electrode-electrolyte interface.

The solution side is divided into many layers, the closest layer contains solvent molecules and other ion species and is referred to as the inner helmhltz plane (IHP). The distance for IHP is x1. Solvated ions from the diffusion layer can approach the electrode only to distance x2. This outer layer is referrd to as the outer helmholtz plane (OHP). The interaction of the solvated ions with the electrode is from a distance due to the electrostatic forces. These extend into the bulk solution.

The excess charge density in the diffusion layer is σd, therefore total charge density on the solution of the double layer σs is given by

$$\sigma s = \sigma i + \sigma d = - \sigma M$$

The double layer thickness is less than 100°A.

The potential profile across the double layer is as shown in the figure 2-11.

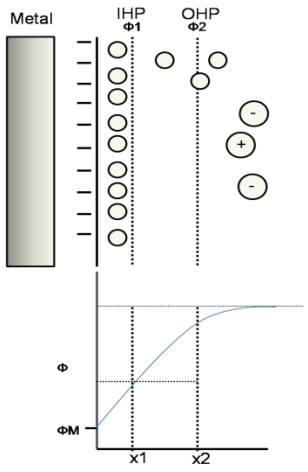

Figure 2-11 Potential profie across the double layer region in the absence of specific adsorption of ions. Φ is the inner potential. Adapted from Bard & Faulkner, Wiley and sons.

2-2-3-2 ITO Macro electrode

Performing CV on macro electrode is used to confirm the electro activity of the film before going through the effort of patterning the microelectrode. The former contains a redox couple species while the latter is used as a conducting electrolyte.

Cyclic voltammetry (CV) on the ITO electrodes was performed using the 1 mM K_3 $Fe(CN)_6$ potassium ferricyanide in 0.1 M KCl electrolyte on the macroelectrode. A PDMS gasket of 3 mm diameter was used to hold the solution on the macroelectrode. An Ag/AgCl electrode is used as the reference/counter

electrode. CV is performed at different scan rates to check the redox activity and the peak-to-peak separation (ΔEp) values, which indicates the electron transfer rate. The smaller the value of ΔEp, the faster is the rate of electron transfer.

CV was performed on ITO macro electrode to check for the electrochemical activity of the electrode with the standard solution of K_3 Fe $(CN)_6$ in KCl solution. Figure 2-12 depicts CV's obtained using scan rates of 100mV/s, 200mV/s and 500mV/s. The ΔEp values at these scan rates are 105 mV, 170 mV and 265 mV. The increasing peak-to-peak separation with scan rate indicates a slower electron transfer kinetics, which indicates that the nernstian concentrations cannot be maintained and hence the reaction is quasi-reversible.

Scan rate: 100 mV/s

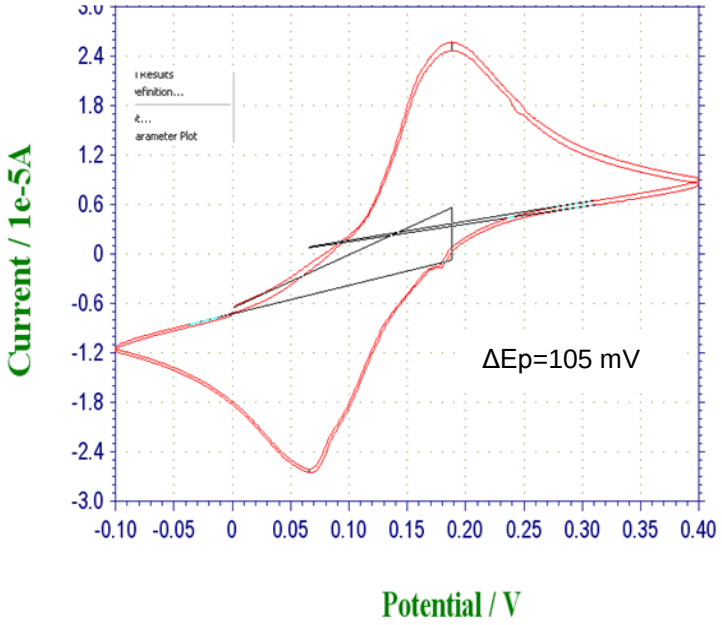

(a)

Scan rate: 200 mV/s

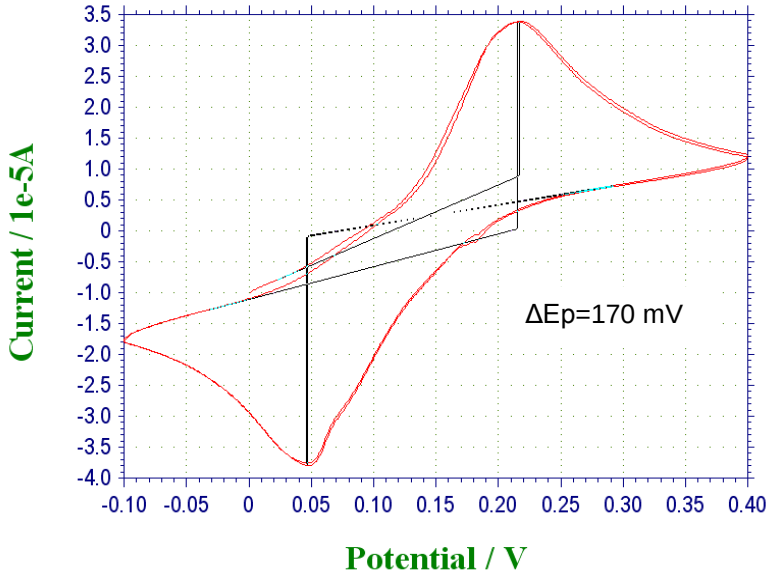

(b)

Scan rate: 500 mV/s

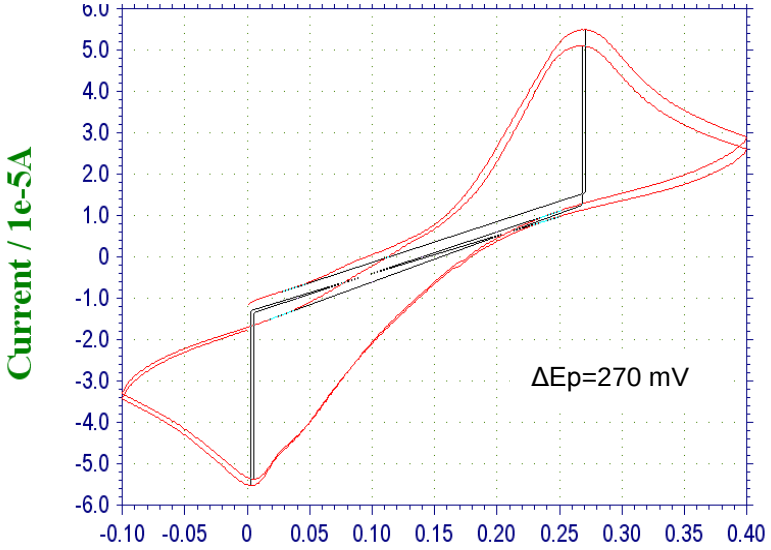

(c)

Figure 2-12 CV's of ITO macroelectrodes, a), b) and c) scans show the scan rates of 100, 200 and 500 mV respectively.

Microelectrode

The ITO coated glass substrate was patterned using microfabrication process and cyclic voltammetry (CV) was performed using the 1 mM $K_3Fe(CN)_6$ in 0.1 M KCl electrolyte on the microelectrode. The area of the microelectrode was the same area of the opening in the insulation of the device, which was approximately 20µm in diameter. A PDMS gasket was used to hold the solution. An Ag/AgCl electrode is used as the reference electrode/counter electrode.

Scan rate: 1000 mV/s

The electrode was scanned at a rate of 1000mV/s. At microelectrode size it is important to scan at high scan rates to capture the redox activity on the electrode. The peak-to-peak separation for the 20µm diameter electrode is 70 mV.

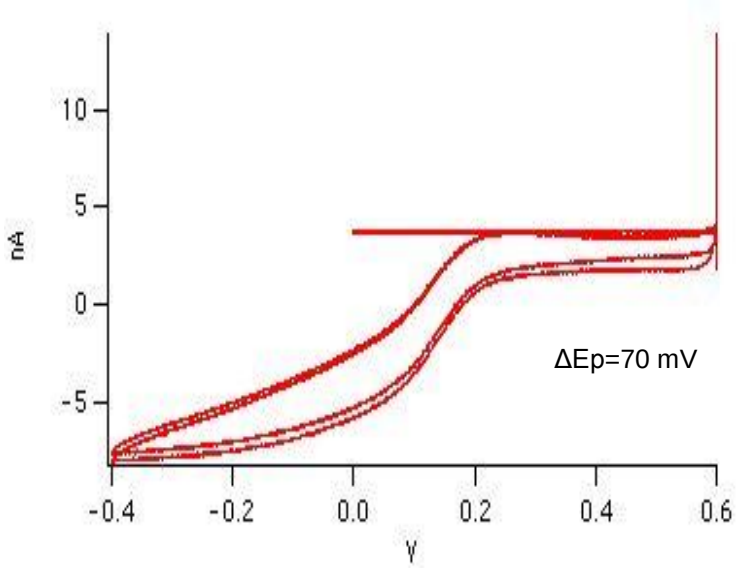

Figure 2-13 CV for the ITO microelectrode device.

2-2-4 Nitrogen doped Diamond like carbon (DLC:N)

Diamond-like carbon (DLC) films are hard amorphous films with interesting properties. DLC films can be hard, have low coefficient of friction and are chemically inert (Grill 1993). Depending on the deposition conditions, these films can be fully amorphous or diamond like. DLC can be prepared by various deposition techniques including sputtering from a graphite target (Robertson 1993; Grill 1999; Gao, Chen et al. 2008). Undoped DLC films prepared by sputtering are not highly conductive because of the presence of diamond like sp^3 hybridized states (Chhowalla, Ferrari, et al. 2000). It is important to have low resistivity for electrochemical applications because high series resistance on the working electrode leads to current dependent potential drop within the electrode. The two ways of reducing the series resistance used were, nitrogen doping in-

situ during the deposition process (Kleinsorge, Ferrari et al. 2000) (Gao, Chen et al. 2008), and sputter a highly conductive film below the DLC:N layer. ITO is preferred because it can maintain the transparent property of the electrode whereas depositing a metallic adhesion layer will make the electrodes opaque. Sputtering at higher temperatures (200°C and above) can further reduce the resistivity of the DLC:N film by significantly decreasing the sp^3 fraction and ordering of graphitic clusters of sp^2 sites (Chhowalla, Ferrari, et al. 2000). Films deposited at higher temperatures like 400°C may contain nanocrystalline graphite.

Adding nitrogen to diamond like carbon can: 1) dope a-C, 2) improve hardness, 3) topological disorder in graphitic bonding and 4) increase conductivity (Silva and Amaratunga 1995; Scharf, Ott et al. 1999), (Kleinsorge, Ferrari et al. 2000). In this study, (DLC:N) was sputtered with parameters of 300 Watts DC power, with the flow of gases Argon (Ar) 10 sccm, and Nitrogen (N) 10 sccm, pressure in the sputtering chamber was maintained at 2 mTorr and the substrate temperature was maintained at 200°C. The flow of the gas was controlled using mass flow controllers. The substrate was heated with the halogen lamps that are placed just above the substrate holder in the sputtering chamber. The time to sputter approximately 100 nm of DLC:N film is about 1 Hour. The thickness of the DLC:N was measured with a profilometer and found to be 115 nm. This type of film was also sputtered at a higher temperature of 400°C.

2-2-5 Nitrogen doped Diamond like Carbon (DLC:N) on ITO

DLC:N is sputtered on top of an ITO base layer to create a transparent, conductive electrode material with excellent electrochemical properties. A graphite target (Williams Advanced Materials Inc, Buffalo, NY, USA) with 99.99% purity and 75 mm in diameter and 3 mm thick was used. Sputtering of the two films was sequential (when both the films were being sputtered in-house), without breaking the vacuum and using a multi-target sputter source with independent power supplies. For depositing DLC:N, the power supply was switched from RF to DC source. The parameters were the same for DLC:N and ITO as stated in the previous sections when describing these individual films. The thickness of the films was measured using a profilometer (Alpha step 200, Tencor, San Jose, CA, USA).

The DLC:N on ITO microelectrodes we developed exhibit desirable electrochemical properties. First, they can be fabricated by the regular sputtering process which is micro fabrication compatible. Second, they exhibit a smooth surface, which would provide lower capacitance charging current as lower double layer capacitance is suitable for electrochemical detection. Third, they are much cheaper compared with the carbon fiber electrodes (CFE) and other noble metal electrodes. Finally and most importantly, they have excellent electrochemical properties such as large working window, low noise level, small double layer capacitance, and low and stable background current and high sensitivity. In addition the DLC:N electrodes can be optically transparent if deposited around or

below 40 nm thickness. The transmittance value of such a film could be around 70% when sputtered at a temperature of 200°C.

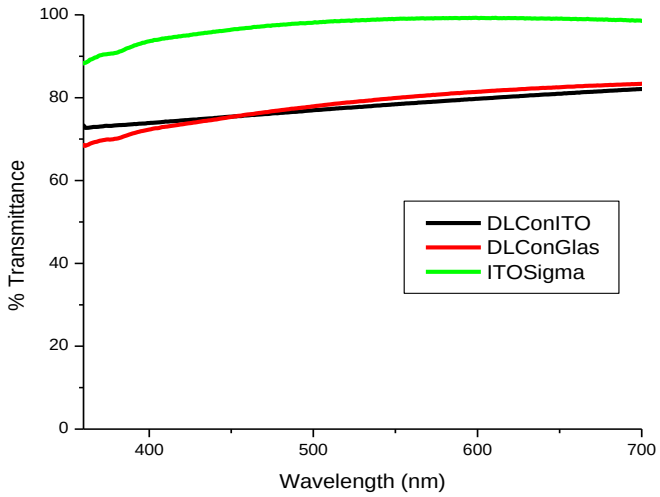

Figure 2-14 Transmittance curve for DLC:N 40 nm sputtered at 200°C on ITO 30nm. The other two transmittance curves are DLC:N on glass and ITO on glass.

The sheet resistance of such a film deposited on ITO was 96 Ω and had a resistivity of 6.7×10^{-4} Ω-cm. As these can be deposited onto normal glass slides, this is a desirable property in many biological applications as it enables viewing the cells using an inverted microscope simultaneously when performing electrochemical measurements.

For a thicker film of DLC:N, 110 nm sputtered on ITO at 200°C the transmittance values are shown in figure 2-15 are around 45%. This means that with increase in thickness the transmittance values of DLC:N on ITO will decrease. The film at even this thickness is transparent and it can be

successfully used to image cells on the electrode using a microscope. The resistivity values for DLC:N (110nm) on ITO (30nm) is 1.68×10^{-3} Ω-cm.

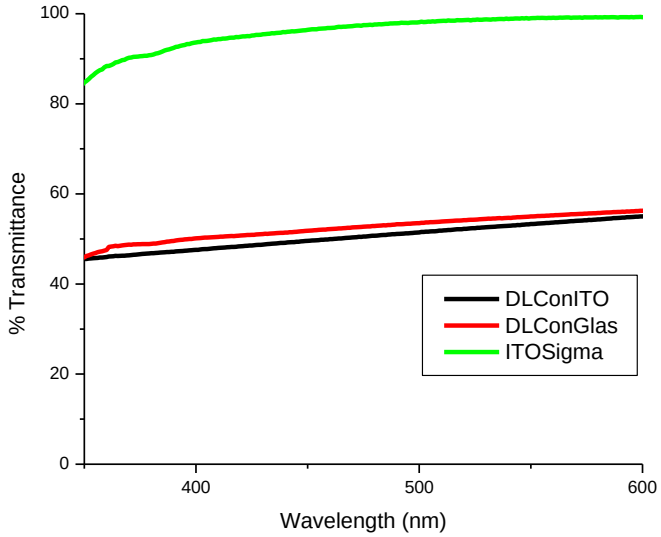

Figure 2-15 Transmittance curve for DLC:N 110 nm sputtered at 200°C on ITO 30 nm. The other two transmittance curves are DLC:N on glass and ITO on glass.

2-2-6 Surface properties by AFM

Atomic force microscopy was performed to analyze the surface properties of the deposited DLC films. Figure 2-16 shows an AFM image of DLC sputtered on a glass substrate. The as-deposited DLC film on glass has an average grain size of 5 nm and surface roughness of 1.5 nm.

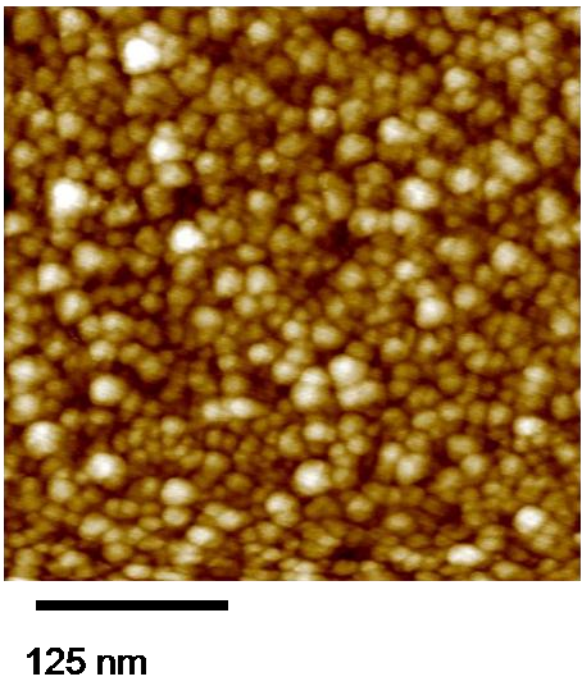

Figure 2-16 AFM image of the DLC:N film deposited on glass substrate, image shows very smooth surface and grain size of the film.

2-2-6-1 Electrical properties of the DLC:N on ITO film

A Four-point probe was used to measure the resistivity of the as-deposited DLC:N on ITO film. As we have pointed out, in electrochemical detection, it is desirable to have sensing electrodes of low resistivity to minimize the series resistance. From the four point probe the sheet resistance and the resistivity of the film can be calculated by the equation of $\rho = R_s t$ where, R_S is the sheet resistance and t this thickness of the film. The resistivity values for DLC:N (110nm) on ITO (30nm) sputtered at 200°C is 1.68×10^{-3} Ω-cm and the values for DLC:N (40nm) on ITO (30nm) were 6.7×10^{-3} Ω-cm.

2-2-6-2 Raman spectroscopy of the DLC film

Raman spectroscopy is a non-destructive technique used to characterize the structure of carbon. When light is scattered from a molecule or crystal, most photons are elastically scattered. The scattered photons have the same frequency and, therefore, wavelength, as the incident photons. However, a small fraction of light is scattered at optical frequencies different from, and usually lower than, the frequency of the incident photons. The process of inelastic scatter is termed the Raman effect. The scattering can occur with a change in vibrational, rotational or electronic energy of a molecule.

The Raman spectra of a wide range of disordered and amorphous carbons have been measured under excitation from 785 to 229 nm. The *G* peak in carbon arises from vibrations of sp^2 sites in both ring and chain configurations, and is a good indicator of disorder (Chhowalla, Ferrari, et al. 2000).

A Raman spectroscopic scan is shown in figure 2-17. The structure properties can usually be derived from the characteristics of the D peak (1355 cm^{-1}) and the G peak (1550 cm^{-1}). The broadened D peak and G peak indicate the sputtered DLC film appears to be highly disordered.

The increase in the conductivity of the nitrogen doped film has been reported due to the reasons like a downward shift of the Fermi level or the widening of the conduction band, and the density of states increase at Fermi level (Gao, Chen et al. 2008).

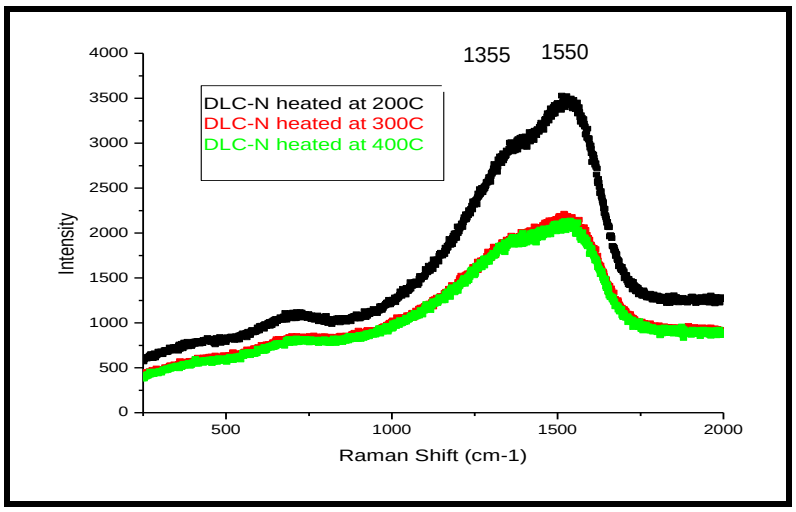

Figure 2-17 Raman spectroscopic scan of the DLC:N films on glass substrate. The broadened G, D peaks indicates the highly disordered DLC film. The spectroscopy was performed with devices annealed in an inert chamber after sputtering. The black line spectra indicate the sample annealed at 200°C whereas the red line and the green line indicate the samples annealed at 300°C and 400°C.

2-2-6-3 Electrochemical characteristics of the DLC:N on ITO macroelectrodes

Cyclic voltammetry experiments were performed on the DLC:N on ITO electrodes using the ferricyanide solution. As we can see from figure 2-18, there are obvious oxidation and reduction peaks. The peak-to-peak separation (ΔEp) values are 230 mV with a scan rate of 50 mV/s and 290 mV with a scan rate of 200 mV/s.

Scan rate: 50 mV/s

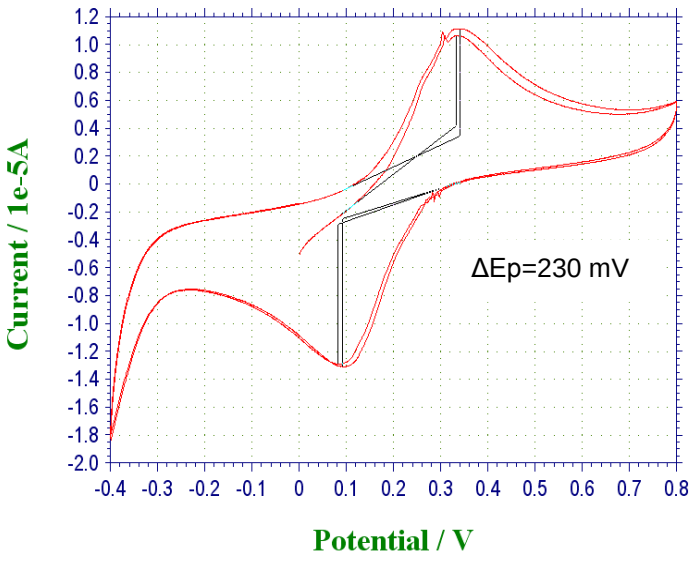

(a)

Scan rate: 200mV/s

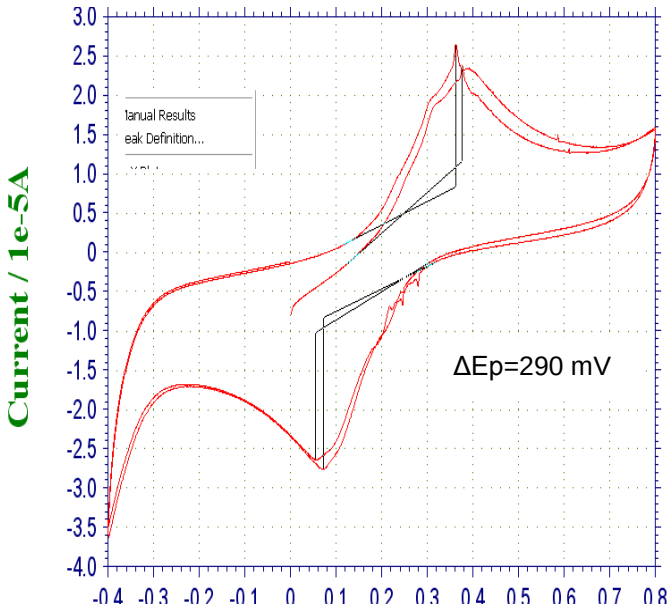

(b)

Figure 2-18 Cyclic voltammograms of with DLC:N on ITO macroelectrode on glass substrate for the 1 mM $K_3Fe(CN)_6$ in 0.1 M KCl analyte. Scan rates are 50 mV/s for a) and b) 200 mV/s.

DLC:N on ITO Microelectrode

Cyclic voltammetry experiments were performed on the DLC:N on ITO electrodes using ferricyanide solution. As we can see from figure 2-19, the peak-to-peak separation value for this microelectrode scanned at the rate of 1000mV/s is 130 mV for a 20µm electrode. The oxidation peak for the DLC:N on ITO microelectrodes are distinct, the peaks are hardly observable at slower scan rates in microelectrodes. If the scan rates are too slow the current becomes limited by the diffusion of the analyte.

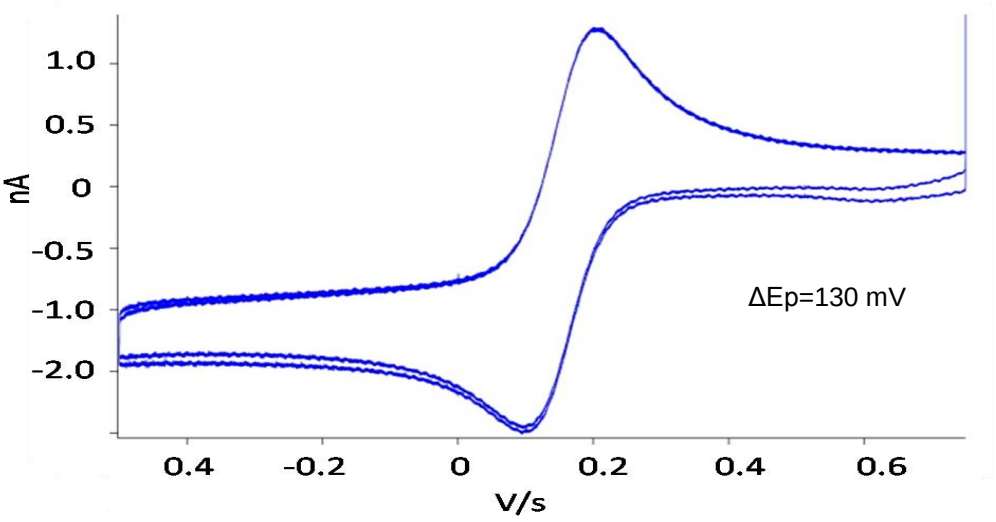

Figure 2-19 CV of DLC:N on ITO of a 20 µm electrode scanned at 1000mV/s.

2-2-6-4 CV of DLC:N on ITO (Plasma treated)

The RF plasma oxidation at ambient temperature can cause erosion of graphite and DLC films but they do not cause appreciable damage to DLC surfaces with diamond like properties. The results suggest that erosion by low energy ions is very selective to the sp^2 (and hence an increase in ΔEp values) and *sp* states compared to the sp^3 state of carbon.

It is an important step during the optimization of the etch process to make sure the erosion of the DLC:N is minimal, if any at all. It is also possible that over-exposure to plasma can cause the DLC:N film surface to become totally recluse of electro activity, so it is a good exercise to perform CV each time the surface is exposed to plasma. To make sure that the film is still present after the plasma treatment it would be better to sputter thicker layer such that it does not totally get depleted. The ΔEp value for a plasma treated DLC:N on ITO is 550 mV. This indicates the electron transfer rate has slowed considerably in comparison with the untreated DLC:N on ITO, which has ΔEp values in the 200 mV range. This could be due to the oxidation of Sp^2 states. These oxidized states may not participate in the electron transfer process resulting in an increase ΔEp value.

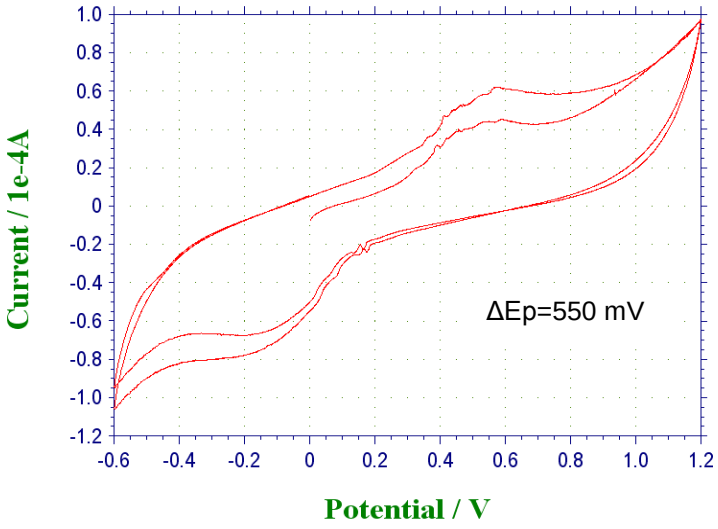

Figure 2-20 Cyclic voltammograms of the DLC:N on ITO (Plasma treated) in 1 mM $K_3Fe(CN)_6$ in 0.1 M KCl.

2-2-6-5 CV Scan of DLC:N on ITO sputtered at different temperatures

We sputtered the DLC:N on ITO substrates at different temperatures and then performed the CV measurements. Figure 2-21 depicts a CV performed at scan rate of 100 mV/s for the substrates sputtered at 200ºC, 300ºC and 4.00ºC. The ΔEp are 200 mV, 130 mV and 110 mV respectively for substrates sputtered at 200ºC, 300ºC and 400ºC. This indicates a faster electron transfer rate for the substrates sputtered at higher temperatures because of the graphitization of the film, and the resistivity decrease due the decreasing hopping distance between SP^2 clusters (Chhowalla, Ferrari, et al. 2000).

CV of DLC:N on ITO sputtered at 200ºC:

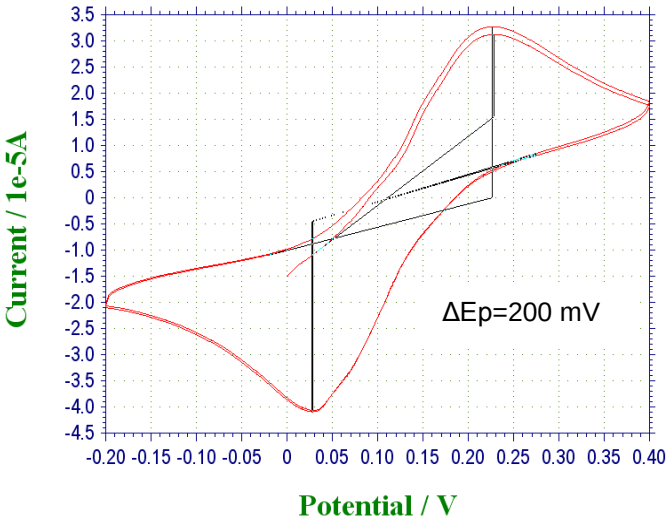

(a)

CV of DLC:N on ITO sputtered at 300ºC:

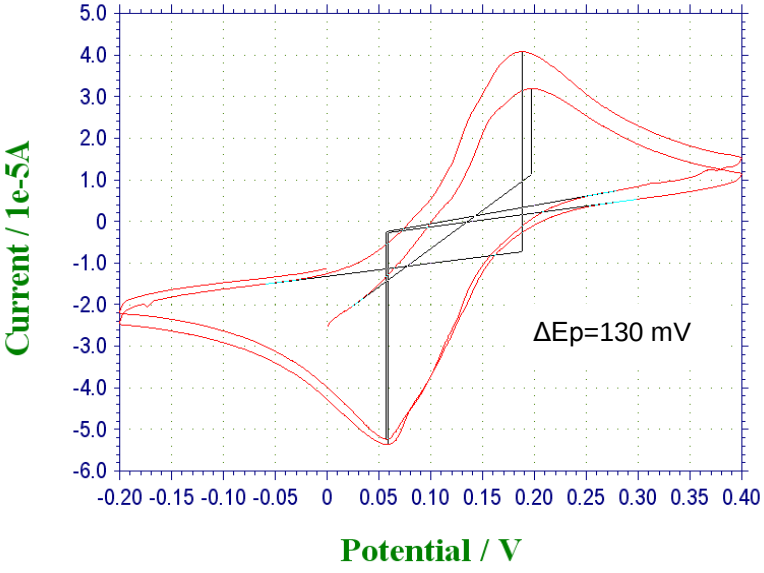

(b)

CV of DLC:N on ITO sputtered at 400ºC

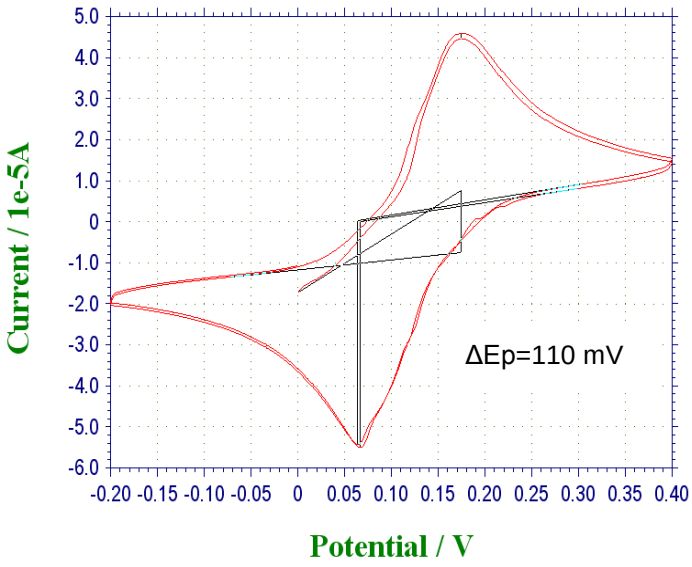

(c)

Figure 2-21 Cyclic voltammograms of the DLC:N on ITO 1 mM $K_3Fe(CN)_6$ in 0.1 M KCl with substrate annealed at different temperatures. a), b) and c) are all have a scan rate of 100 mV/s but have been heated at 200°C, 300°C and 400°C respectively.

2-2-6-6 Resistivity and ΔEp values for the DLC:N sputtered at different temperatures with same deposition conditions and time

The DLC:N on ITO samples sputtered at higher temperatures was found to have lower resistivity values. The decreased ΔEp (mV) values indicate a faster electron transfer rate. This is the result of DLC:N on ITO deposited at higher

temperatures. The deposition at higher temperature leads to graphitization of carbon films and hence high conductivity. Deposition above 200°C causes a sharp decrease in sp^3 bonding (Chhowalla, Robertson et al. 1997). In fact films deposited at 400°C show incorporation of nanocrystalline graphite (Chhowalla, Ferrari et al. 2000).

DLC:N on ITO	Substrate heated at Temperature (ºC)	Resistivity Ω-cm	ΔEp (mV)
	200°C	1.20×10-3	200
	300°C	1.00×10-3	130
	400 ºC	8.4×10 -4	110

Table 2-2 Resistivity and peak-to-peak separation values for film sputtered at different temperatures.

2-2-7 Specific capacitance of electrode materials

There are two methods to measure the specific capacitance of a microelectrode. One way is to find the capacitive current of the electrode using the cyclic voltammetry, and since the scan rate at which the sample is being scanned is known, the capacitance can be calculated using the formula $C = \Delta i / 2\omega$, where Δi is the capacitive current difference between the forward scan and the reverse scans, and ω is the scan rate. Another method is to apply sine wave excitation voltage and calculate the capacitance from the resulting sinusoidal current using Pulse software. The typical specific capacitance values measured for an electrode area of 400 μm^2 are 9 $\mu F/cm^2$ for an ITO electrode, 12.5 $\mu F/cm^2$ for Au electrode, 17.5 $\mu F/cm^2$ for DLC:N on ITO electrode and 25 $\mu F/cm^2$ for an Pt electrode deposited and patterned by the similar process in our lab.

2-2-8 Platinum

Platinum of thickness 100 nm was deposited by supplying an RF power of 200W to a platinum target. The Argon flow rate was 20 sccm under chamber pressure of 4 mTorr and the deposition was carried out at ambient temperature. Depositions of 3 min will a 30 nm thin film. A layer of titanium is deposited at 100 watts with 20 sccm of argon flow at 4 mTorr. A deposition time of 12 minutes gives a 20 nm thick film. The ΔEp values are 115 mV for a sample scanned at 100mV/s and 155 mV for a sample scanned at 200 mV.

Macroelectrode: *CV of Pt (30 nm)*

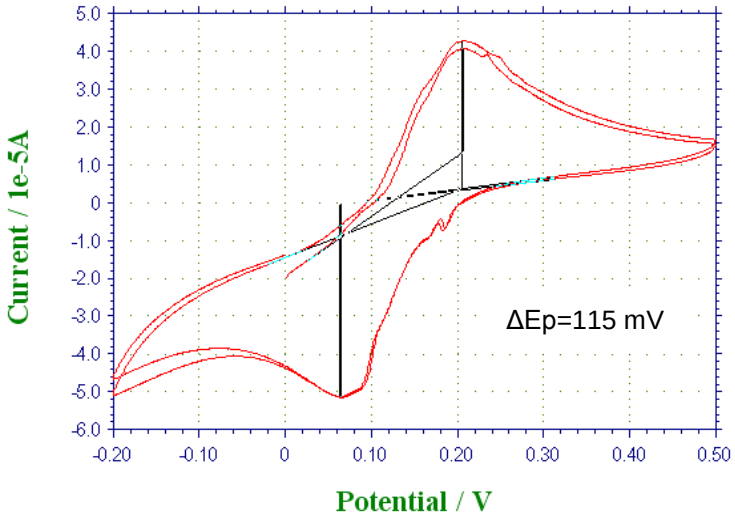

(a)

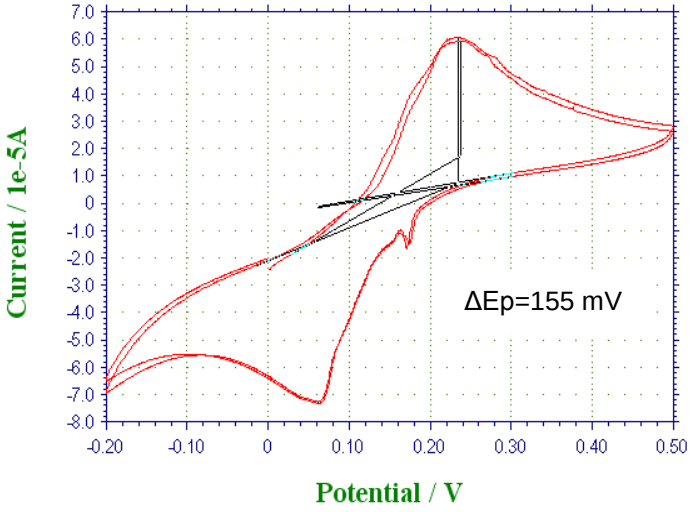

(b)

Figure 2-22 CV of platinum macro electrode with a) scan rate of 100mV/s and b) scan rate of 200 mV/s.

2-2-9 Gold

Gold deposition requires an adhesion layer of Titanium. This base layer of 50nm was deposited by supplying RF power of 100 W to a Titanium target, with an Argon flow rate of 30 sccm, a chamber pressure of 4 mTorr and the deposition was carried out at ambient temperature. Gold deposition was done without breaking the vacuum at the same chamber pressure, substrate temperature and Argon flow rate by switching the RF power supply of 100 W to the gold target. The thickness of the Gold film was 100 nm. The ΔEp value for a sample scanned at 100 mV/s is 100mV and the sample scanned at 200mV/s has a peak-to-peak separation value of 120 mV.

Macroelectrode: *CV of Gold device*

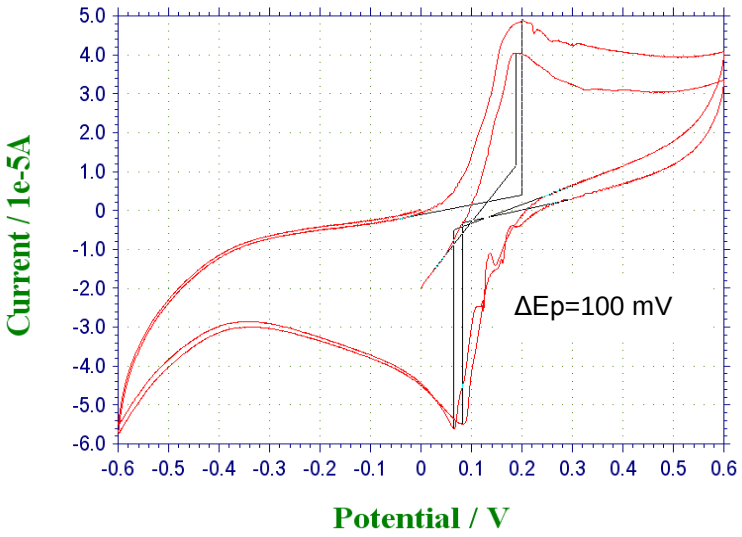

(a)

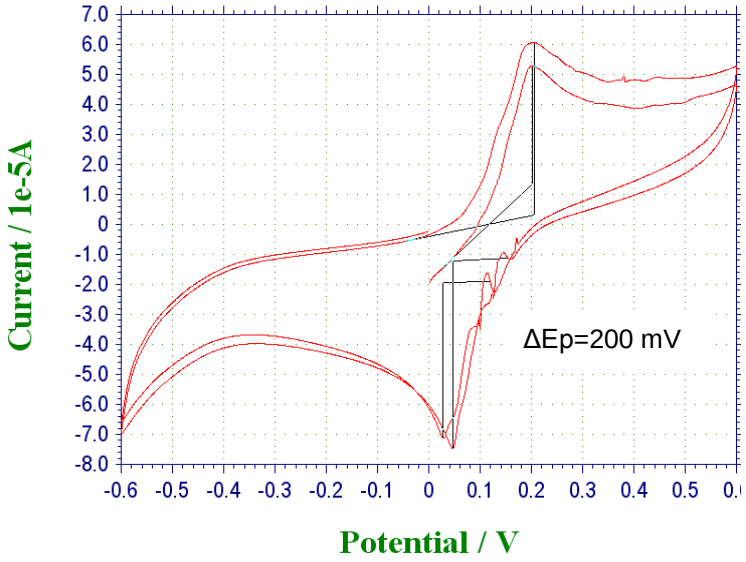

(b)

Figure 2-23 CV of Gold macro electrode with a) scan rate of 100mV/s, b) scan rate of 200 mV/s, and c) 500mV/s.

Microelectrode

The microelectrode of diameter 20µm scanned at a rate of 1000mV/s has a peak-to-peak separation of 70 mV.

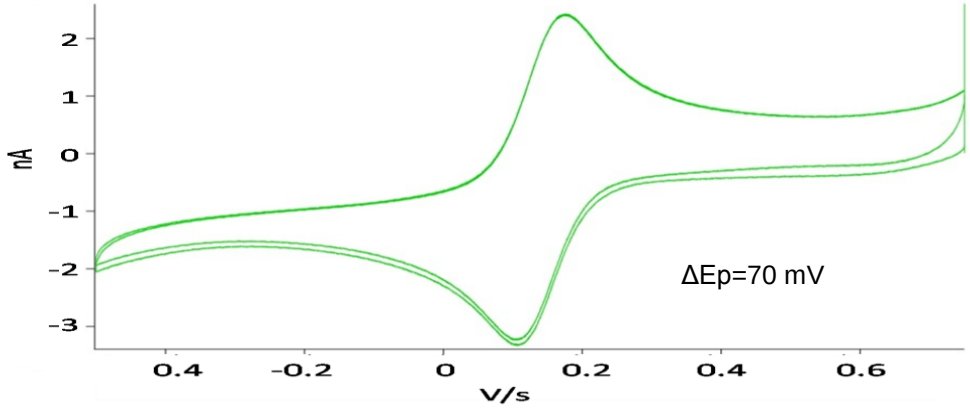

Figure 2-24 CV of Gold microelectrode with scan rate of 1000 mV/s.

2-2-10 Teflon AF film

Teflon 1600 AF is from a family of amorphous fluoropolymers (Mihailov and Lazare 1993; Ding, Wang et al. 2001). These polymers are soluble in specific solvents for that particular type of the Teflon series. These films have excellent mechanical, electrical and optical properties (Resnick and Buck 2002). They can be made into thin films by spin coating (Mayer, Kriebel et al. 2003). This solution also can be used to dip coat as well. These films can withstand high temperatures and can be cured to make durable films. The advantage of using a Teflon films is that it is transparent, completely inert and totally biocompatible (Resnick 1989; Makohliso, Giovangrandi et al. 1998). We use Teflon AF 1600 series which can give very thin films when spin coated. Actually, the viscosity of the solution can be determined by using the percentage of Teflon pellets in the dissolving solvent. The more the percentage of Teflon pellets the more viscous the solution is. Teflon films can easily withstand temperatures of up to 300°C for the 1600 series. These properties vary depending on the series of Teflon AF used.

Teflon films on the glass substrates were prepared by spin coating 5% FSM 660 (Fluor alkyl monosilane), (Cytonix, Bethesda, MD USA), as an adhesion layer at 3500 rpm for 30 seconds on glass slides followed by baking at 100 ºC for 10 min. 2% Teflon AF (DuPont, Wilmington, DE, USA) in FC-75 and FC-770 solvent (3M, MN, USA) solution was then spun on it at 3000 rpm for 30 s

followed by baking in three steps: 115 ºC for 15 min, 230 ºC for 15 min and 300 ºC for 2hr.

2-2-10-1 Patterning of Teflon

For patterning Teflon AF, substrates were spin coated at 3000 rpm with S 1813 (Rohm and Haas, USA) photoresist for 30 seconds followed by a bake of 1 min. This process was repeated another time to cover any pin holes that remained on the substrate after the first coat of photoresist. Transparency masks (Output City, OR, USA) were used to pattern the Teflon-coated substrate using mask alligner (OAI Model 200 IR) with UV exposure of 14 sec. The photoresist was developed with MF 321 (Rohm and Haas, USA) developer for 1 min 40 sec, washed with DI water and blow dried with air to remove the moisture.

The 2% Teflon film was etched with two different protocols: In the first protocol, the Teflon film was RIE etched using 1000 watt power, 20 sccm of CF_4, 20 sccm of CHF3 at 250 mTorr pressure. The time it took to etch the 220nm film was about 20 sec, in the second protocol the Teflon film with thickness of 220 nm was RIE etched using 500 watt power, 50 sccm of oxygen gas at 250 mTorr pressure. The time it took to etch the 220nm film was about 22 sec. The etch rate is 10 nm/sec.

Though both the processes can be used to etch Teflon, the protocol using the RIE with oxygen gives a much cleaner etch and is gentler to the underlying electrode surface.

2-2-11 PDMS gasket processing

The PDMS gaskets were made of poly (dimethyl siloxane) (PDMS, Dow Corning Corp., Midland, MI USA). The curing agent was mixed with the monomer in a ratio of 1:20, or sometimes 1:10. It was left in the atmosphere for an hour, until all bubbles are removed. The mixture I was then baked in an oven at 60 °C for 45 minutes to make a thick slab. The slab was cut into wells by using a using a hollow punch with diameters of 3 mm or sometimes just holes of small dimensions are cut using a blade.

References

Arnell, R. D. and P. J. Kelly (1999). "Recent advances in magnetron sputtering." Surface and Coatings Technology **112**(1-3): 170-176.

Banovec, A. and M. Kern "Comparison between chemical and pulsed laser etching of indium tin oxide thin films." Vacuum **43**(5-7): 737-739.

Beensh-Marchwicka, G., L. Kròl-Stepniewska, et al. (1982). "Effect of the oxygen pressure during sputtering on the properties of thin CuOx films." Thin Solid Films **88**(1): 33-39.

Burda, C., Y. Lou, et al. (2003). "Enhanced Nitrogen Doping in TiO2 Nanoparticles." Nano Letters **3**(8): 1049-1051.

Dayton, M. A., J. C. Brown, et al. (1980). "Faradaic electrochemistry at microvoltammetric electrodes." Analytical Chemistry **52**(6): 946-950.

de Sande, J. C. G., C. N. Afonso, et al. (1992). "Optical properties of laser-deposited a-Ge films: a comparison with sputtered and e-beam-deposited films." Appl. Opt. **31**(28): 6133-6138.

Ferrari, A. C. "Determination of bonding in diamond-like carbon by Raman spectroscopy." Diamond and Related Materials **11**(3-6): 1053-1061.

Ferrari, A. C. and J. Robertson (2001). "Resonant Raman spectroscopy of disordered, amorphous, and diamondlike carbon." Physical Review B **64**(Copyright (C) 2010 The American Physical Society): 075414.

Ferreira, N. G., L. L. G. Silva, et al. (2002). "Kinetics study of diamond electrodes at different levels of boron doping as quasi-reversible systems." Diamond and Related Materials **11**(8): 1523-1531.

Ganesh, V., S. K. Pal, et al. (2006). "Self-assembled monolayers (SAMs) of alkoxycyanobiphenyl thiols on gold--A study of electron transfer reaction using cyclic voltammetry and electrochemical impedance spectroscopy." Journal of Colloid and Interface Science **296**(1): 195-203.

Gao, Y., X. Chen, et al. (2008). "Magnetron sputtered diamond-like carbon microelectrodes for on-chip measurement of quantal catecholamine release from cells." Biomed Microdevices **10**(5): 623-629.

Grill, A. (1993). "Review of the tribology of diamond-like carbon." Wear **168**(1-2): 143-153.

Grill, A. (1999). "Electrical and optical properties of diamond-like carbon." Thin Solid Films **355-356**: 189-193.

Hawley, M. D. and S. W. Feldberg (1966). "Nuances of the ECE Mechanism. I. Development of the Theoretical Relationships for Chronoamperometry1a." The Journal of Physical Chemistry **70**(11): 3459-3464.

Hellgren, N., M. P. Johansson, et al. (1999). "Role of nitrogen in the formation of hard and elastic CNx thin films by reactive magnetron sputtering." Physical Review B **59**(Copyright (C) 2010 The American Physical Society): 5162.

Joshi, R. N., V. P. Singh, et al. (1995). "Characteristics of indium tin oxide films deposited by r.f. magnetron sputtering." Thin Solid Films **257**(1): 32-35.

Kaufman, J. H., S. Metin, et al. (1989). "Symmetry breaking in nitrogen-doped amorphous carbon: Infrared observation of the Raman-active G and D bands." Physical Review B **39**(Copyright (C) 2010 The American Physical Society): 13053.

Kelly, P. J. and R. D. Arnell (2000). "Magnetron sputtering: a review of recent developments and applications." Vacuum **56**(3): 159-172.

Khanna, A., D. G. Bhat, et al. (2006). "Growth and characterization of chromium oxide thin films prepared by reactive ac magnetron sputtering." Journal of Vacuum Science & Technology A: Vacuum, Surfaces, and Films **24**(5): 1870-1877.

Kim, D. S., T. E. Fischer, et al. (1991). "The effects of oxygen and humidity on friction and wear of diamond-like carbon films." Surface and Coatings Technology **49**(1-3): 537-542.

Laux, S., N. Kaiser, et al. (1998). "Room-temperature deposition of indium tin oxide thin films with plasma ion-assisted evaporation." Thin Solid Films **335**(1-2): 1-5.

Laviron, E. (1979). "A.C. polarography and faradaic impedance of strongly adsorbed electroactive species: Part I. Theoretical and experimental study of a quasi-reversible reaction in the case of a Langmuir isotherm." Journal of Electroanalytical Chemistry **97**(2): 135-149.

Lindgren, T., J. M. Mwabora, et al. (2003). "Photoelectrochemical and Optical Properties of Nitrogen Doped Titanium Dioxide Films Prepared by Reactive DC Magnetron Sputtering." The Journal of Physical Chemistry B **107**(24): 5709-5716.

Mailly, F., A. Giani, et al. (2001). "Anemometer with hot platinum thin film." Sensors and Actuators A: Physical **94**(1-2): 32-38.

Mardare, D., M. Tasca, et al. (2000). "On the structural properties and optical transmittance of TiO2 r.f. sputtered thin films." Applied Surface Science **156**(1-4): 200-206.

May, C. and J. Strümpfel (1999). "ITO coating by reactive magnetron sputtering-comparison of properties from DC and MF processing." Thin Solid Films **351**(1-2): 48-52.

Miyake, H., S. Ye, et al. (2002). "Electroless deposition of gold thin films on silicon for surface-enhanced infrared spectroelectrochemistry." Electrochemistry Communications **4**(12): 973-977.

Musil, J., J. Lestina, et al. (2001). "Pulsed dc magnetron discharge for high-rate sputtering of thin films." Journal of Vacuum Science & Technology A: Vacuum, Surfaces, and Films **19**(2): 420-424.

Nagaoka, T. and T. Yoshino (1986). "Surface properties of electrochemically pretreated glassy carbon." Analytical Chemistry **58**(6): 1037-1042.

Nicholson, R. S. (1965). "Theory and Application of Cyclic Voltammetry for Measurement of Electrode Reaction Kinetics." Analytical Chemistry **37**(11): 1351-1355.

O'Dea, J. J. and J. G. Osteryoung (1993). "Characterization of quasi-reversible surface processes by square-wave voltammetry." Analytical Chemistry **65**(21): 3090-3097.

Palshin, V., E. I. Meletis, et al. (1995). "Characterization of ion-beam-deposited diamond-like carbon films." Thin Solid Films **270**(1-2): 165-172.

Resnick, P. and W. Buck (2002). Teflon® AF: A Family of Amorphous Fluoropolymers with Extraordinary Properties**:** 25-33.

Resnick, P. R. (1989). "The preparation and properties of a new family of amorphous fluoropolymers: teflon® AF." Journal of Fluorine Chemistry **45**(1): 100-100.

Pihel, K., Q. D. Walker, et al. (1996). "Overoxidized Polypyrrole-Coated Carbon Fiber Microelectrodes for Dopamine Measurements with Fast-Scan Cyclic Voltammetry." Analytical Chemistry **68**(13): 2084-2089.

Robertson, J. (1993). "Deposition mechanisms for promoting sp3 bonding in diamond-like carbon." Diamond and Related Materials **2**(5-7): 984-989.

Ruske, F., V. Sittinger, et al. (2005). "Hydrogen doping of DC sputtered ZnO:Al films from novel target material." Surface and Coatings Technology **200**(1-4): 236-240.

Scharf, T. W., R. D. Ott, et al. (1999). "Structural and tribological characterization of protective amorphous diamond-like carbon and amorphous CN[sub x] overcoats for next generation hard disks." Journal of Applied Physics **85**(6): 3142-3154.

Schiller, S., G. Beister, et al. (1984). "Reactive high rate D.C. sputtering: Deposition rate, stoichiometry and features of TiOx and TiNx films with respect to the target mode." Thin Solid Films **111**(3): 259-268.

Sigmund, P. (1969). "Theory of Sputtering. I. Sputtering Yield of Amorphous and Polycrystalline Targets." Physical Review **184**(Copyright (C) 2010 The American Physical Society): 383.

Silva, S. R. P. and G. A. J. Amaratunga (1995). "Doping of rf plasma deposited diamond-like carbon films." Thin Solid Films **270**(1-2): 194-199.

Sreenivas, K., M. Sayer, et al. (1989). "Properties of D.C. magnetron-sputtered lead zirconate titanate thin films." Thin Solid Films **172**(2): 251-267.

Teixeira, V., H. N. Cui, et al. (2002). "Amorphous ITO thin films prepared by DC sputtering for electrochromic applications." Thin Solid Films **420-421**: 70-75.

Thornton, J. A. (1974). "Influence of apparatus geometry and deposition conditions on the structure and topography of thick sputtered coatings." Journal of Vacuum Science and Technology **11**(4): 666-670.

Wen-Fa, W. and et al. (1994). "Effect of sputtering power on the structural and optical properties of RF magnetron sputtered ITO films." Semiconductor Science and Technology **9**(6): 1242.

Williams, P. (1979). "The sputtering process and sputtered ion emission." Surface Science **90**(2): 588-634.

Yang, C.-Y., S. E. Babcock, et al. (1998). "Microstructure of electron-beam-evaporated epitaxial yttria-stabilized zirconia/CeO2 bilayers on biaxially textured Ni tape." Physica C: Superconductivity **307**(1-2): 87-98.

http://www.basinc.com/mans/EC_epsilon/Techniques/CycVolt/cv_analysis.html

CHAPTER 3

DEVICE MICROFABRICATION

3-1 Overview of patterning using photolithography

As discussed in chapter 2, DLC:N on ITO is an appropriate, cytophilic material for making electrodes, whereas Teflon AF is an appropriate cytophobic material for insulating inactive areas of the chip. This chapter describes the process I developed to fabricate a fully functional microdevice using these materials.

Fabrication of such devices is best performed in extremely clean environments, hence handling and storage become integral parts of this process. Most of the microfabrication is done in some kind of a clean room. I had access to a class 100 clean room in our facility. A class 100 room must meet the specification that there are less than 100 particles per cubic foot with a size greater than 5 μm.

Photolithography is a process for transferring a pattern with micron-sized features onto a substrate using selective illumination, as shown in figure 3-1. The first step is to design a photomask with the desired pattern. The photomask is laid out using software such as autocad or adobe illustrator. Once the design is ready, the photomask is fabricated using either a printing process (in the case of low-cost transparency soft masks) or e-beam lithography to make a high-resolution hard mask. The size of the smallest feature on the pattern sets the

minimum resolution, which is sometimes specified in dpi (dots per inch). For printing a 20 µm size feature on a transparency, a resolution of at least 20,000 dpi is needed (Deng, Tien et al. 1999; Michel, Bernard et al. 2001; Linder, Wu et al. 2003; Du, Lo et al. 2008). The maximum resolution currently available for transparency photomasks is 25,000 dpi (Deng, Tien et al. 1999) and the approximate cost of printing a pattern on an A4-sized transparency is $ 150 (http://www.outputcity.com/).

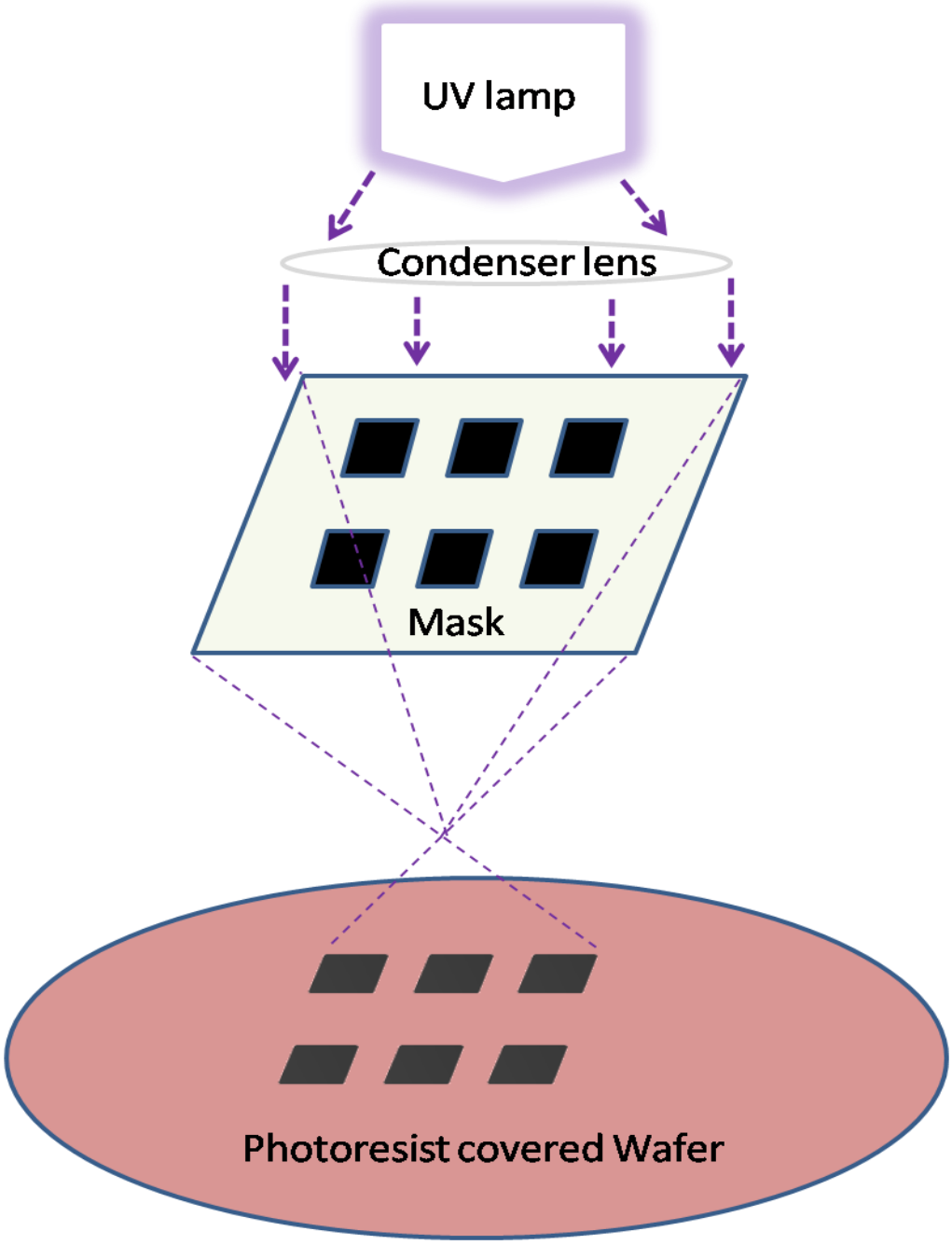

Figure 3-1 Process of photolithography.

The substrate is cleaned to eliminate organic and inorganic impurities from the surface. An ultraviolet light (UV) sensitive polymer, known as photoresist, is spin coated onto the substrate. The substrate is soft baked to remove solvents from the photoresist. The patterned mask is placed on this polymer-coated substrate. When UV light is exposed on this mask, the structure of the photoresist is chemically changed in the areas where the light passes through the mask. In the case of a positive photoresist, the exposed material becomes more soluble and is removed when the substrate is immersed in the developer solution. Following development, the sample is rinsed and dried.

There are two ways of transferring the photoresist pattern, to pattern other materials on the device. In the lift-off process, a film is deposited on top of the patterned photoresist. The underlying photoresist is then removed in a stripping solution, which also selectively removes the overlying film. An alternative approach is to pattern photoresist on top of the film to be patterned. Then an etching process is used to selectively remove regions of the film that are not protected by overlying photoresist.

3-2 Detailed fabrication process

Reagents: S1813 positive photoresist (Rohm & Hass, PA, USA), MF-321 developer (Rohm & Hass, PA,USA), PDMS (Sylgard 184, Dow Corning, MI, USA), Teflon (Dupont, USA), FC-770 (3M, MN , USA), acetone, isopropanol, sulphuric acid, phosphoric acid and all other reagents were obtained from (Sigma Aldrich, MO, USA) unless otherwise noted.

Equipment: A CEE model 100 CB was used for spin coating (Brewer science, MO, USA), the mask alligner / exposure system was model 200IR (OAI, CA, USA), conductive films were sputtered using an ATC 2000-V sputtering system (AJA international, Inc, MA, USA) and etching of Teflon AF was carried out using RIE with a Precision 5000 mark II (Applied materials Inc., CA, USA),. An inverted microscope (Olympus, model IX-50, USA), was used for imaging cells whereas amperometric measurements were carried out using an EPC-9 potentiostat amplifier (HEKA Electronik, Lambrecht, Germany).

3-2-1 Fabrication Process

Borosilicate/glass slides, 25×75 mm, were cleaned with acetone, isopropanol and DI water. The substrate was then cleaned using sulphuric acid and phosphoric acid in a ratio of 4:1 for 10 min. The substrate was blow dried with air and left on a hot plate for two minutes to remove the moisture.

Indium tin oxide (ITO, target from Kurt J. Lesker, Pittsburg PA, USA) was sputter deposited (ATC 2000-V, AJA international, Inc, MA, USA) using 180 watts RF power, with inflow of argon at 20 sccm and a pressure of 4 mTorr for 20 mins at 50ºC to obtain a film thickness of ~100 nm. Without breaking the vacuum, diamond-like carbon (DLC), was subsequently deposited using 300 watts DC power, a pressure of 2 mTorr, Ar flow of 10 sccm, N2 flow of 2 sccm and a temperature 200°C for 1 hr. The thickness of the film is ~110 nm. In some

cases the ITO-coated slides were purchased commercially (Sigma-Aldrich, St. Louis, MO USA).

The conductive films were patterned using photolithography. S1813 positive photoresist (Rohm & Hass, PA,USA) was spin coated (CEE Model 100, Brewer Science,MO, USA) onto the substrate at 3000 rpm with an acceleration of 1100 rpm for 30 s. The substrate was then heated at 115 ºC on a hot plate for 2 min. A transparency photomask photoplotstore.com and/or outputcity.com) was used with a mask aligner (OAI Model 200 IR San Jose, CA, USA) and illuminated with ~10.5 mW/cm^2 UV light for 14 sec. The photoresist was developed with MF 321 (Rohm & Hass, PA,USA), washed with DI water and blown dry with compressed air. The photoresist was subsequently post-baked on the hot plate for about 3 min.

The DLC:N was etched for ~ 30 s using oxygen plasma RIE with a power of 500 watts, and a flow of 50 sccm O_2 (Precision 5000 mark II Applied Materials, CA, USA). The ITO thin film was then wet etched for ~100 s using 37% HCl. The substrate was thoroughly washed with DI water and then dipped in acetone to lift-off the photoresist and exposes the patterned DLC:N on ITO.

An adhesion layer of FSM 600 (Cytonix, MD, USA), 5% by volume in ethanol, was spin-coated onto the device at 3500 rpm for 30 s and then baked on a hotplate for 10 min at 95ºC. Teflon AF-1600 pellets (DuPont, DE, USA) were dissolved (2% wt/wt) in FC-75 or FC-770 (3M, MN, USA). Teflon pellets were sonicated in the solvent at 40ºC for 1 hour or until the solution was totally clear.

Alternatively, a 6% Teflon solution obtained from DuPont was diluted to 2%. The 2% Teflon solution was spin coated on the device at 3000 rpm for 30 s followed by baking on a hot plate at 115ºC for 15 min. Subsequently the temperature was increased to 225 ºC for another 15 min and then to 300 ºC for 1 hr. Following cooling, the Teflon-coated substrate was rinsed with acetone and heated to 95 ºC for 2 min.

S1813 photoresist was spin coated on the Teflon-coated device and baked as previously described. Sometimes multiple coatings were required to totally cover the Teflon. A second photomasks determined the pattern of openings in the Teflon that serve as electrode / docking sites or connection pads. The photoresist was exposed through the mask for 14 s using the mask aligner and developed with MF 321. Openings in Teflon were made using RIE at 500 W, a pressure of 250 mTorr pressure and a gas flow rate of 50 sccm O_2. It took ~17 sec to etch at a 2% film of Teflon with an average thickness is 250 nm. Subsequently the S1813 photoresist was removed using acetone followed by washing with ethanol and DI water and then blown dry with compressed air.

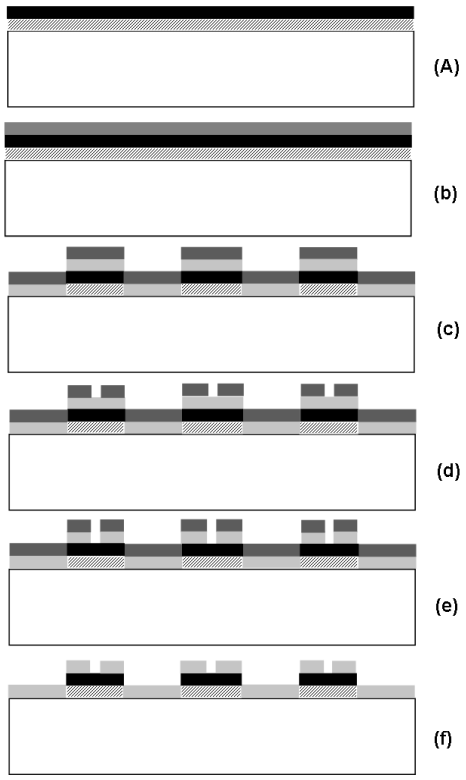

Figure 3-2 a) DLC:N sputtered on an ITO coated glass substrate, b) photoreist spin coated, c) DLC:N on ITO films etched and coated with teflon and photoresist, d) photoresist patterned on Teflon, e) Teflon film etched and f) photoresist lif-off for a final device.

3-2-2 Images of a patterened device

Figure 3-2 shows a fabricated device. The electrodes were arranged in clusters of ten in order to allow imaging of each cluster in a single field of view when using a 40X objective lens on an inverted microscope. There are 4 clusters on each device, for a total of 40 electrodes,.

(a) (b) (c)

Figure 3-3 Images of the electrode / docking sites on the fabricated device.

3-2-3 Device Layout and Connectivity

Connection pads (3 mm × 3 mm) for each of the 40 electrodes are laid out on the edge of the chip (figure 2a), whereas the working electrodes / docking sites are laid out in 4 sets of 10 near the center of the chip (figure 2b). Each set of 10 electrodes is arranged in a square pattern that can fit within the field of view of a 40X microscope objective lens. The device is placed in a custom-built holder that mounts on the microscope stage (figure 2c). A plastic cover containing numbered holes facilitates connecting a metal pin to the desired electrode. The metal pin, in turn, is connected to the headstage of an EPC-9 potentiostat amplifier. A PDMS

gasket serves to hold the drop of solution containing cells over the working electrode. A Ag/AgCl wire is placed in the drop of solution to serve as the ground / reference electrode.

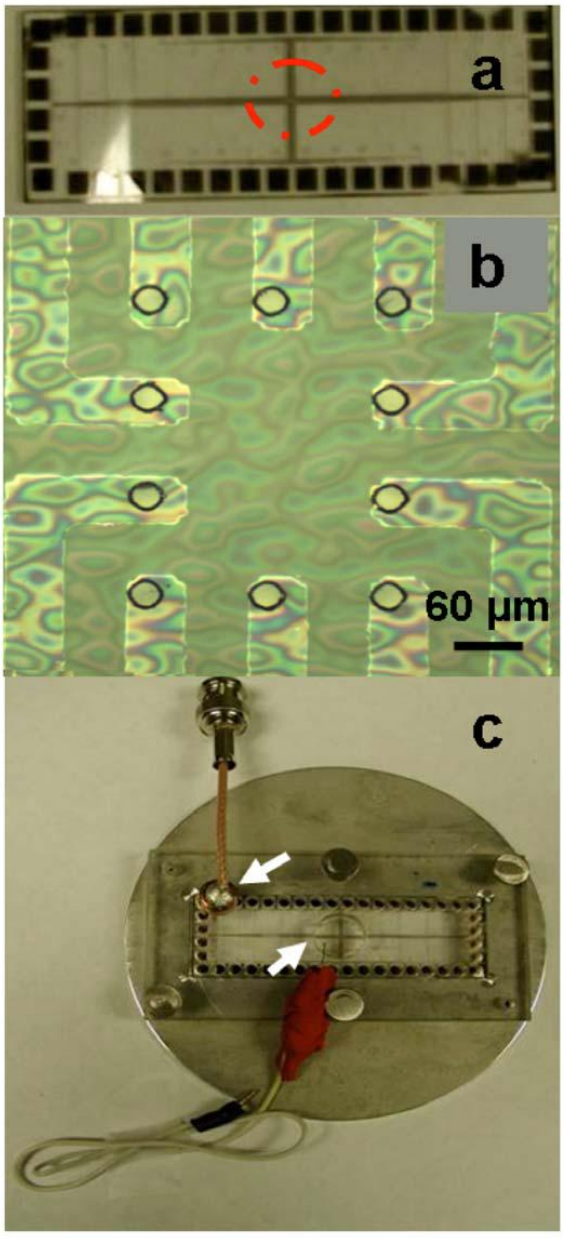

Figure 3-4 Photos of device and recording configuration. a) a microfabricated device of dimensions 25×75 mm with 40 microelectrodes in the center of the device (dashed circle). Connection to the chip is made via the connection pads arranged around the circumference of the chip, b) photomicrograph of the center of the chip depicting one of the four sets of 10 microelectrode / docking sites, c) Photo of chip in custom-made holder which facilitates connection of the amplifier input to a connection pad (upper arrow) and insertion of a Ag/AgCl ground / reference electrode in the drop of solution confined to the middle part of the chip (lower arrow). The chip plus holder is placed on an inverted microscope to observe cell docking to electrodes.

3-3 Troubleshooting

The following table was created to aid in troubleshooting the fabrication process.

Problem	Possible Reason	Solution
Opaque areas on the glass slide	Acetone has dried or slide not thoroughly cleaned	Blow dry as soon as the substrate is rinsed
Pin holes on the photoresist	Photo resist has expired or there were bubbles on the substrate	Prevent bubbles while putting photoresist on the substrate. Order a new photoresist if expired
Photoresist lifts off unintended	Substrate over/under exposed. Inadvertent spill of a drop of some other solvent during the process in the developer.	Check the power of the lamp and figure the exact time. Change the developer
Sputtered electrode peels off or does not give the intended electrical or electrochemical results	Substrate not properly developed. Excess sonication. Sputtering chamber contaminated hence bad deposited electrode.	If the problem is limited to a substrate or two then other substrates can be used or else pattern a new set of substrates. Don't leave sonication unattended. Clean the sputtering chamber.
Non transparent or rough Teflon film	Teflon granules not fully dissolved in the solvent	Sonicate Teflon granules enough such that the solution

		is totally clear.
Teflon or electrode surface is damaged after RIE	Bad correlation between plasma power and etch time. Non uniform coating of photoresist on Teflon	Optimize the etching time precisely. Depends on the thickness of the Teflon film and etch parameters like power, gas content, etc.
Cells do not adhere well enough on the docking areas after appropriate time to settle down	Cells might be unhealthy. If primary cells are being used, they vary from time to time	Use healthy cells. Use a different batch of primary cells.
Absence of electrochemical activity during recording	Teflon is not completely etched or the areas have been etched too much that there are no more microelectrodes present	Before beginning actual cell recordings it is advisable to do a cyclic voltammetry recording using ferricyanide as a test analyte to check the responsiveness of the electrode.

Table 3-1 shows some possible issues that could be faced during the process of fabricating the device and how to overcome them.

References

Deng, T., J. Tien, et al. (1999). "Using Patterns in Microfiche as Photomasks in 10-μm-Scale Microfabrication." Langmuir **15**(19): 6575-6581.

Du, Y., E. Lo, et al. (2008). "Method of Bottom-Up Directed Assembly of Cell-Laden Microgels." Cellular and Molecular Bioengineering **1**(2): 157-162.

Linder, V., H. Wu, et al. (2003). "Rapid Prototyping of 2D Structures with Feature Sizes Larger than 8 μm." Analytical Chemistry **75**(10): 2522-2527.

Michel, B., A. Bernard, et al. (2001). "Printing meets lithography: soft approaches to high-resolution patterning." IBM J. Res. Dev. **45**(5): 697-719.

http://www.outputcity.com

CHAPTER 4

TARGETING OF CELLS TO ELECTRODE DOCKING SITES

Selective targeting of cells to electrodes is desired so that, ideally, every electrode has a cell adhered in order to be able to collect data. It is desirable that only a single cell is near each electrode so that extra cells do not introduce a significant amperometric background current. INS-1 cells were used in early experiments as a readily available cell line to test for specific targeting of cells to electrode docking sites in our novel DLC:N / Teflon microdevice. This was followed by experiments with bovine adrenal chromaffin cells that secrete electroactive catecholamine's.

4-1 Selective targeting of INS-1 cells to electrode docking sites

The cytophilic (DLC:N) and the cytophobic (Teflon AF) properties on the surface of this microfbarictaed bio-chip can be seen in the following images. The first image on the left in figure 4-1 shows cells loaded and before wash. Some cells come together and form clumps when they are unable to find a suitable surface to adhere to, others are weakly adhered to the surface, whereas other cells are floating in the cell medium. After a gentle wash, as seen in the middle image, the cells which are docked to the electrodes stay in place, while most of the excess cells are washed away. Washing multiple times decreases the density of cells on the Teflon (cytophobic) surface, but care has to be taken about how aggressively the device is washed. The cells on the electrodes could also be

washed away along with the cells on insulating material. The image on the right shows a totally clean device following repetitive washes which can be reused. Thorough cleaning of the device before reuse is carried out by washing it with acetone and ethanol or with a mild detergent.

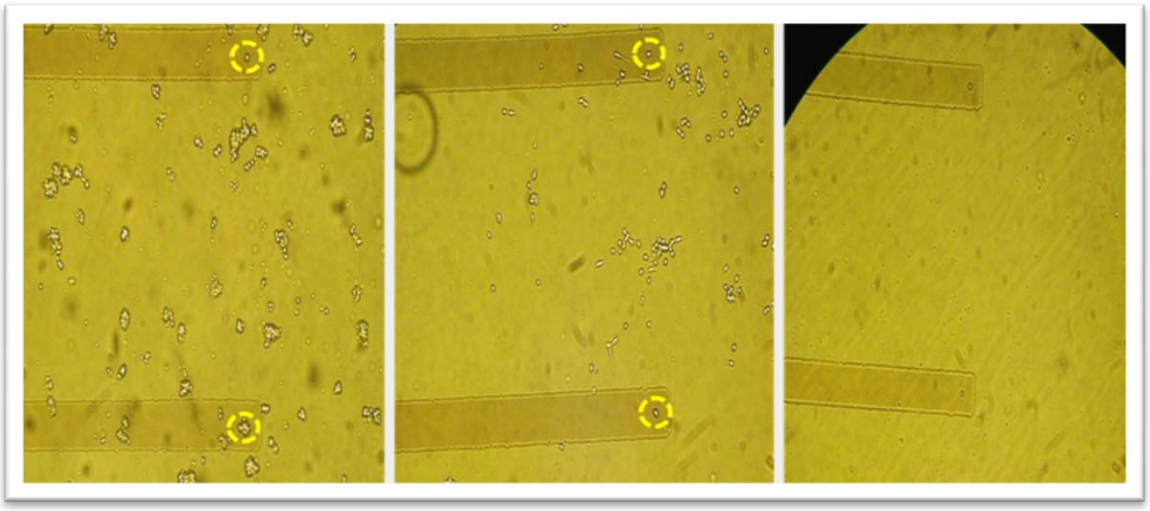

Figure 4-1 Progressive washing of the device to remove cells demonstrates that gentle washes remove cells from the cytophobic Teflon insulation whereas more thorough washing removes cells from the electrode docking sites. Washout of all the cells allows reuse of the device. The image on the left depicts a high density of INS-1 cells following the loading of the cells on the device for 2 hrs. The middle image demonstrates reduction of cells on the Teflon surface following a gentle wash. The right image shows that more extensive washing removes nearly all cells from the device.

Figure 4-2 is another example image of an selective targeting of an individual INS-1 cell to an electrode docking site. Cells are virtually absent on the insulating Teflon cytophobic film.

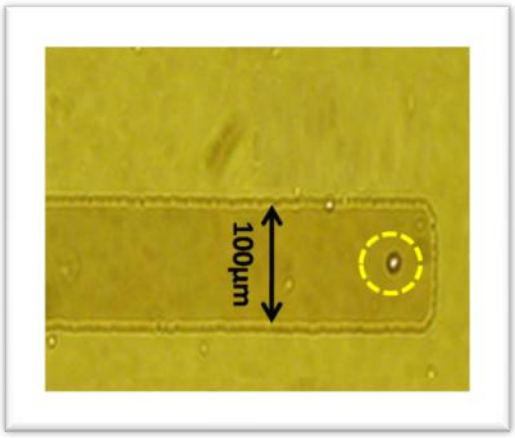

Figure 4-2 Single INS-1 cell docked to an electrode

4-2 Selective targeting of chromaffin cells to electrode / cell docking sites

The targeting of chromaffin cells was tested for both larger and single-cell-sized electrode openings. Figure 4-3 is the image of chromaffin cells docked on a 40 µm DLC:N electrode patterned with Teflon AF as the insulation material. The cells were allowed to settle for 2 hrs and then washed. A clump of cells is visible on cell docking site area of the electrode whereas the insulating Teflon areas are virtually cell free.

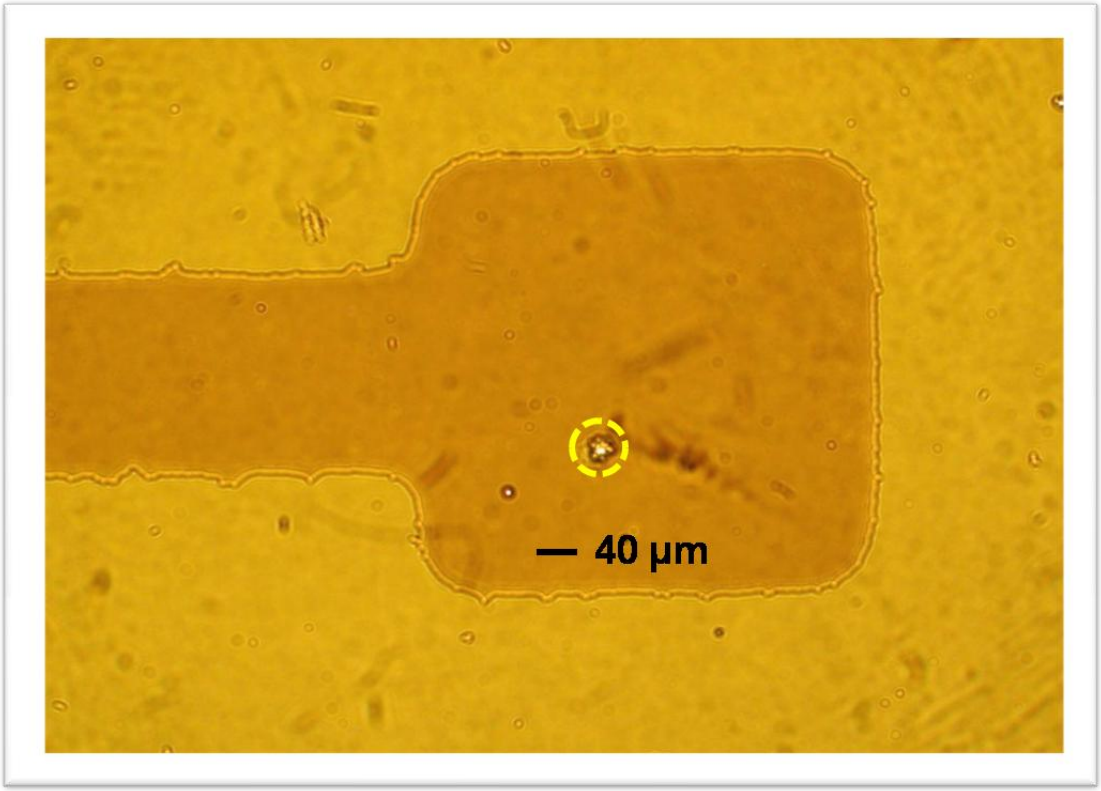

Figure 4-3 Image of docking of a small cluster of cells on a 40 µm patterned device.

Docking of cells on ~20 µm electrode is shown in figure 4-4 before wash. The cells were allowed to settle for 30 min before being washed. The image before wash shows high density of chromaffin cells on the electrode area. Gentle washing was carried out by removing excess cell media with a pipette followed by addition of bath solution. This was repeated several times to decrease the cell density on the cytophobic Teflon surface.

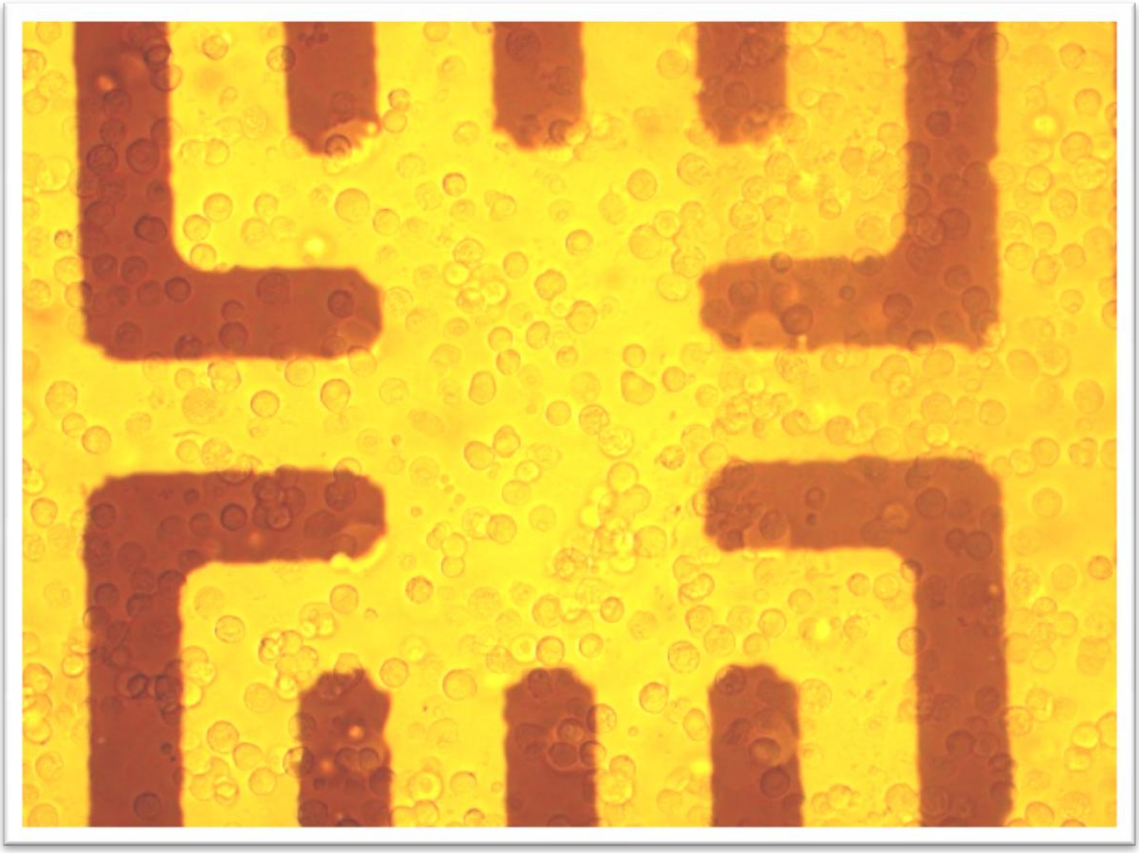

Figure 4-4 Photograph of chromaffin cells before wash.

The photograph in figure 4-5 a) shows cell occupancy of seven out of the ten electrode docking sites after wash. Some of the sites are occupied by single cells whereas multiple cells can be seen on other electrodes. The ratio of single cells to clumps depends on cell culture conditions in that cell clumping is more prevalent when cells are in culture for longer than 24 hours. We quantified cell attachment on 14 electrode arrays and found that 92 of the possible 140 electrode / docking sites (66%) are occupied by cells. Since some cells remain on the Teflon AF surface, we quantified the density of cells on the electrodes (DLC:N surface) versus the Teflon AF surface, b) The data indicate that cells

preferentially attach to the DLC:N electrode surface by a ratio of greater than 19:1.

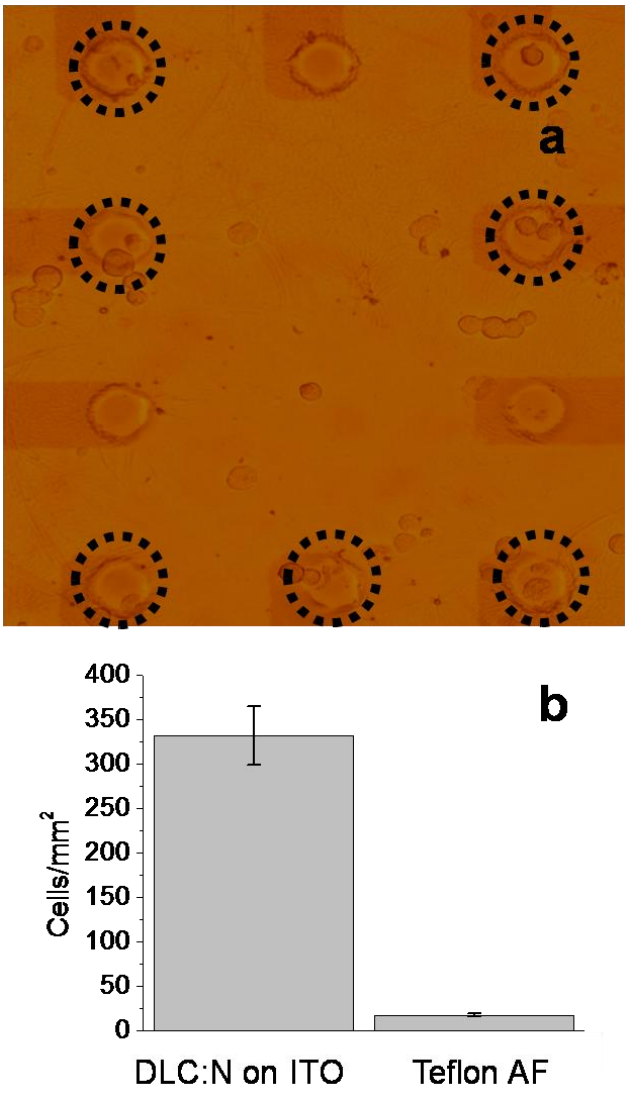

Figure 4-5 Cells are successfully targeted to electrodes. a) Sample photomicrograph depicting 7 out of 10 electrodes occupied by cells. b) Bar graph quantifying the density of cells observed on DLC:N electrodes versus on the Teflon AF insulating film. The error bars are the SEM measured from 14 electrode arrays.

4-3 Cell isolation and culture methods

4-3-1 INS-1 cells

The INS-1 cell line originates from cells isolated from an x-ray-induced rat transplantable insulinoma (M. Asfari, 1992, Y. Yang and K. D. Gillis, 2004). These cells were a kind gift from C. Wollheim, University of Geneva, Switzerland. These cells were maintained in culture media consisting of RPMI 1640 medium supplemented with 50 µM 2-mercaptoethanol (Acros Organics), 2 mM L-glutamine, 10 mM HEPES, 100 units/ml Penicillin, 100 g/ml streptomycin, 1 mM Sodium Pyruvate and 10% fetal bovine serum. The cells were cultured in 25 cm^2 tissue culture flasks and incubated at 37ºC in 5% CO_2, 95% air. The medium was replaced every alternate day and cells were passed once per week. For passing the cells, 2 ml of Trypsin/EDTA (0.05% Trypsin with EDTA 4Na, 1X; Univ. of Missouri Cell Core) was added to the flask. After cells had detached, which takes about 2 minutes, 3 ml of serum-containing medium was added to inactivate trypsin. The liquid medium in the flask is rolled gently to detach the cells from the flask. The cell suspension was then centrifuged at 1000 rpm for 5 minutes. This medium is removed and new medium added. Again the centrifugation step is repeated to wash the trypsin from the medium. The cells were then split 1:10, placed in a new culture flask and returned to the incubator. A portion of the remaining cells were sometimes used for experiments following resuspension in bath solution at a final concentration of 10^6 cells/ml.

4-3-2 Chromaffin cells

Chromaffin cells were harvested from bovine adrenal glands once per week (U. Ashery, A. Betz, 1999, Y. Yang, T. J. Craig, 2007). Harvested cells are maintained in 25 cm^2 polystyrene cell culture flasks at a density of ~10^6 cells in 5 ml of culture media per flask (Dulbecco's modified Eagles medium supplemented with 10% (v/v) fetal bovine serum and 1% penicillin/streptomycin) and kept in the incubator for use over a period of 1-5 days after preparation. Just before the experiment, the cell-containing media is triturated to detach the cells from the flask and also to break up cell clumps into individual cells. A few ml of cell-containing media is removed from the culture flask and put into a 10 ml plastic tube. This sample is centrifuged at 1000 rpm for about 5 minutes, the supernatant is removed and standard bath solution is added to the cells. The standard bath solution consists of (in mM): 150 NaCl, 5 KCl, 5 $CaCl_2$, 2 $MgCl_2$, 10 glucose, and 10 HEPES titrated to pH 7.2 with NaOH. The final cell concentration in the standard bath solution is ~10^6 cells/ml. 50 μL of the cell suspension was loaded onto the chip device for experimentation.

4-3-3 Cell quantification

The cell images were quantified using the image J software. The total insulated area and the total docking site area was calculated. The difference between the insulated area and the docking sites gives the net insulated area. The cells were measured using the cell-counter plug-in from the image J software. The total cells on the insulated and the cells on the docking sites are counted, and the then the number of cells are divided the net insulating area and the net area of the docking sites respectively to get the cells/cm^2. These values were plotted as column bars to compare the adhesion between the cytophilic electrode and the cytophobic insulating area.

References

U. Ashery, A. Betz, T. Xu, N. Brose, and J. Rettig, "An efficient method for infection of adrenal chromaffin cells using the Semliki Forest virus gene expression system, Europe Journal of Cell Biology, vol. 78, pp. 525-32, 1999.

Y. Yang, T. J. Craig, X. Chen, L. F. Ciufo, M. Takahashi, A. Morgan, and K. D. Gillis, "Phosphomimetic Mutation of Ser-187 of SNAP-25 Increases both Syntaxin Binding and Highly Ca2+-sensitive Exocytosis, The Journal of General Physiology, vol. 129, p. 233, 2007.

M. Asfari, "Establishment of 2-mercaptoethanol-dependent differentiated insulin-secreting cell lines, Endocrinology, vol. 130, pp. 167-178, 1992.

Y. Yang and K. D. Gillis, "A highly Ca-sensitive pool of granules is regulated by glucose, PKC, and cAMP in insulin-secreting INS-1 cells, The Journal of General Physiology, vol. 124, pp. 641-651, 2004.

CHAPTER 5

CELL RECORDINGS AND ANALYSIS

5-1 Experimental setup

The experimental setup for measuring cell exocytosis is shown in figure 5-1. The chip device was placed in a custom holder which facilitates connection of the amplifier to the selected electrode. A copper pin with a short wire was used to connect the contact pad at the edge of the chip to the head stage of the EPC-9 patch-clamp amplifier (HEKA, Lambrecht, Germany) and HEKA Pulse software was used for the amplifier control and data acquisition. A small reservoir made with PDMS holds the cell-containing solution. A Ag/AgCl wire electrode was inserted into the drop of solution to serve as the reference electrode for amperometric recordings. A +700 mV potential was applied to the working microelectrode relative to the Ag/AgCl reference, and current from the working electrode is monitored and recorded by the computer. To minimize pickup of external electrical noise, the chip and the head stage were shielded.

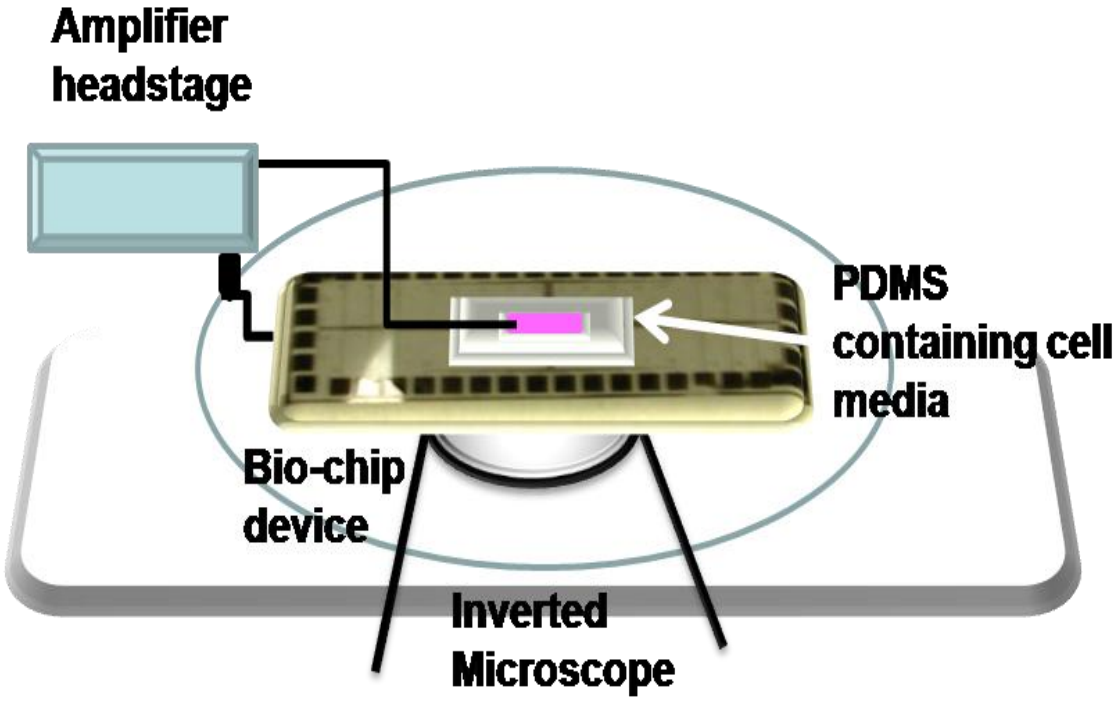

Figure 5-1 Schematic of the set-up for amperometric measurements.

5-2 Stimulation and recording

50 μL of a cell suspension is placed in the PDMS gasket and a few minutes are allowed for settling of the cells. Then 50 μL of the high-K^+ solution is added to the cell containing media to stimulate catecholamine release. This elevation of the extracellular K^+ concentration causes the cell to depolarize. This causes the voltage-gated Ca^{2+} channels to open and there is influx of Ca^{2+} which triggers exocytosis. When the catecholamines are released from each vesicle and reach the working electrode, they oxidize, resulting in a spike of faradaic current. Amperometric current are low-pass filtered at a cut-off frequency of 2.9 kHz and sampled at a frequency of 10 kHz. Amperometric spikes were recorded

in sweeps of 120 seconds duration. The pulse software was used for recording amperometric currents and analysis of spike parameters (Mosharov and Sulzer 2005; Mosharov 2008) was carried out using freely available software (Borges lab; Segura et. al; 2000 and Sulzer Lab).

5-3 Amperometric Recordings

It is important to note that the response from each cell is quite variable as is also the case for recording using carbon-fiber electrodes. Shown in figure 5-2 is a sample recording from a single cell for a period of 2 minutes. Shown in the inset is a portion of the recording on an expanded time scale. Note the expanded time scale is necessary to resolve the dynamics of individual spikes which typically occur over a timescale of tens of milliseconds.

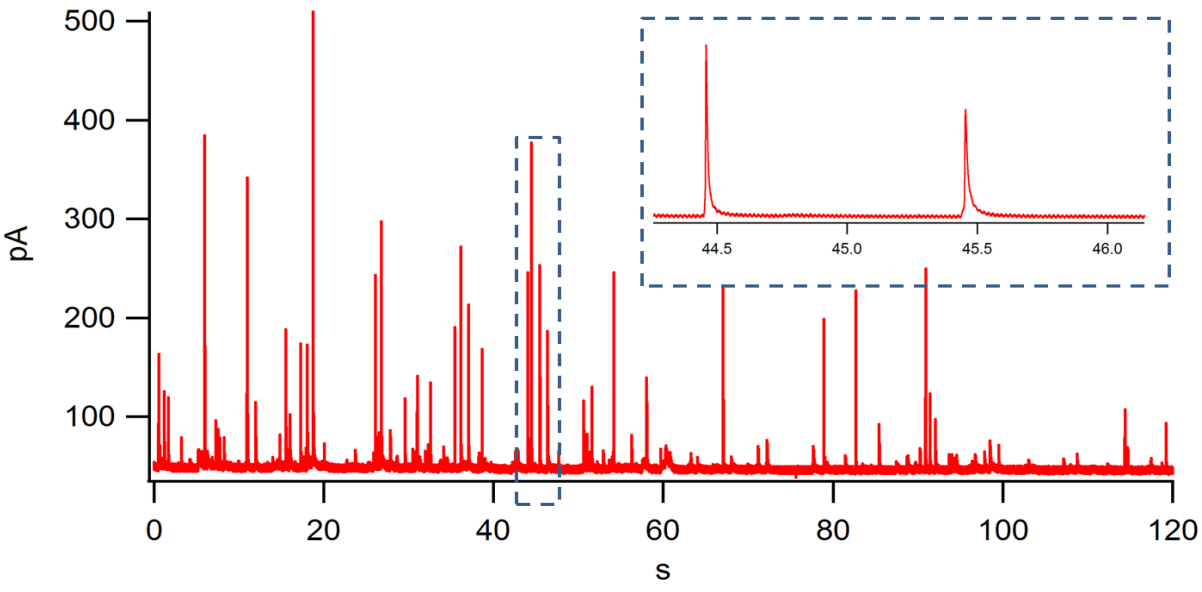

Figure 5-2 Recordings from single bovine chromaffin cells using a DLC:N on ITO electrode.

5-4 Individual Cell recordings

5-4-1 DLC:N on ITO

Figure 5-3 a) and b) show sample recordings from two individual cells in order to illustrate typical cell-to-cell variability. The difference in the amperometric responses may reflect both differences in cell secretion and the sensitivity of the electrode. Larger spike amplitudes (I_{max}) indicate more rapid release of molecules upon vesicle fusion or perhaps a more sensitive (e.g., cleaner) electrode. Variability in the spike area (Q) occur from the same cell, indicate the number of molecules released from a vesicle, and are thought to reflect variability in the size of the fusing vesicles. The spike frequency indicates the rate that vesicles are fusing near the electrode and varies quite a bit from cell to cell and depends on the type of stimulus applied. The duration that the spike exceeds the half-maximal value ($t_{1/2}$) indicates how long it takes for a vesicle to release its contents, although it may also be affected by the sensitivity / cleanliness of the electrode. There is a tendency for I_{max} and $t_{1/2}$ to be inversely correlated, i.e., more sensitive electrodes tends to detect large and fast spikes. Further information about interpretation of spike parameters can be found in the review (Segura, Brioso et al. 2000) (Mosharov, Sulzer. 2005).

The background (dc) current is an important electrode-dependent parameter. It is desirable for the background current to be small and stable to reduce shot noise. In Figure 5-3 a) it can be seen that the background current decays during this recording. In fact, the background current can take many

minutes to stabilize following application of the voltage, and this changing background is most apparent in platinum electrodes (data not shown). Larger electrodes have larger background currents, larger capacitance values and larger noise, which may explain why the background current in figure 5-3 a) is smaller than that in figure 5-3 b).

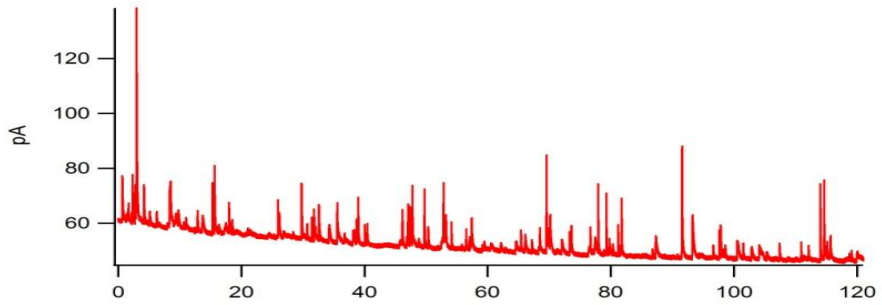

(a)

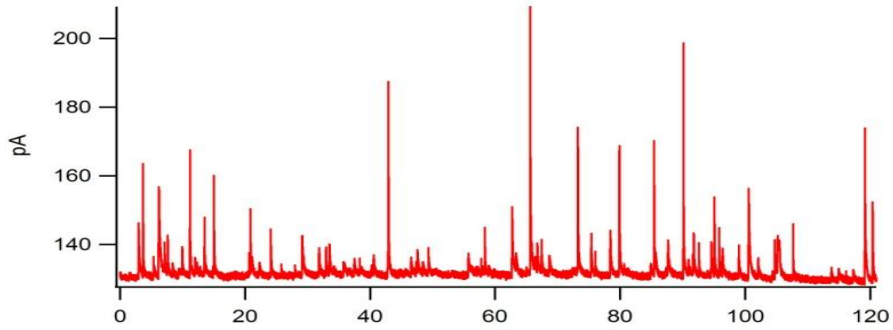

(b)

Figure 5-3 Recordings from single bovine chromaffin cells using a DLC:N on ITO electrode a) cell 1 and b) cell (2).

5-4-2 Recordings with Au electrodes

Figure 5- 4 a) and b) show sample recordings from two individual cells using Au electrodes. The spike frequencies of these sample recordings are higher than those shown for DLC:N electrodes (figure 5-3), but this was not a consistent finding and I don't find evidence that the electrode material affects the rate of exocytosis. However, the spike amplitudes (I_{max}) and areas (Q) tend to be larger with Au electrodes compared to DLC:N or carbon-fiber electrodes will be discussed later in the chapter.

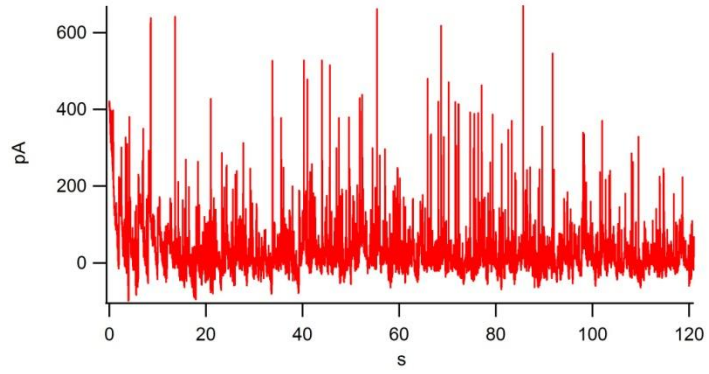

(a)

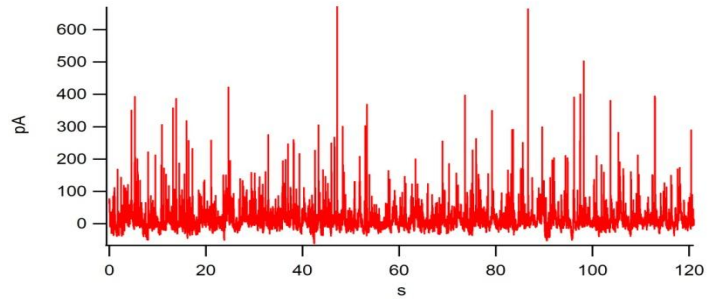

(b)

Figure 5-4 Recordings from two single bovine chromaffin cells using an Au electrode, a) cell 1 and b) cell2.

5 -5 Spike Analysis

Following acquisition, amperometric data was filtered before the spike characteristics were analyzed. Pickup of line frequency interference (60Hz and harmonics) was reduced using software written by Dr. Gillis. Software "decimation", i.e., averaging adjacent samples, was also used as a form of low-pass filtering. Typically 20-50 adjacent samples were averaged to resulting in a time resolution of 2-5 ms per sample

Figure 5-5 a) is a 10 second expanded recording of a regular spike plotted in IGOR (red trace) overlapped with a decimated spike (black trace). Every 50 samples were averaged to produce a single point for the "decimated" trace. The process of decimation is performed to reduce noise which can have a standard deviation in the pA range and thus obscure smaller features in the spike such as the "foot signal". On the other hand, if the data are filtered too much with decimation then the spike amplitude could be reduced and the spike time course could be prolonged, thus resulting in a loss of information. As it can be seen in figure 5-5 a), a decimation factor of 50 (5 ms per sample time resolution) does not significantly modify the spike shapes for this particular recording. This indicates that spike information has been lost after decimation, but we did not analyze foot signals in this study and so lower decimation factors may be necessary when resolving these fast pre-spike features.

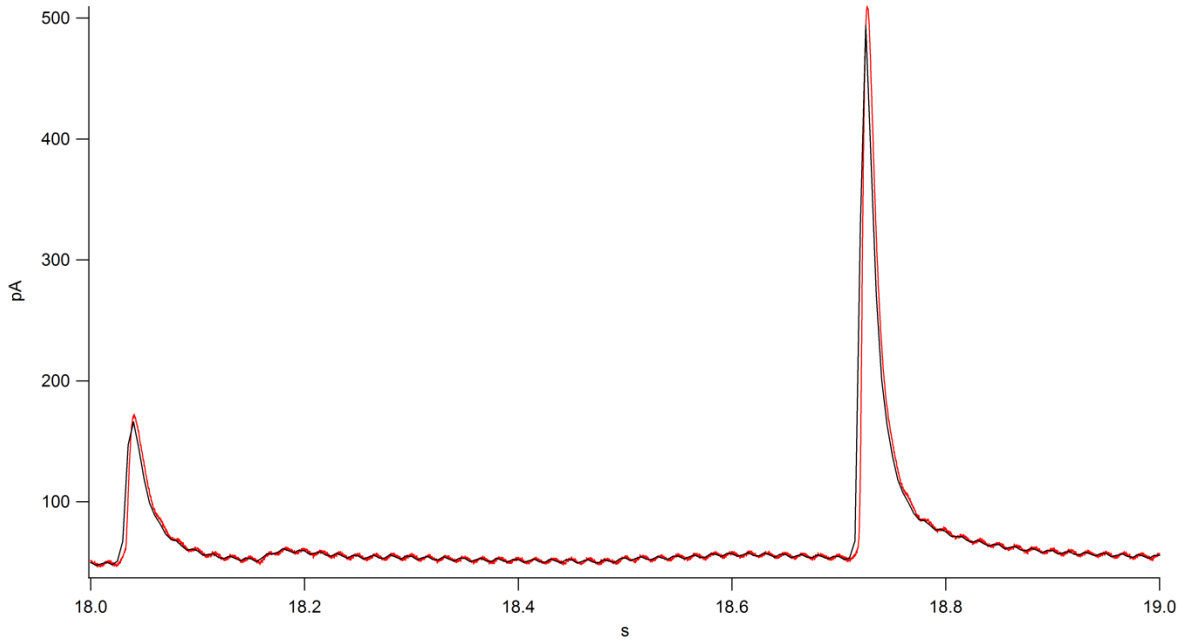

(a)

Features of interest for each quantal release event, i.e., amperometric spike, are summarized in figure 5-5 b). Since spike parameters usually vary quite a bit but from spike-to-spike, histograms are compiled to summarize data obtained under a given condition.

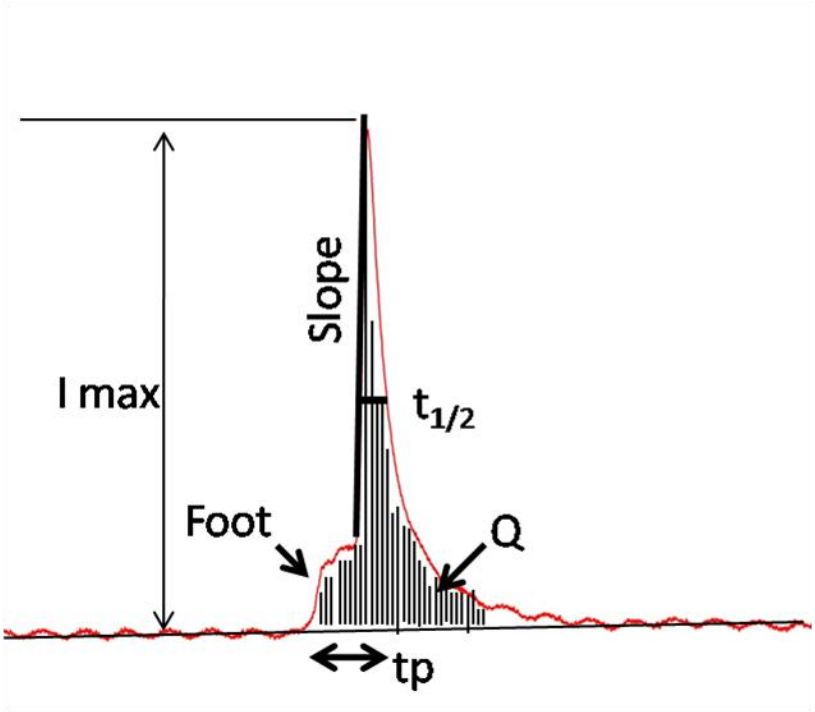

(b)

Figure 5-5 a) Recording on DLC:N electrode before (red trace) and after (black trace) 50-fold decimation, b) Sample spike with a foot signal illustrating parameters which are typically measured.

Criterion must be selected on whether to accept or reject an amperometric event. I rejected spikes which showed multiple rising phases, i.e., overlapping spikes. We also rejected spike with amplitudes smaller than 10 pA and times-to-peak greater than 40 ms for DLC:N electrodes. For Au electrodes, spike amplitudes smaller than 15 pA and times-to-peak greater than 40 ms were rejected.

5-5-1 Spike analysis from individual cells on DLC:N on ITO electrode

Figure 5-6 depicts typical histograms of spike parameters obtained through analysis of a two minute recording containing 103 analyzable spikes using a DLC:N electrode. This analysis was performed using software from the Borges lab (Segura et. al; 2000 and the Sulzer lab). Histograms are displayed for six spike parameters I_{max}, Q, $Q^{1/3}$, $t_{1/2}$, t_p and slope. For each spike, the integral of area under the curve gives the charge (Q) and is related to the number of moles of molecule detected. The histogram for Q (figure 5-6) shows this parameter has a wide, non-Gaussian distribution (Finnegan, Pihel et al. 1996). Note, however, that the distribution of $Q^{1/3}$ is approximately normally distributed. The explanation for this is that the distribution of vesicle diameter in cells is believed to be approximately Gaussian. Since Q is proportional to vesicle volume (assuming vesicles contain a uniform concentration of catecholamines), a histogram of $Q^{1/3}$ is used to illustrate the distribution of vesicle size (Travis and Wightman 1998).

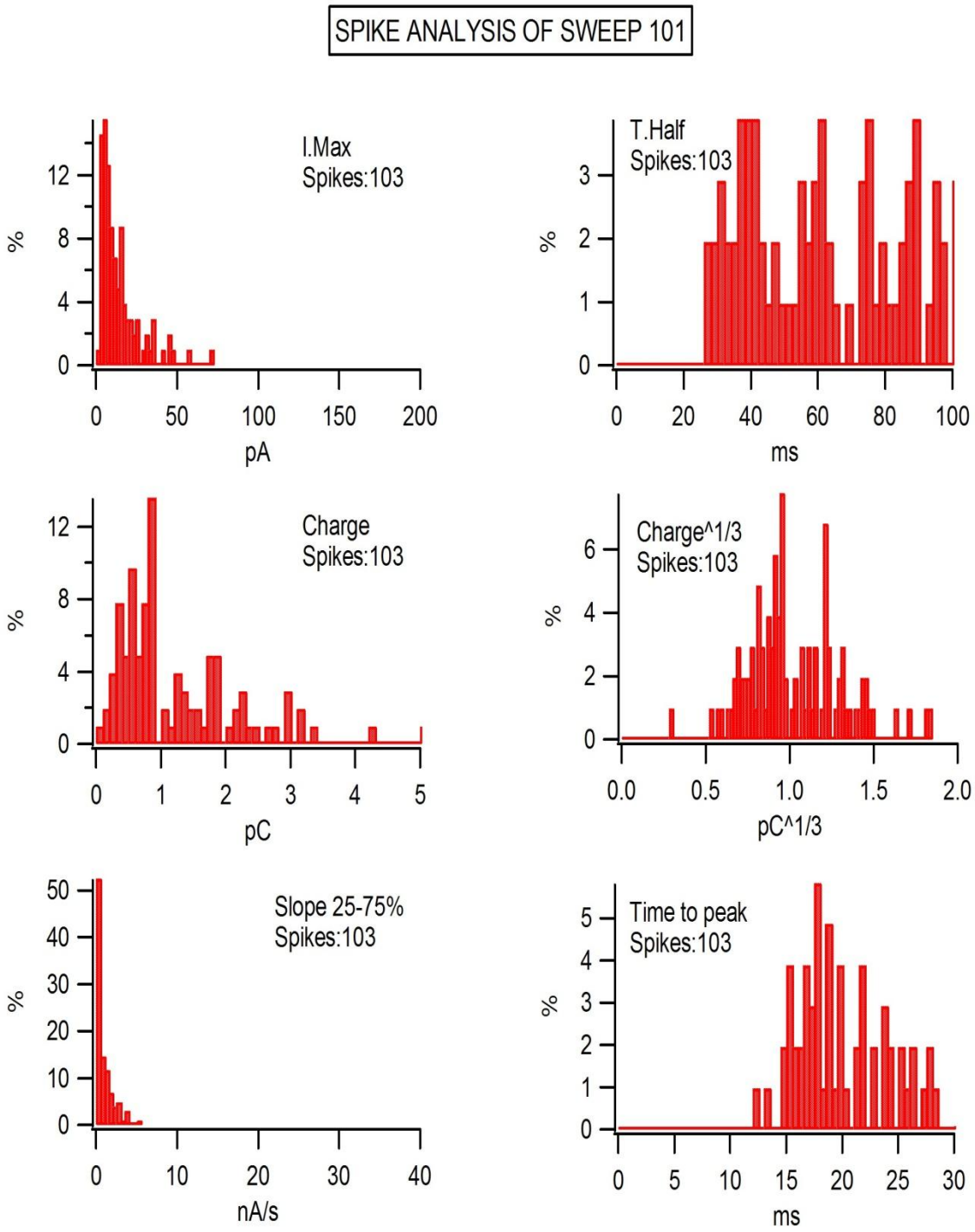

Figure 5-6 Quantification of a single cell on a DLC:N on ITO electrode for a 120 sec recording.

5-5-2 Quantification of cells with DLC:N on ITO electrode

Figure 5-7 depicts a bar graph from 24 individual cells. The values on top of each histogram indicate the number of spikes for that particular cell and the histograms indicate the median value of I max, Q and t1/2 for bovine chromaffin cells. This type of analysis was to illustrate cell-to-cell (and electrode-to-electrode) variability. The number of analyzable release events varied from 6 to 107 events for the 24 cells analyzed. It can be seen in b) that the median value of Q generally ranges from 1.0 to 1.5 pC with the noted exception of the ninth cell.

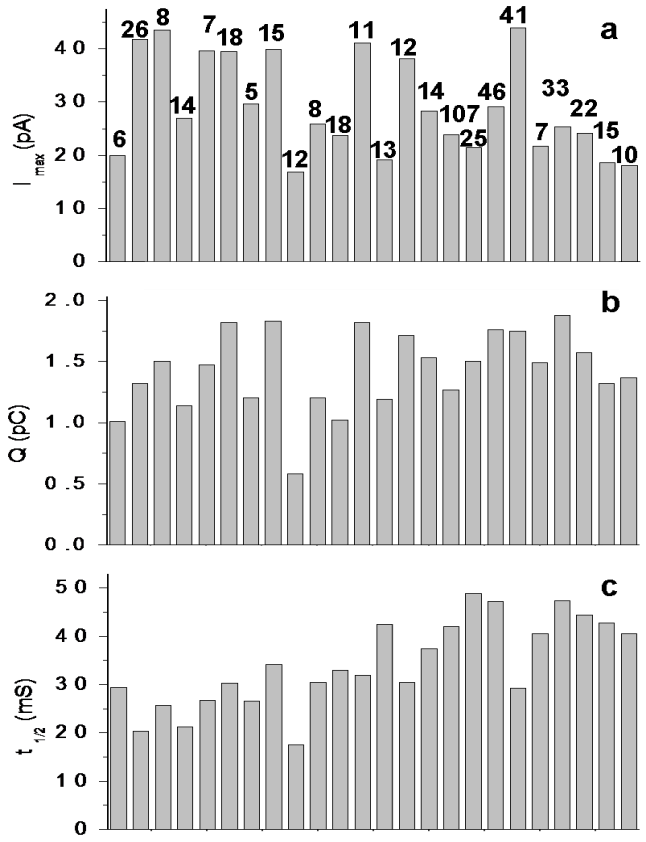

Figure 5-7 Quantification of the consistency of measured spike parameters between different cells and electrodes. Each bar indicates the median value of each parameter for each of 24 cells. The number above each bar denotes the number of spikes recorded from that particular cell.

5-5-3 Cumulative analysis of events with DLC:N on ITO electrode

Figure 5-8 shows histograms accumulated from analysis of 24 cells with 493 total release events. The median values are 26.9 pA for I max, 1.49 pC for *Q* and 33.0 ms for t1/2 and $Q^{1/3}$ of 1.06 pC and are similar to values reported for chromaffin cells using carbon fiber electrodes.

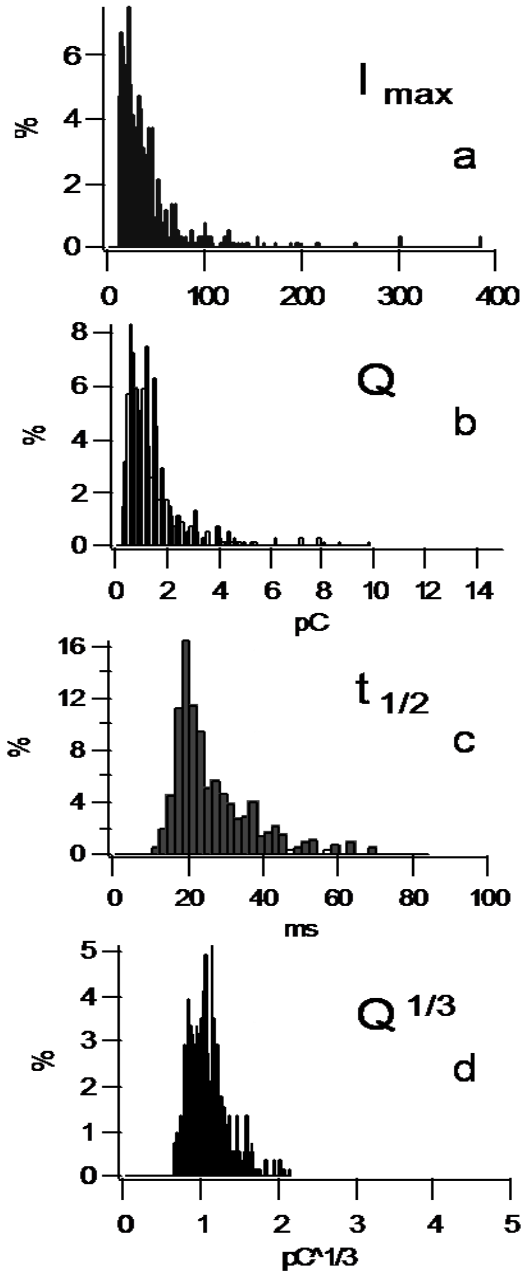

Figure 5-8 Quantitative analysis of 493 spikes recorded from 24 cells. Histograms depict: a) spike amplitude (Imax), b) spike area or charge (Q), c) duration that the spike exceeds the half-maximal amplitude (t1/2) and d) cube root of charge ($Q^{1/3}$).

5-6 Quantification of spike parameters recorded with Au electrode

Figure 5-6 depicts typical histograms of spike parameters obtained through analysis of a two-minute recording containing 337 analyzable spikes using a Au electrode. As before, the histogram for Q shows a wide, non-Gaussian distribution, whereas the $Q^{1/3}$ histogram is approximately Gaussian distributed. This is because of the reasons explained earlier during the analysis of DLC:N on ITO electrode. The median Q values seem to be in the 2.0 -2.2 pC range. These values are comparatively more than the values for the carbon fiber, but conform with our groups unpublished results (data not shown).

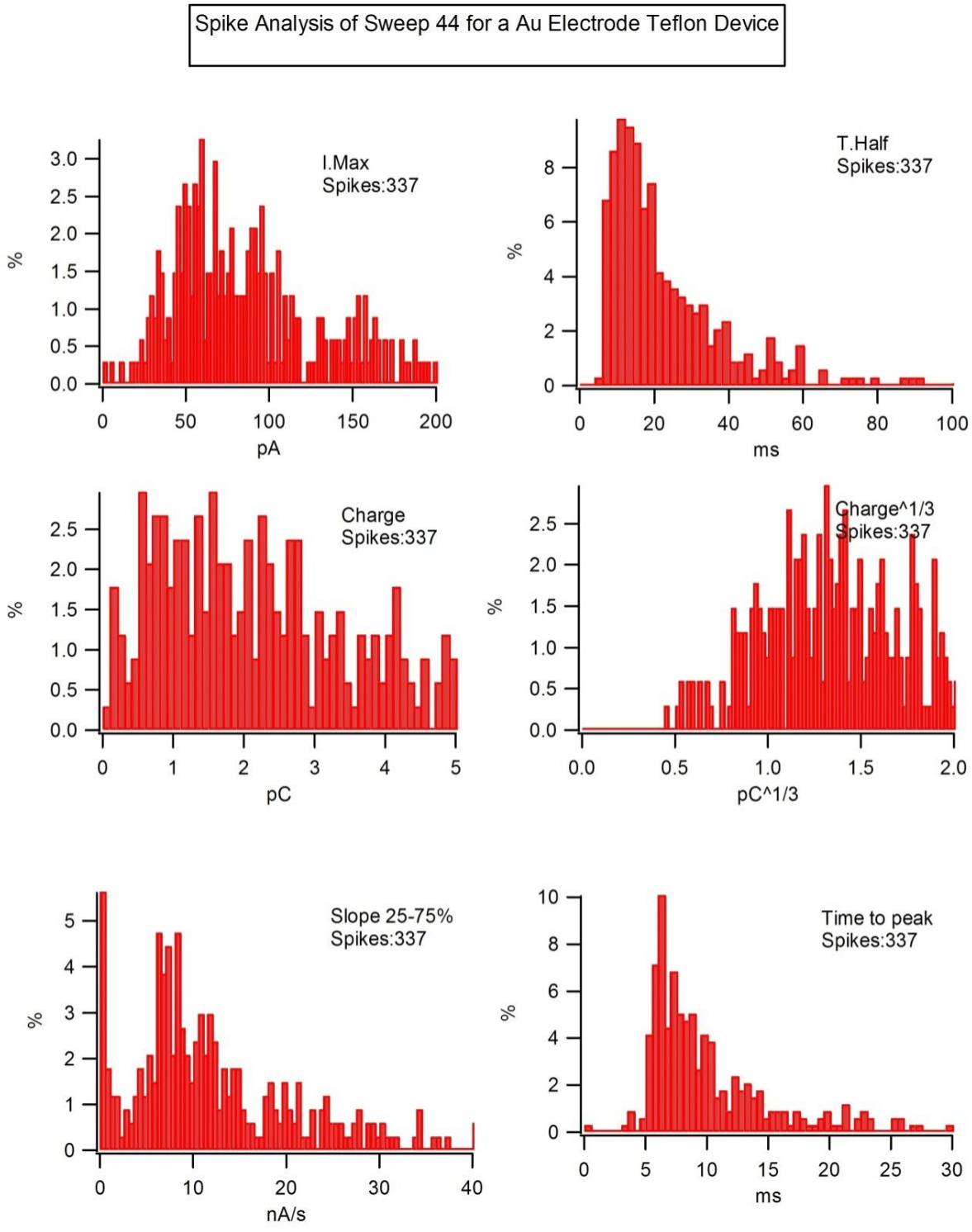

Figure 5-9 Quantification of spike parameters for a single cell on a Au electrode over a 120 sec recording.

Figure 5-10 depicts a bar graph from 6 individual bovine chromaffin cells. The values on top of each histogram indicate the number of spikes for that particular cell. This type of analysis was to illustrate cell-to-cell variability on Au electrodes. The number of release events varied 67 to 191 events for the 6 cells analyzed. The median Q values were in the range of 1.2 – 1.8 pC from this group of cells.

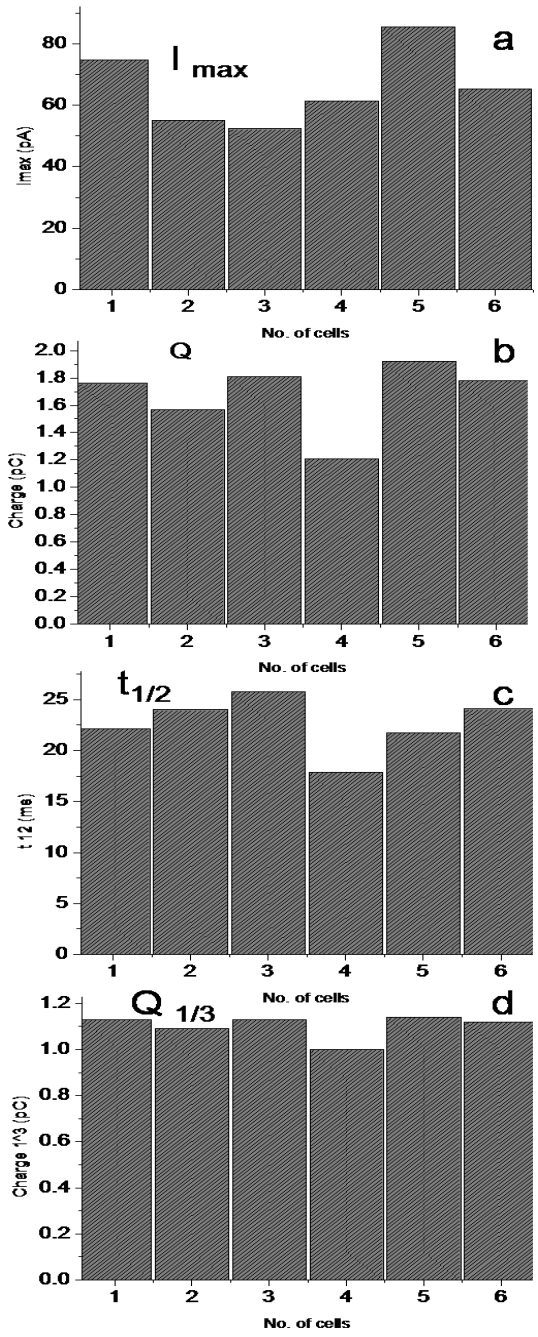

Figure 5-10 Quantification of the consistency of measured spike parameters between different cells and electrodes. Each bar indicates the median value of each parameter for each of 6 cells. The number above each bar denotes the number of spikes recorded from that particular cell.

Figure 5-11 shows histograms of 1226 release events obtained from 6 cells. The median values are 96.7 pA for I max, 2.83 pC for *Q* and 20.96 ms for t1/2. The Q values are markedly larger than what I found for DLC electrodes or what is commonly reported for carbon fiber electrodes. Table 5-1 compares the mean +/- SD values of spike parameters between the DLC and Au electrodes. Next I apply a statistical test to determine if the differences in Q values are statistically significant.

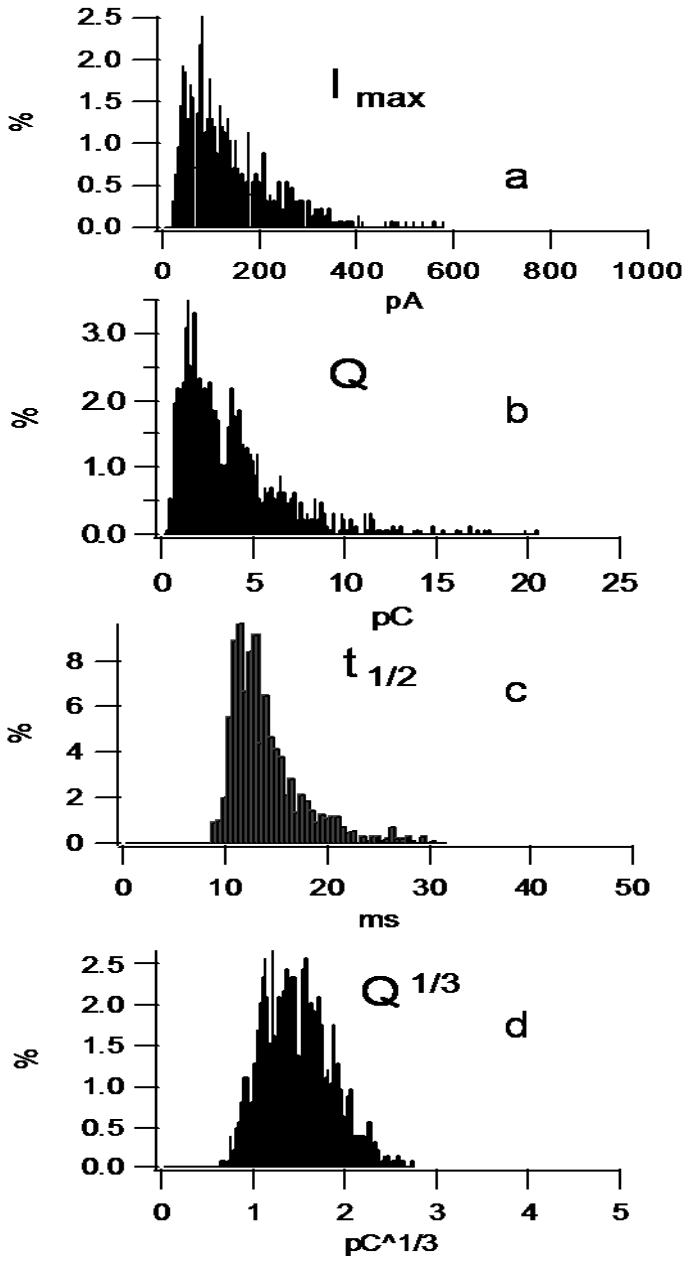

Figure 5-11 Quantitative analysis of 1226 spikes recorded from how many 6 cells. Histograms depict: a) spike amplitude (Imax), b) spike area or charge (Q) and c) Duration that the spike exceeds the half-maximal amplitude (t1/2) and d) Cube root of charge ($Q^{1/3}$).

Spike parameters for DLC on ITO electrodes	
Imax (pA): (mean ± s.d)	39.18 ± 34.35
Charge (pC)	1.43 ± 1.12
t1/2 (ms)	26.77 ± 11.45
Number of spikes	504
Number of cells	28
Spike parameters for Au electrodes	
Imax (pA): (mean ± s.d)	120.63 ± 84.16
Charge (pC):	3.66 ± 2.90
t1/2 (ms):	24.48 ± 11.27
Number of spikes	1226
Number of cells	6

Table 5-1 Quantitative comparison of cumulative values from DLC:N on ITO electrode and Au electrode.Data are mean ± s.d values.

5-7 Two Independent Sample Wilcoxon Rank Sum Test: (Mann-Whitney Test)

The Mann-Whitney test, also called the rank sum test, is a nonparametric test that compares two unpaired groups. To perform this test it ranks all the values from low to high, not considering to which group each value belongs. If two values are the same, then they both get the average of the two ranks for which they tie. The smallest number gets a rank of 1. The largest number gets a rank of N, where N is the total number of values in the two groups. It then sums the ranks in each group, and reports the two sums. If the sums of the ranks are very different, the *p* value will be small. If the *p* value is small, the idea that the difference is a coincidence can be rejected, and it can be concluded that the populations have different medians.

If the samples size 20 or less is small, and there are no ties, it calculates an exact *p* value. If the samples are large, or if there are ties, it approximates the *p* value from a Gaussian approximation. Here, the term Gaussian has to do with the distribution of sum of ranks, and does not imply that the underlying data need to follow a Gaussian distribution. The approximation is quite accurate with large samples.

The software used for this test was from UCLA online source,

The results from applying the test to compare Q values between the DLC:N and Au electrode are give a *p* value for this comparison was found to be .000368.The *p* value indicates the Q values are significantly different with high confidence.

The quantitative comparison of spikes between the DLC:N and Au microelectrodes show significant differences in the Q (pC). The Q value of 1.43 ± 1.12 pC with the DLC:N electrode is comparable to the carbon fiber values (Ales, Tabares et al. 1999; Amatore, Arbault et al. 2009), but, the Q values of 3.66 ± 2.90 for the Au electrode are higher than what is usually reported. The number of electrons donated per each oxidized catecholamine molecule is usually assumed to be two, although it may be possible for as many as four electrons be transferred per catecholamine following intracyclization reaction (Adams, Murrill et al. 1972; Tse, McCreery et al. 1976). Intracycliization is usually thought to be too slow to occur during the time course of an individual amperometric spike but perhaps Au electrodes catalyze these reactions at a higher rate than carbon-based electrodes, thus explaining the difference in Q values. Another possibility is that Au promotes release of large vesicles, perhaps by triggering vesicle-vesicle fusion within the cell before exocytosis. Finally, it should be noted that the experiments with Au and DLC electrodes were not performed in a paired fashion with the same batches of cells. It will be important to perform paired experiments in the future to verify the difference between the electrodes.

In any case, my results clearly demonstrate that our microfabricated device consisting of DLC:N on ITO electrodes insulated with Teflon AF is an effective alternative to carbon-fiber microelectrodes for higher-throughput studies of quantal exocytosis.

References

Adams, R. N., E. Murrill, et al. (1972). "6-Hydroxydopamine, a new oxidation mechanism." European Journal of Pharmacology **17**(2): 287-292.

Ales, E., L. Tabares, et al. (1999). "High calcium concentrations shift the mode of exocytosis to the kiss-and-run mechanism." Nat Cell Biol **1**(1): 40-44.

Amatore, C., S. p. Arbault, et al. (2009). "Invariance of Exocytotic Events Detected by Amperometry as a Function of the Carbon Fiber Microelectrode Diameter." Analytical Chemistry **81**(8): 3087-3093.

Finnegan, J. M., K. Pihel, et al. (1996). "Vesicular quantal size measured by amperometry at chromaffin, mast, pheochromocytoma, and pancreatic beta-cells." J Neurochem **66**(5): 1914-1923.

Mosharov, E. V. (2008). "Analysis of single-vesicle exocytotic events recorded by amperometry." Methods Mol Biol **440**: 315-327.

Mosharov, E. V. and D. Sulzer (2005). "Analysis of exocytotic events recorded by amperometry." Nat Methods **2**(9): 651-658.

Segura, F., M. A. Brioso, et al. (2000). "Automatic analysis for amperometrical recordings of exocytosis." Journal of Neuroscience Methods **103**(2): 151-156.

Travis, E. R. and R. M. Wightman (1998). "SPATIO-TEMPORAL RESOLUTION OF EXOCYTOSIS FROM INDIVIDUAL CELLS." Annual Review of Biophysics and Biomolecular Structure **27**(1): 77-103.

Tse, D. C. S., R. L. McCreery, et al. (1976). "Potential oxidative pathways of brain catecholamines." Journal of Medicinal Chemistry **19**(1): 37-40.

http://www.graphpad.com/articles/interpret/analyzing_two_groups/mann_whitney.htm

http://www.socr.ucla.edu/htmls/ana/TwoIndependentSampleWilcoxonRankSum_

Analysis.html

CHAPTER 6

INCORPORATING Pt NANOPARTICLES ON ELECTRODES IN ORDER TO IMPROVE SENSITIVITY FOR DETECTING THE RELEASE OF CATECHOLAMAINES OR OTHER ELECTROACTIVE ANALYTES FROM CELLS

6-1 Introduction

Reactive oxygen and nitrogen species (ROS and RNS) are involved in the regulation of many biological processes such as reactivity, proliferation and apoptosis (Buttke and Sandstrom 1994; McNeil and Manning 2002; Abrams and White 2004). Reactive oxygen species (ROS) is a collective term that includes oxygen radicals such as superoxide (O 2 ·-), hydroxyl (OH ·), peroxyl (RO 2 ·), and hydroperoxyl (HO 2 ·) (Bayr 2005). Reactive nitrogen species (RNS) include Peroxynitrite, nitrogen dioxide, and other reactive nitrogen species that are formed in the reaction of nitric oxide (NO) with the superoxide anion (O'Donnell, Eiserich et al. 1998; ICHINOSE, SUGIURA et al. 2000). Nitric oxide (NO) is the smallest molecule found in nature (Chen, Wang et al. 2008), is an important bio-regulatory molecule (Malinski and Taha 1992), and plays an important role as a cell-signaling molecule, anti-infective agent and, as most recently recognized, an antioxidant (Patel, McAndrew et al. 1999). If the production of these species increases in comparison to the scavenging ability of the cell pathologies, neurodegenerative disorders can result from oxidative stress (Coyle and

Puttfarcken 1993; Olanow 1993; Sies 1997; Finkel and Holbrook 2000). Hypertension (Wei, Christman et al. 1985), atherosclerosis (VanBenthuysen, McMurtry et. al. 1987), diabetes (Baynes 1991; Giugliano, Ceriello et al. 1996), Parkinson's disease (Jenner 2003) and ageing (Beal 1995) have also been related to oxidative stress. Though these species were considered to be toxic by-products of metabolism in the past, more recent studies have shown that these are signaling molecules to control processes such as programmed cell death, pathogen defense and systemic signaling (Mittler 2002).

6-2 Detection of reactive species

Many studies have used surface modification of the carbon fiber electrode to detect release of reactive species from the cells (Deinhammer, Ho et al. 1994; Tarpey and Fridovich 2001; Engelmann, Bobier et al. 2003; Tian, Mao et al. 2005). Superoxide, hydrogen peroxide, nitric oxide, peroxynitrile are the main species types (Kohen, Vellaichamy et al. 2000; Arbault, Sojic et al. 2004; Campese, Ye et al. 2004; Patwell, McArdle et al. 2004; McArdle, Pattwell et al. 2005; Amatore, Arbault et al. 2006; Amatore, Arbault et al. 2007). Platinum and platinzed surfaces are also often used as electrochemical electrode materials to detect reactive species because they yield properties such as high sensitivity and good reproducibility, and mesoporous microelectrodes retain the high rates of mass transport typical of conventional microelectrodes, whereas their high surface area greatly enhances their catalytic activity (Evans, Elliott et al. 2002;

Karam and Halaoui 2008) (Karyakin, Puganova et al. 2003; Spegel, Heiskanen et al. 2008).

Whereas there are reports of release of reactive oxygen or nitrogen species from human endothelial cells being detected using electrodes patterned on microchips (Oni, Pailleret et al. 2004) the development of this technology is still in early stages.

6-3 Incorporating Pt nanoparticles on the DLC:N on ITO electrode

Here I report preliminary experiments to measure release of electroactive substance from cells using micropatterned electrodes consisting of Pt nanoparticles sputter-deposited on the surface of DLC:N. The nanoparticle size is a function of sputtering time and working distance, the smaller the sputter time and smaller the working distance, the smaller the size of the nanoparticle. We sputtered Pt nanoparticles for times ranging from 5 to 45 seconds. The size of the particles for these sputter times ranged from 0.8 nm - 2.0 nm. The thickness of the sputtered DLC:N film was also varied between 20 nm and 40 nm.

The first step in testing the microfabricated electrodes was to perform cyclic voltammetry (CV) with ferricyanide to see how the Pt nanoparticles affect the electrochemical sensitivity of the DLC:N microelectrode that I have previously characterized. As will be described in the next section, the CV on devices with small Pt nanoparticles have a larger peak-to-peak separation (ΔEp) which indicates slower electron transfer kinetics. Importantly, this slowing of electron

transfer kinetics was not noted for nanoparticles larger than ~ 1 nm or for bulk-deposited Pt. An intriguing question is what is the physical mechanism for nanoparticles to change the electrochemical properties of the electrode? Though small nanoparticles are known to be capable of charge storage (Yun, Mueller et al. 2009) which may impede the electron transfer process, further research is warranted to find the exact reason for this change.

The next step was to measure amperometric currents from depolarized bovine chromaffin cells using the Pt nanoparticle-coated electrodes. The microdevice with small nanoparticles detected amperometric spikes with durations of seconds, which are orders of magnitude longer than the duration of spikes that are typically recorded that result from exocytosis of catecholamines. These broad spikes were infrequent, typically occurring two or three times in a recording of 120 sec duration. This suggests the possibility that the nanoparticle electrodes are detecting release of an electroactive analyte that is not normally detected by conventional electrodes, such as ROS or RNS. Another possibility is that the nanoparticles amplify the electrochemical signal originating from exocytosis of catecholamines. The possibility that nanoparticles amplify electrochemical electrode signals has been suggested previously (McNeil, Greenough et al. 1992; Cooper, Greenough et al. 1993; Manning, McNeil et al. 1998; Tolias, McNeil et al. 1999) (Gobi and Mizutani 2000).

6-4 Measurement of electrode sensitivity using Cyclic Voltammetry

6-4-1 CV of conventional DLC:N micropatterned electrode

CV with 0.1mM Fe (CN)6 in 0.1M KCl was performed at the scan rate of 100mV/s to check for the peak-to-peak separation between the oxidation and reduction of the species on the device. In the example of figure 6-1 ΔEp = 231 mV.

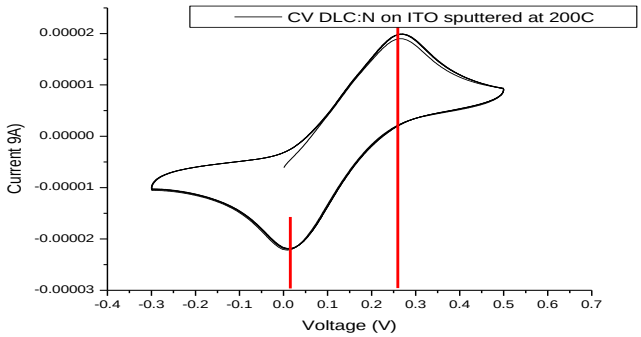

Figure 6-1 CV of DLC:N on ITO sputtered at 200°C.

6-4-2 DLC:N(20nm)-ITO-Pt NP's 10 s sputter

CV was carried out under the same conditions. In the example of figure 6-2, ΔEp = 540mV.

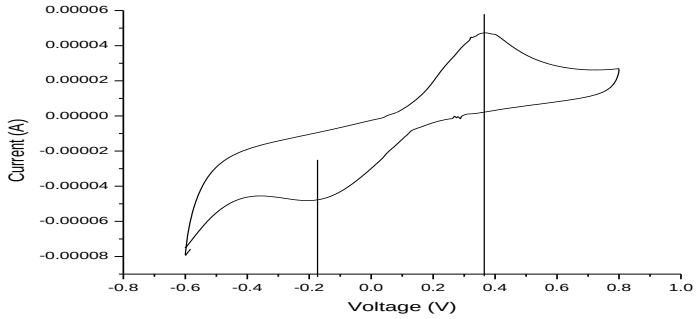

Figure 6-2 CV of DLC:N on ITO-Pt NPs 10 Sec sputtered at 200°C.

6-4-3 Capacitance values for DLC:N(20nm)-ITO-Pt NP's 10 Sec sputter

The capacitance of the 20 μm-diameter electrodes were measured using cyclic voltammetry at 100 mV/s. Devices with nanoparticles had capacitance values approximately double that of same-sized electrodes without nanoparticles. This may be due to the increased surface area or the charge storage property of the Pt nanoparticles.

DLC:N on ITO with & without Pt nanoparticles	
DLC:N on ITO	25.4 μF/cm2
DLC:N(20nm)-ITO-Pt NPs 10 Sec sputter	50.3 μF/cm2

Table 6-1 Comparison of capacitance values between a device with and without particles.

6-5 Comparison of spikes between a conventional DLC:N on ITO electrode and DLC:N sputtered with Pt nanoparticles

Figure 6-3 (a) is a recording from bovine chromaffin cells stimulated with a high K+ solution using a 20 μm diameter DLC:N electrode. The recording contains spikes resulting from quantal exocytosis of catecholamines with typical parameters such as I max, Q and t ½. For a recording of 120 sec from an depolarized chromaffin cell with a clean electroactive DLC:N on ITO electrode, 50-150 spikes with average amplitudes of 30-50 pA, charge of 1.3-1.7 pC and half-width of 15-25 ms is expected. The electrode was held at a constant potential of 600 mV. Signals were low-pass filtered with a cut-off frequency of 2.9 kHz and sampled at 10 kHz.

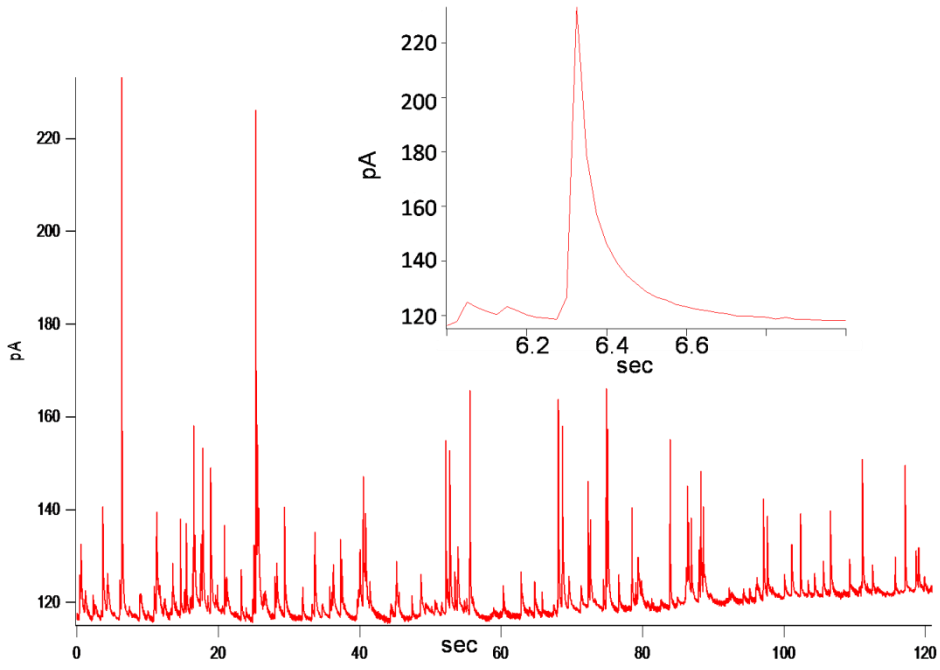

(a)

Figure 6-3 b) shows a recording from a 20 µm electrode, as explained in the preceding paragraph, the only difference with this electrode is that it has been sputtered for 10 sec with Pt nanoparticles. The expected nanoparticle size for this sputter time is ~ 0.8 nm. The recorded spikes are markedly longer in duration (t1/2) and lower in frequency, although their amplitude (Imax) is similar to recordings without nanoparticles. Only 5 spikes could be detected in a two-minute recording.

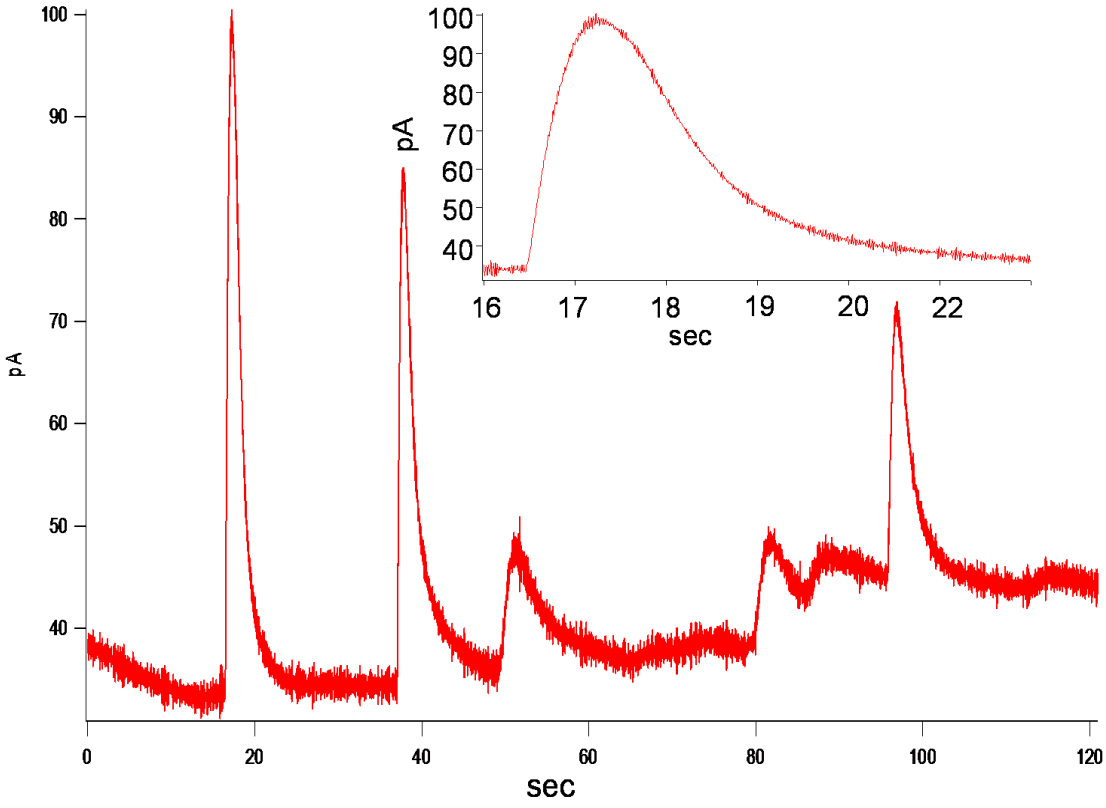

(b)

As can be seen in inset of figure 6-3 b) the spikes recorded with Pt nanoparticles had t1/2 values in the 2 – 4 second range. This is very different

from a device without nanoparticles which have t1/2 values of tens of milliseconds. Consequently, the spike charge (Q) is also ~100x larger, with values in the 150-200 pC range. As previously stated the values obtained with DLC:N on ITO is 26.8 ms for t1/2 and 1.43 pC for Q. I recorded at least 25 spikes from 5 cells on the nanoparticle-sputtered device.

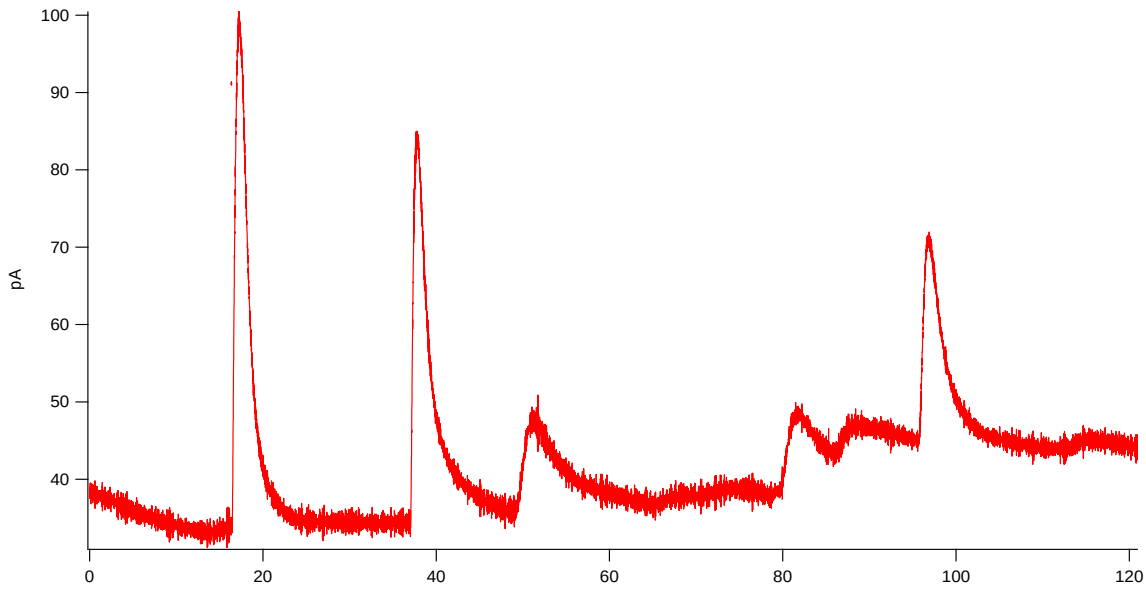

(c)

Figure 6- 3 Amperometric spikes of a) DLC:N on ITO for a duration of 120sec, the inset shows one spike on an expanded scale, b) DLC:N (20nm) on ITO with Pt NPs for a duration of 120sec, c) another sample of a two minute recording from a single cell.

Long-duration spikes with wide t ½ were also reported during measurement of release of reactive species from fibroblasts (Amatore, Arbault et al. 2008), myocytes (Spegel, Heiskanen et al. 2008), macrophages (Amatore, Arbault et al. 2008), bovine embryos (Adams, Puchades et al. 2008), neutrophyls and phagocytes (Amatore, Arbault et al. 2008), and glial cells (McNeil and Manning 2002).

6-5-1 Long-term (10 min) cell recording

Figure 6-4 a), b) and c) depict amperometric recordings obtained over a 10 minute period from a single cell. Each sweep is a two-minute recording. The electrode was held at 600 mV. Three spikes are evident in figure 6-4 a), the amplitude of the first spike is ~50 pA and t ½ is in the 5-8 sec range. The second and the third spikes have smaller amplitudes but the half-widths are still seconds in duration.

Sweep 113(0-2 min)

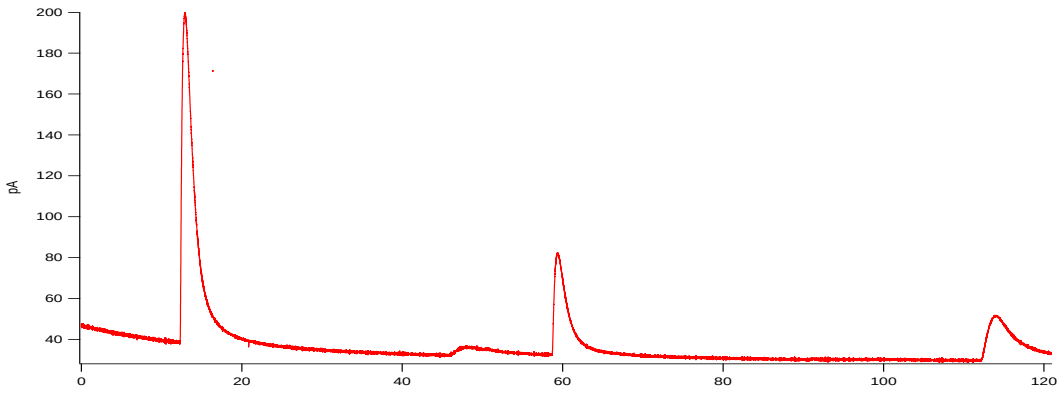

(a)

The following two minute recording shows spikes with 50 pA amplitude, and 10-15 sec values of t ½ . Note that a smaller bump in current is evident immediately proceeding many of the larger amperometric spikes. It is interesting to speculate that these may be pre-spike foot signals representing transmitter release from a fusion pore as described previously (Ales, Tabares et al. 1999)

Sweep 114 (2- 4 min)

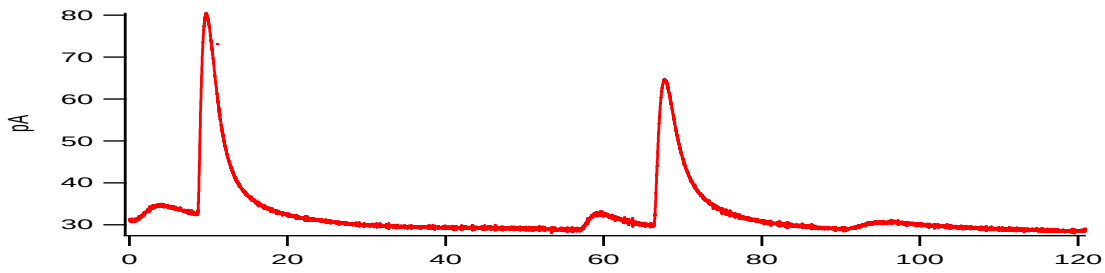

(b)

Sweep 118 (8- 10 min)

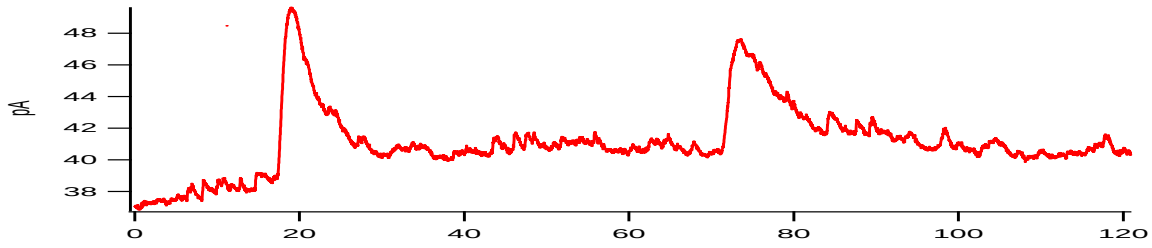

(c)

Figure 6-4 Amperometric spikes from the DLC:N on ITO-Pt NPs 10 Sec sputtered at 200°C from different cells for a period of 10 minutes from the same cell.

It could be inferred from the above recordings that release of an electoactive analyte from the cell occurred for a period of at least 10 minutes. The spike amplitudes decreased over this period but the half-widths grew wider.

6-5-2 Effects of electrode potential on the long-duration spikes

The electrode potential was varied in order to probe the potentials where oxidation of the electroactive analyte occurs. Figure 6-5 a) shows recordings from the electrode held at 600 mV. Long-duration amperometric spikes are clearly evident.

Sweep 28 600 mV

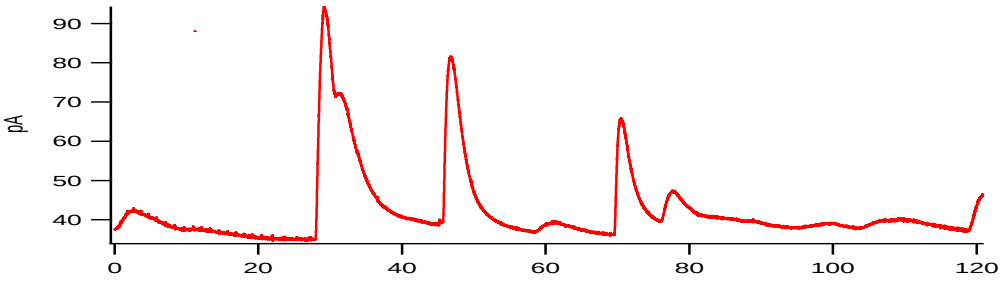

(a)

Figure 6-5 b) shows recordings with electrode potential held at 800 mV. There is no apparent change in the ability of the electrode to record the long-duation spikes.

Sweep 95 800 mV

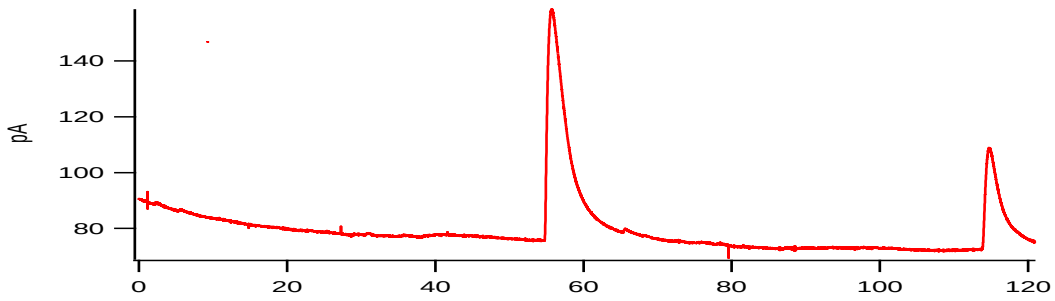

(b)

Figure 6-5 Amperometric spikes from the DLC:N on ITO-Pt NPs 10 Sec sputtered at 200°C from different cells at varying electrode potentials a) 600 mV and b) 800 mV.

Next, the device was cleaned with plasma for 30 Sec; to perform amperometric measurements. The wide spikes were still visible at voltage 600 mV as can be seen in sweep figure 6-6 a), when the voltage was raised to 1000 mV as can be seen in b), all the spikes look like the regular amperometric spikes without the broadening effect.

Raising the voltage to 1000 mV does not disassociate or dissolve the Pt nanoparticles. The particles remain intact as explained above when wide spikes are observed even after reverting from 1000 mV to 600 mV. Large spikes are not evident after stepping the electrode potential to + 500 mV (figure. 6-6 c). This probably means that the species is being oxidized at potential closer to 600 mV than to 500 mV.

Sweep 152 600 mV

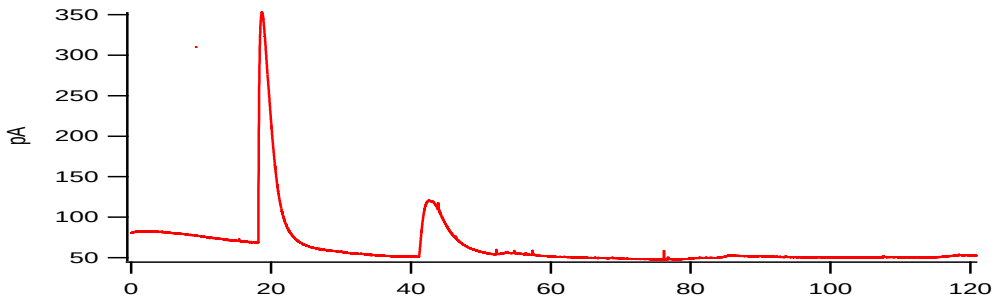

(a)

Sweep 154 1000 mV

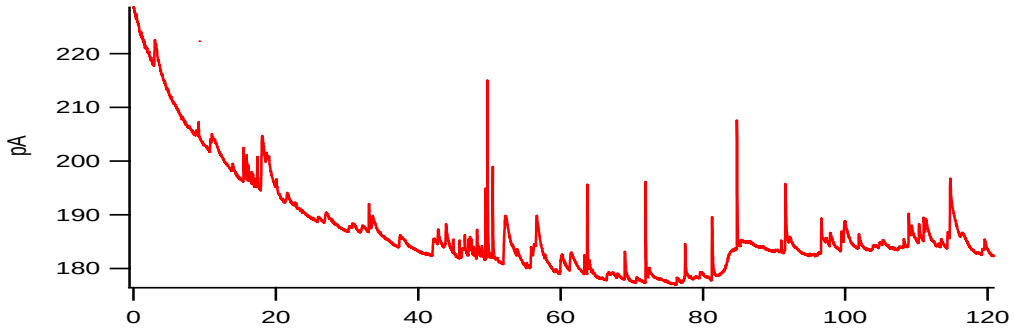

(b)

Sweep 157 500 mV

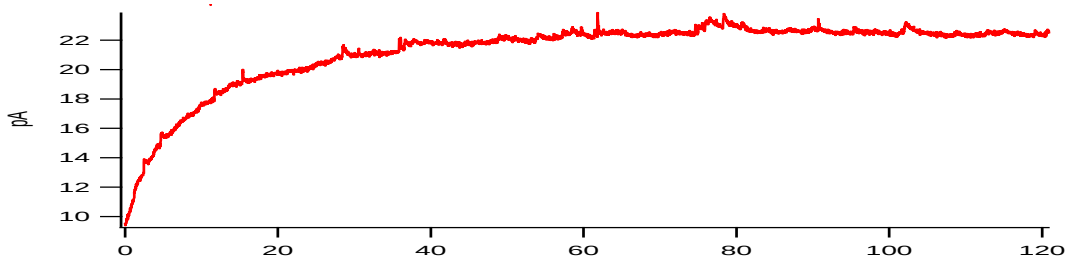

(c)

Figure 6-6 Amperometric spikes from the DLC:N on ITO-Pt NPs 10 Sec sputtered at 200°C treated with plasma and tested at varying voltage a) 600mV, b) 1000 mV and c) 500 mV.

It is important to note that the device gives regular spikes and not the broadened spikes when the voltage is raised from 600 mV to 1000 mV. The reason for this could be that the nanoparticles may be at a different potential relative to the DLC:N on ITO film due to the Coulombic charge energy. Thus once catecholamines are oxidized to quinones on the DLC, perhaps they are reduced again on the nanoparticles. This would allow subsequent oxidation again on the DLC to amplify the total charge measured because more than two electrons would be transferred per catecholamine molecule. In this way the catecholamine would act to discharge the stored charge of the nanoparticles. Increasing the potential from 600 mV to 1000 mV may have discharged the nanoparticles so that they are no longer at a potential whereby they can reduce the quinones, thus normal amperometric spikes are evident.

6-5-3 Spike Analysis

DLC:N (20nm) -ITO-Pt NP's 10 Sec sputter

The parameters measured from amperometric spikes were I max (pA), t ½ and Q (pC), As can be seen in the table below and the consequent tables on the sweep analysis pages, though the amplitude of these spikes are similar to regular amperometric spikes, the charge and half-width have larger values.

Sweep analysis 90

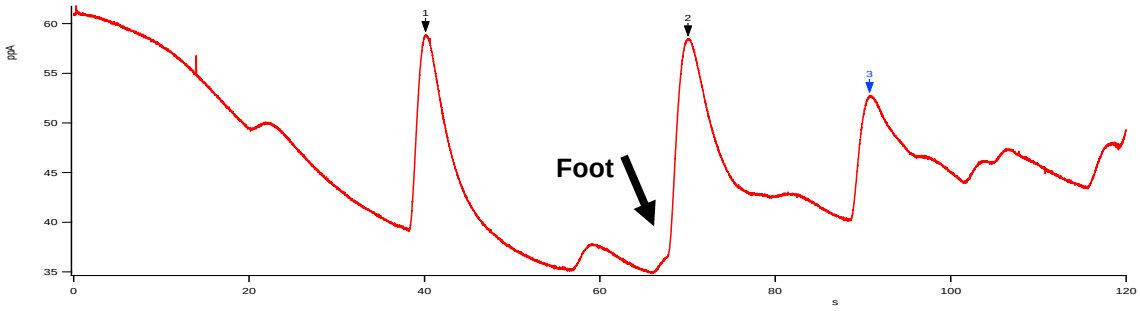

t1/2 (mS)	Imax (A)	Q (C)
3217.846	1.97989e-11	7.23870e-11
4471.313	2.19653e-11	1.01009e-10

Analysis of the foot signal

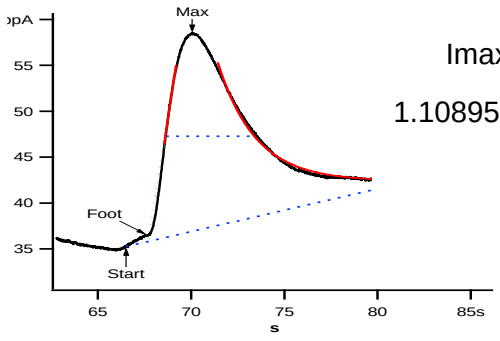

Imax (A)	t1/2 (mS)	Q (C)
1.10895e-12	1045.50	1.39250e-13

(a)

Sweep analysis 113

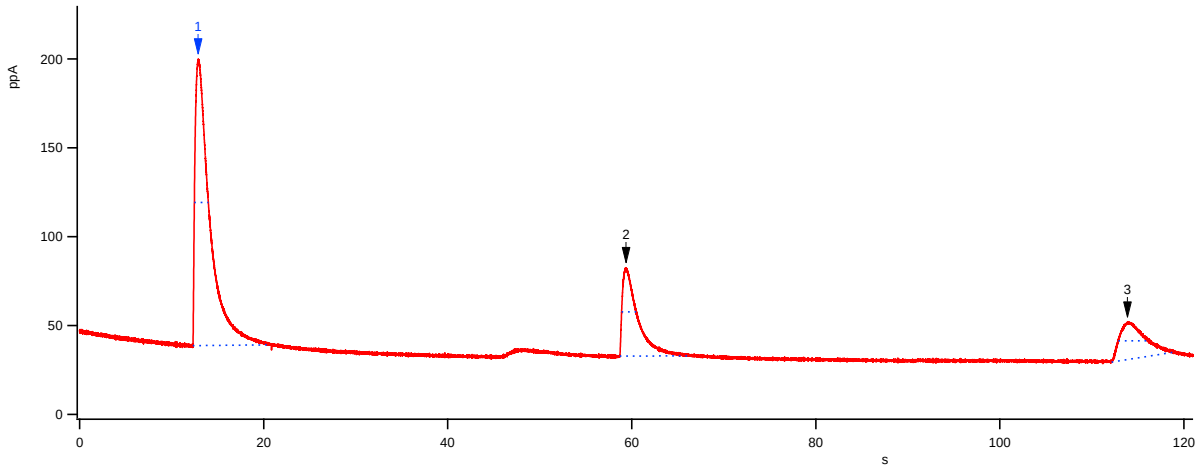

t1/2 (mS)	Imax (A)	Q (C)
1516.365	1.61223e-10	3.01210e-10
1566.952	4.95810e-11	9.59568e-11
3203.262	2.10106e-11	6.63950e-11

Mean I max = 77 pA Mean t ½ = 2095 mS Mean Q = 154 pC

(b)

Figure 6-7 Analysis of amperometric spikes from DLC:N on ITO-Pt NPs 10 Sec sputtered at 200°C a) analysis from one individual cell with foot , b) analysis from another spike without foot.

6-6 Conclusions

From the data and analysis presented in the chapter a few informed conclusions could be made: 1) The properties of the DLC:N on ITO microelectrode change with the sputtering of Pt nanoparticles, 2) The device is detecting an unknown electroactive substance released from the cells with the Pt sputtered device. One possibility is that the released substances are reactive oxygen species or reactive nitrogen species such as NO. 3) In one experiment, increasing the electrode potential from 600mV to 1000 mV eliminated the long-duration amperometric spikes.

There are a couple of experiment that could be performed to confirm that the spikes being detected are coming from the reactive species: 1) Repeat the experiments at various potentials many times to confirm the holding potential at which these spikes are detected and 2) Inhibit the release of catecholamines by using a exocytosis inhibitor like botulinum toxin and perform the same experiment.

The first series of experiments will provide the exact voltage window in which the big spikes are being detected and will provide insight into which species are likely to be oxidized at that particular potential, and the second set of experiments will confirm if these spikes are from the reactive species as the release of catecholamine is blocked by the inhibitor.

If the big spikes are visible from the recordings of cells with inhibited exocytosis, then other possible processes like amplification of catecholamines by the process of multiple redox activity should be looked into.

In conclusion it could be said, that this was a successful demonstration of a carbon based electrode (Diamond like carbon on Indium tin oxide) with good electrochemical properties that could be incorporated with Pt nanoparticles (all batch-process compatible) in probable detection of reactive species from chromaffin cells. This study would complement the other research going on to study oxidative stress using a microfabricated device, the thorough and quick understanding of which might provide important progress in understanding of some ailments and their cure.

References

Abrams, J. M. and M. A. White (2004). "Coordination of cell death and the cell cycle: linking proliferation to death through private and communal couplers." Current Opinion in Cell Biology **16**(6): 634-638.

Adams, K. L., M. Puchades, et al. (2008). "In Vitro Electrochemistry of Biological Systems." Annual Review of Analytical Chemistry **1**(1): 329-355.

Adams, R. N., E. Murrill, et al. (1972). "6-Hydroxydopamine, a new oxidation mechanism." European Journal of Pharmacology **17**(2): 287-292.

Albillos, A., G. Dernick, et al. (1997). "The exocytotic event in chromaffin cells revealed by patch amperometry." Nature **389**(6650): 509-512.

Ales, E., L. Tabares, et al. (1999). "High calcium concentrations shift the mode of exocytosis to the kiss-and-run mechanism." Nat Cell Biol **1**(1): 40-44.

Ales, E., L. Tabares, et al. (1999). "High calcium concentrations shift the mode of exocytosis to the kiss-and-run mechanism." Nat Cell Biol **1**(1): 40-44.

Allen, M., B. Myer, et al. (2001). "<I>In vitro</I> and <I>in vivo</I> investigations into the biocompatibility of diamond-like carbon (DLC) coatings for orthopedic applications." Journal of Biomedical Materials Research **58**(3): 319-328.

Amatore, C., S. Arbault, et al. (2009). "Quantitative investigations of amperometric spike feet suggest different controlling factors of the fusion pore in exocytosis at chromaffin cells." Biophys Chem **143**(3): 124-131.

Amatore, C., S. Arbault, et al. (2006). "Monitoring in real time with a microelectrode the release of reactive oxygen and nitrogen species by a single macrophage stimulated by its membrane mechanical depolarization." Chembiochem **7**(4): 653-661.

Amatore, C., S. Arbault, et al. (2008). "Real-time amperometric analysis of reactive oxygen and nitrogen species released by single immunostimulated macrophages." Chembiochem **9**(9): 1472-1480.

Amatore, C., S. Arbault, et al. (2007). "Electrochemical detection in a microfluidic device of oxidative stress generated by macrophage cells." Lab Chip **7**(2): 233-238.

Amatore, C., S. Arbault, et al. (2008). "Triangulation mapping of oxidative bursts released by single fibroblasts by amperometry at microelectrodes." Anal Chem **80**(24): 9635-9641.

Amatore, C., S. Arbault, et al. (2008). "Electrochemical monitoring of single cell secretion: vesicular exocytosis and oxidative stress." Chem Rev **108**(7): 2585-2621.

Amatore, C., S. p. Arbault, et al. (2009). "Invariance of Exocytotic Events Detected by Amperometry as a Function of the Carbon Fiber Microelectrode Diameter." Analytical Chemistry **81**(8): 3087-3093.

Andersson, H. and A. v. d. Berg (2004). Microfluidic devices for cellomics**:** 1-22.

Andersson, H. and A. van den Berg (2003). "Microfluidic devices for cellomics: a review." Sensors and Actuators B: Chemical **92**(3): 315-325.

Andersson, H. and A. van den Berg (2004). "Microfabrication and microfluidics for tissue engineering: state of the art and future opportunities." Lab Chip **4**(2): 98-103.

Andersson, H. and A. van den Berg (2004). "Microtechnologies and nanotechnologies for single-cell analysis." Current Opinion in Biotechnology **15**(1): 44-49.

Angleson, J. K. and W. J. Betz (1997). "Monitoring secretion in real time: capacitance, amperometry and fluorescence compared." Trends Neurosci **20**(7): 281-287.

Arbault, S., N. Sojic, et al. (2004). "Oxidative stress in cancer prone xeroderma pigmentosum fibroblasts. Real-time and single cell monitoring of superoxide and nitric oxide production with microelectrodes." Carcinogenesis **25**(4): 509-515.

Archer, D. A., M. E. Graham, et al. (2002). "Complexin regulates the closure of the fusion pore during regulated vesicle exocytosis." J Biol Chem **277**(21): 18249-18252.

Arnell, R. D. and P. J. Kelly (1999). "Recent advances in magnetron sputtering." Surface and Coatings Technology **112**(1-3): 170-176.

Ashery, U., F. Varoqueaux, et al. (2000). "Munc13-1 acts as a priming factor for large dense-core vesicles in bovine chromaffin cells." EMBO J **19**(14): 3586-3596.

Bai, H.-J., M.-L. Shao, et al. (2009). "Patterned Au/Poly(dimethylsiloxane) Substrate Fabricated by Chemical Plating Coupled with Electrochemical Etching for Cell Patterning." Langmuir **25**(17): 10402-10407.

Banovec, A. and M. Kern "Comparison between chemical and pulsed laser etching of indium tin oxide thin films." Vacuum **43**(5-7): 737-739.

Bao, M. and W. Wang (1996). "Future of microelectromechanical systems (MEMS)." Sensors and Actuators A: Physical **56**(1-2): 135-141.

Bashir, R. (2004). "BioMEMS: state-of-the-art in detection, opportunities and prospects." Advanced Drug Delivery Reviews **56**(11): 1565-1586.

Baynes, J. W. (1991). "Role of oxidative stress in development of complications in diabetes." Diabetes **40**(4): 405-412.

Bayr, H. (2005). "Reactive oxygen species." Critical Care Medicine **33**(12): S498-S501 410.1097/1001.CCM.0000186787.0000164500.0000186712.

Beal, M. F. (1995). "Aging, energy, and oxidative stress in neurodegenerative diseases." Annals of Neurology **38**(3): 357-366.

Becker, H. and C. Gärtner (2000). "Polymer microfabrication methods for microfluidic analytical applications." Electrophoresis **21**(1): 12-26.

Beebe, D. J., G. A. Mensing, et al. (2002). "PHYSICS AND APPLICATIONS OF MICROFLUIDICS IN BIOLOGY." Annual Review of Biomedical Engineering **4**(1): 261-286.

Beensh-Marchwicka, G., L. Kròl-Stepniewska, et al. (1982). "Effect of the oxygen pressure during sputtering on the properties of thin CuOx films." Thin Solid Films **88**(1): 33-39.

Borges, R., M. Camacho, et al. (2008). "Measuring secretion in chromaffin cells using electrophysiological and electrochemical methods." Acta Physiologica **192**(2): 173-184.

Brannon-Peppas, L. (1995). "Recent advances on the use of biodegradable microparticles and nanoparticles in controlled drug delivery." International Journal of Pharmaceutics **116**(1): 1-9.

Britland, S., E. Perez-Arnaud, et al. (1992). "Micropatterning proteins and synthetic peptides on solid supports: a novel application for microelectronics fabrication technology." Biotechnol Prog **8**(2): 155-160.

Bruns, D. (2004). "Detection of transmitter release with carbon fiber electrodes." Methods **33**(4): 312-321.

Burda, C., Y. Lou, et al. (2003). "Enhanced Nitrogen Doping in TiO2 Nanoparticles." Nano Letters **3**(8): 1049-1051.

Buttke, T. M. and P. A. Sandstrom (1994). "Oxidative stress as a mediator of apoptosis." Immunology Today **15**(1): 7-10.

Campese, V. M., S. Ye, et al. (2004). "Reactive oxygen species stimulate central and peripheral sympathetic nervous system activity." Am J Physiol Heart Circ Physiol **287**(2): H695-703.

Carmignoto, G. (2000). "Reciprocal communication systems between astrocytes and neurones." Progress in Neurobiology **62**(6): 561-581.

Ceccarelli, B., W. P. Hurlbut, et al. (1973). "TURNOVER OF TRANSMITTER AND SYNAPTIC VESICLES AT THE FROG NEUROMUSCULAR JUNCTION." J. Cell Biol. **57**(2): 499-524.

Chang, J. C., G. J. Brewer, et al. (2000). "Microelectrode Array Recordings of Patterned Hippocampal Neurons for Four Weeks." Biomedical Microdevices **2**(4): 245-253.

Chen, G., P. Gavin, et al. (1995). "Observation and quantitation of exocytosis from the cell body of a fully developed neuron in Planorbis corneus." J. Neurosci. **15**(11): 7747-7755.

Chen, X. X., Y. Wang, et al. (2008). "A novel amperometric sensor for the determination of nitric oxide, and its application in rat liver cells." Microchimica Acta **161**(1): 255-263.

Chicharro, M., A. Sánchez, et al. (2004). "Capillary electrophoresis of neurotransmitters with amperometric detection at melanin-type polymer-modified carbon electrodes." Analytica Chimica Acta **523**(2): 185-191.

Chow, R. H., L. von Ruden, et al. (1992). "Delay in vesicle fusion revealed by electrochemical monitoring of single secretory events in adrenal chromaffin cells." Nature **356**(6364): 60-63.

Ciolkowski, E. L., K. M. Maness, et al. (1994). "Disproportionation During Electrooxidation of Catecholamines at Carbon-Fiber Microelectrodes." Analytical Chemistry **66**(21): 3611-3617.

Cooper, J. M., P. L. Foreman, et al. (1995). "Glutamate oxidase enzyme electrodes: microsensors for neurotransmitter determination using electrochemically polymerized permselective films." Journal of Electroanalytical Chemistry **388**(1-2): 143-149.

Cooper, J. M., K. R. Greenough, et al. (1993). "Direct electron transfer reactions between immobilized cytochrome c and modified gold electrodes." Journal of Electroanalytical Chemistry **347**(1-2): 267-275.

Corey, J. M., A. L. Brunette, et al. (1997). "Differentiated B104 neuroblastoma cells are a high-resolution assay for micropatterned substrates." Journal of Neuroscience Methods **75**(1): 91-97.

Coyle, J. and P. Puttfarcken (1993). "Oxidative stress, glutamate, and neurodegenerative disorders." Science **262**(5134): 689-695.

Cummings, E. B. and A. K. Singh (2003). "Dielectrophoresis in Microchips Containing Arrays of Insulating Posts:â€‰ Theoretical and Experimental Results." Analytical Chemistry **75**(18): 4724-4731.

Das, C. M., F. Becker, et al. (2005). "Dielectrophoretic Segregation of Different Human Cell Types on Microscope Slides." Analytical Chemistry **77**(9): 2708-2719.

Dayton, M. A., J. C. Brown, et al. (1980). "Faradaic electrochemistry at microvoltammetric electrodes." Analytical Chemistry **52**(6): 946-950.

de Sande, J. C. G., C. N. Afonso, et al. (1992). "Optical properties of laser-deposited a-Ge films: a comparison with sputtered and e-beam-deposited films." Appl. Opt. **31**(28): 6133-6138.

Deinhammer, R. S., M. Ho, et al. (1994). "Electrochemical oxidation of amine-containing compounds: a route to the surface modification of glassy carbon electrodes." Langmuir **10**(4): 1306-1313.

Deng, T., J. Tien, et al. (1999). "Using Patterns in Microfiche as Photomasks in 10-μm-Scale Microfabrication." Langmuir **15**(19): 6575-6581.

Ding, S.-J., P.-F. Wang, et al. (2001). "A novel structural amorphous fluoropolymer film with an ultra-low dielectric constant." Materials Letters **49**(3-4): 154-159.

Dittrich, P. S. and A. Manz (2006). "Lab-on-a-chip: microfluidics in drug discovery." Nat Rev Drug Discov **5**(3): 210-218.

Du, Y., E. Lo, et al. (2008). "Method of Bottom-Up Directed Assembly of Cell-Laden Microgels." Cellular and Molecular Bioengineering **1**(2): 157-162.

El-Ali, J., P. K. Sorger, et al. (2006). "Cells on chips." Nature **442**(7101): 403-411.

Engelmann, M. D., R. T. Bobier, et al. (2003). "Variability of the Fenton reaction characteristics of the EDTA, DTPA, and citrate complexes of iron." BioMetals **16**(4): 519-527.

Evans, S. A. G., J. M. Elliott, et al. (2002). "Detection of Hydrogen Peroxide at Mesoporous Platinum Microelectrodes." Analytical Chemistry **74**(6): 1322-1326.

Falconnet, D., G. Csucs, et al. (2006). "Surface engineering approaches to micropattern surfaces for cell-based assays." Biomaterials **27**(16): 3044-3063.

Fang, Q., K. Berberian, et al. (2008). "The role of the C terminus of the SNARE protein SNAP-25 in fusion pore opening and a model for fusion pore mechanics." Proceedings of the National Academy of Sciences **105**(40): 15388-15392.

Ferrari, A. C. "Determination of bonding in diamond-like carbon by Raman spectroscopy." Diamond and Related Materials **11**(3-6): 1053-1061.

Ferreira, N. G., L. L. G. Silva, et al. (2002). "Kinetics study of diamond electrodes at different levels of boron doping as quasi-reversible systems." Diamond and Related Materials **11**(8): 1523-1531.

Fiedler, S., S. G. Shirley, et al. (1998). "Dielectrophoretic Sorting of Particles and Cells in a Microsystem." Analytical Chemistry **70**(9): 1909-1915.

Finkel, T. and N. J. Holbrook (2000). "Oxidants, oxidative stress and the biology of ageing." Nature **408**(6809): 239-247.

Finnegan, J. M., K. Pihel, et al. (1996). "Vesicular Quantal Size Measured by Amperometry at Chromaffin, Mast, Pheochromocytoma, and Pancreatic β-Cells." Journal of Neurochemistry **66**(5): 1914-1923.

Finnegan, J. M., K. Pihel, et al. (1996). "Vesicular quantal size measured by amperometry at chromaffin, mast, pheochromocytoma, and pancreatic beta-cells." J Neurochem **66**(5): 1914-1923.

Fox, M., D. Esveld, et al. (2006). "Electroporation of cells in microfluidic devices: a review." Analytical and Bioanalytical Chemistry **385**(3): 474-485.

Fu, A. Y., H.-P. Chou, et al. (2002). "An Integrated Microfabricated Cell Sorter." Analytical Chemistry **74**(11): 2451-2457.

Fubini, B. and A. Hubbard (2003). "Reactive oxygen species (ROS) and reactive nitrogen species (RNS) generation by silica in inflammation and fibrosis." Free Radical Biology and Medicine **34**(12): 1507-1516.

Galli, A., R. D. Blakely, et al. (1998). "Patch-clamp and amperometric recordings from norepinephrine transporters: Channel activity and voltage-dependent uptake." Proceedings of the National Academy of Sciences of the United States of America **95**(22): 13260-13265.

Ganesh, V., S. K. Pal, et al. (2006). "Self-assembled monolayers (SAMs) of alkoxycyanobiphenyl thiols on gold--A study of electron transfer reaction using cyclic voltammetry and electrochemical impedance spectroscopy." Journal of Colloid and Interface Science **296**(1): 195-203.

Gao, Y., X. Chen, et al. (2008). "Magnetron sputtered diamond-like carbon microelectrodes for on-chip measurement of quantal catecholamine release from cells." Biomed Microdevices **10**(5): 623-629.

Gelperina, S., K. Kisich, et al. (2005). "The Potential Advantages of Nanoparticle Drug Delivery Systems in Chemotherapy of Tuberculosis." Am. J. Respir. Crit. Care Med. **172**(12): 1487-1490.

Gil, A., J. Rueda, et al. (2000). "The F-actin cytoskeleton modulates slow secretory components rather than readily releasable vesicle pools in bovine chromaffin cells." Neuroscience **98**(3): 605-614.

Giugliano, D., A. Ceriello, et al. (1996). "Oxidative stress and diabetic vascular complications." Diabetes Care **19**(3): 257-267.

Gobi, K. V. and F. Mizutani (2000). "Efficient mediatorless superoxide sensors using cytochrome c-modified electrodes: surface nano-organization for selectivity and controlled peroxidase activity." Journal of Electroanalytical Chemistry **484**(2): 172-181.

Gong, L.-W., I. Hafez, et al. (2003). "Secretory Vesicles Membrane Area Is Regulated in Tandem with Quantal Size in Chromaffin Cells." J. Neurosci. **23**(21): 7917-7921.

Graham, M. E., R. J. Fisher, et al. (2000). "Measurement of exocytosis by amperometry in adrenal chromaffin cells: Effects of clostridial neurotoxins and activation of protein kinase C on fusion pore kinetics." Biochimie **82**(5): 469-479.

Grill, A. (1993). "Review of the tribology of diamond-like carbon." Wear **168**(1-2): 143-153.

Grill, A. (1999). "Electrical and optical properties of diamond-like carbon." Thin Solid Films **355-356**: 189-193.

Grill, A. (2003). "Diamond-like carbon coatings as biocompatible materials--an overview." Diamond and Related Materials **12**(2): 166-170.

Hafez, I., K. Kisler, et al. (2005). "Electrochemical imaging of fusion pore openings by electrochemical detector arrays." Proceedings of the National Academy of Sciences of the United States of America **102**(39): 13879-13884.

Han, G., P. Ghosh, et al. (2007). "Functionalized gold nanoparticles for drug delivery." Nanomedicine **2**(1): 113-123.

Hans, M. L. and A. M. Lowman (2002). "Biodegradable nanoparticles for drug delivery and targeting." Current Opinion in Solid State and Materials Science **6**(4): 319-327.

Hawley, M. D. and S. W. Feldberg (1966). "Nuances of the ECE Mechanism. I. Development of the Theoretical Relationships for Chronoamperometry1a." The Journal of Physical Chemistry **70**(11): 3459-3464.

Hellgren, N., M. P. Johansson, et al. (1999). "Role of nitrogen in the formation of hard and elastic CNx thin films by reactive magnetron sputtering." Physical Review B **59**(Copyright (C) 2010 The American Physical Society): 5162.

Hensley, K., K. A. Robinson, et al. (2000). "Reactive oxygen species, cell signaling, and cell injury." Free Radical Biology and Medicine **28**(10): 1456-1462.

Hernández, P., I. Sánchez, et al. (1998). "Cyclic voltammetry determination of epinephrine with a carbon fiber ultramicroelectrode." Talanta **46**(5): 985-991.

Heuser, J. E. and T. S. Reese (1973). "EVIDENCE FOR RECYCLING OF SYNAPTIC VESICLE MEMBRANE DURING TRANSMITTER RELEASE AT THE FROG NEUROMUSCULAR JUNCTION." J. Cell Biol. **57**(2): 315-344.

Hilt, J. Z., A. K. Gupta, et al. (2003). "Ultrasensitive Biomems Sensors Based on Microcantilevers Patterned with Environmentally Responsive Hydrogels." Biomedical Microdevices **5**(3): 177-184.

Ho, C.-M. and Y.-C. Tai (1996). "REVIEW: MEMS and Its Applications for Flow Control." Journal of Fluids Engineering **118**(3): 437-447.

Hochstetler, S. E., M. Puopolo, et al. (1999). "Real-Time Amperometric Measurements of Zeptomole Quantities of Dopamine Released from Neurons." Analytical Chemistry **72**(3): 489-496.

Hu, X., P. H. Bessette, et al. (2005). "Marker-specific sorting of rare cells using dielectrophoresis." Proceedings of the National Academy of Sciences of the United States of America **102**(44): 15757-15761.

Huang, Y. and B. Rubinsky (2001). "Microfabricated electroporation chip for single cell membrane permeabilization." Sensors and Actuators A: Physical **89**(3): 242-249.

Huang, Y. and B. Rubinsky (2003). "Flow-through micro-electroporation chip for high efficiency single-cell genetic manipulation." Sensors and Actuators A: Physical **104**(3): 205-212.

Hynes, A. M., H. Ashraf, et al. (1999). "Recent advances in silicon etching for MEMS using the ASE(TM) process." Sensors and Actuators A: Physical **74**(1-3): 13-17.

ICHINOSE, M., H. SUGIURA, et al. (2000). "Increase in Reactive Nitrogen Species Production in Chronic Obstructive Pulmonary Disease Airways." Am. J. Respir. Crit. Care Med. **162**(2): 701-706.

Jackson, M. B. (2007). "In search of the fusion pore of exocytosis." Biophysical Chemistry **126**(1-3): 201-208.

Jain, P. K., K. S. Lee, et al. (2006). "Calculated Absorption and Scattering Properties of Gold Nanoparticles of Different Size, Shape, and Composition: Applications in Biological Imaging and Biomedicine." The Journal of Physical Chemistry B **110**(14): 7238-7248.

Jenner, P. (2003). "Oxidative stress in Parkinson's disease." Annals of Neurology **53**(S3): S26-S38.

Joshi, R. N., V. P. Singh, et al. (1995). "Characteristics of indium tin oxide films deposited by r.f. magnetron sputtering." Thin Solid Films **257**(1): 32-35.

Jun, S. B., M. R. Hynd, et al. (2007). "Low-density neuronal networks cultured using patterned poly-l-lysine on microelectrode arrays." Journal of Neuroscience Methods **160**(2): 317-326.

Karam, P. and L. I. Halaoui (2008). "Sensing of H2O2 at Low Surface Density Assemblies of Pt Nanoparticles in Polyelectrolyte." Analytical Chemistry **80**(14): 5441-5448.

Karyakin, A. A., E. A. Puganova, et al. (2003). "Prussian Blue Based Nanoelectrode Arrays for H2O2 Detection." Analytical Chemistry **76**(2): 474-478.

Kaufman, J. H., S. Metin, et al. (1989). "Symmetry breaking in nitrogen-doped amorphous carbon: Infrared observation of the Raman-active G and D bands." Physical Review B **39**(Copyright (C) 2010 The American Physical Society): 13053.

Kelly, P. J. and R. D. Arnell (2000). "Magnetron sputtering: a review of recent developments and applications." Vacuum **56**(3): 159-172.

Kelly, S., E. M. Regan, et al. (2008). "Patterned growth of neuronal cells on modified diamond-like carbon substrates." Biomaterials **29**(17): 2573-2580.

Khanna, A., D. G. Bhat, et al. (2006). "Growth and characterization of chromium oxide thin films prepared by reactive ac magnetron sputtering." Journal of Vacuum Science & Technology A: Vacuum, Surfaces, and Films **24**(5): 1870-1877.

Koh, T.-W. and H. J. Bellen (2003). "Synaptotagmin I, a Ca2+ sensor for neurotransmitter release." Trends in Neurosciences **26**(8): 413-422.

Kohen, R., E. Vellaichamy, et al. (2000). "Quantification of the overall REACTIVE OXYGEN SPECIES scavenging capacity of biological fluids and tissues." Free Radical Biology and Medicine **28**(6): 871-879.

Kopp, M. U., H. J. Crabtree, et al. (1997). "Developments in technology and applications of microsystems." Current Opinion in Chemical Biology **1**(3): 410-419.

Kotzar, G., M. Freas, et al. (2002). "Evaluation of MEMS materials of construction for implantable medical devices." Biomaterials **23**(13): 2737-2750.

Lafon, E. E. and H. A. Pohl (1981). "Critical fields in cell fusion and dielectrophoresis." Journal of Biological Physics **9**(4): 209-217.

Laux, S., N. Kaiser, et al. (1998). "Room-temperature deposition of indium tin oxide thin films with plasma ion-assisted evaporation." Thin Solid Films **335**(1-2): 1-5.

Laviron, E. (1979). "A.C. polarography and faradaic impedance of strongly adsorbed electroactive species: Part I. Theoretical and experimental study of a quasi-reversible reaction in the case of a Langmuir isotherm." Journal of Electroanalytical Chemistry **97**(2): 135-149.

Lehnert, D., B. Wehrle-Haller, et al. (2004). "Cell behaviour on micropatterned substrata: limits of extracellular matrix geometry for spreading and adhesion." J Cell Sci **117**(1): 41-52.

Lettington, A. H. (1998). "Applications of diamond-like carbon thin films." Carbon **36**(5-6): 555-560.

Lin, R.-Z., C.-T. Ho, et al. (2006). "Dielectrophoresis based-cell patterning for tissue engineering." Biotechnology Journal **1**(9): 949-957.

Lindau, M. and G. Alvarez de Toledo (2003). "The fusion pore." Biochimica et Biophysica Acta (BBA) - Molecular Cell Research **1641**(2-3): 167-173.

Linder, V., H. Wu, et al. (2003). "Rapid Prototyping of 2D Structures with Feature Sizes Larger than 8 µm." Analytical Chemistry **75**(10): 2522-2527.

Lindgren, T., J. M. Mwabora, et al. (2003). "Photoelectrochemical and Optical Properties of Nitrogen Doped Titanium Dioxide Films Prepared by Reactive DC Magnetron Sputtering." The Journal of Physical Chemistry B **107**(24): 5709-5716.

Machado, J. D., C. Alonso, et al. (2002). "Nongenomic regulation of the kinetics of exocytosis by estrogens." J Pharmacol Exp Ther **301**(2): 631-637.

Mailly, F., A. Giani, et al. (2001). "Anemometer with hot platinum thin film." Sensors and Actuators A: Physical **94**(1-2): 32-38.

Makohliso, S. A., L. Giovangrandi, et al. (1998). "Application of Teflon-AF® thin films for bio-patterning of neural cell adhesion." Biosensors and Bioelectronics **13**(11): 1227-1235.

Malacombe, M., M. F. Bader, et al. (2006). "Exocytosis in neuroendocrine cells: new tasks for actin." Biochim Biophys Acta **1763**(11): 1175-1183.

Malinski, T. and Z. Taha (1992). "Nitric oxide release from a single cell measured in situ by a porphyrinic-based microsensor." Nature **358**(6388): 676-678.

Manna, A., T. Imae, et al. (2001). "Synthesis of Dendrimer-Passivated Noble Metal Nanoparticles in a Polar Medium: Comparison of Size between Silver and Gold Particles." Chemistry of Materials **13**(5): 1674-1681.

Manning, P., C. J. McNeil, et al. (1998). "Direct, Real-Time Sensing of Free Radical Production by Activated Human Glioblastoma Cells." Free Radical Biology and Medicine **24**(7-8): 1304-1309.

Manos, P., J. J. Pancrazio, et al. (1999). "Characterization of rat spinal cord neurons cultured in defined media on microelectrode arrays." Neuroscience Letters **271**(3): 179-182.

Mardare, D., M. Tasca, et al. (2000). "On the structural properties and optical transmittance of TiO2 r.f. sputtered thin films." Applied Surface Science **156**(1-4): 200-206.

Markesbery, W. R. (1997). "Oxidative Stress Hypothesis in Alzheimer's Disease." Free Radical Biology and Medicine **23**(1): 134-147.

Marks, G. H., Y. Huang, et al. (1994). "Dielectrophoretic characterization and separation of micro-organisms." Microbiology **140**(3): 585-591.

Markx, G. H., P. A. Dyda, et al. (1996). "Dielectrophoretic separation of bacteria using a conductivity gradient." Journal of Biotechnology **51**(2): 175-180.

Matson, W., P. Langlais, et al. (1984). "n-Electrode three-dimensional liquid chromatography with electrochemical detection for determination of neurotransmitters." Clin Chem **30**(9): 1477-1488.

May, C. and J. Strümpfel (1999). "ITO coating by reactive magnetron sputtering-comparison of properties from DC and MF processing." Thin Solid Films **351**(1-2): 48-52.

Mayer, M., J. K. Kriebel, et al. (2003). "Microfabricated Teflon Membranes for Low-Noise Recordings of Ion Channels in Planar Lipid Bilayers." Biophysical Journal **85**(4): 2684-2695.

McArdle, F., D. M. Pattwell, et al. (2005). "Intracellular generation of reactive oxygen species by contracting skeletal muscle cells." Free Radical Biology and Medicine **39**(5): 651-657.

McDonald, J. C., D. C. Duffy, et al. (2000). "Fabrication of microfluidic systems in poly(dimethylsiloxane)." Electrophoresis **21**(1): 27-40.

McDonald, J. C. and G. M. Whitesides (2002). "Poly(dimethylsiloxane) as a Material for Fabricating Microfluidic Devices." Accounts of Chemical Research **35**(7): 491-499.

McNeil, C. J., K. R. Greenough, et al. (1992). "Electrochemical Sensors for Direct Reagentless Measurement of Superoxide Production by Human Neutrophils." Free Radical Research **17**(6): 399 - 406.

McNeil, C. J. and P. Manning (2002). "Sensor-based measurements of the role and interactions of free radicals in cellular systems." Reviews in Molecular Biotechnology **82**(4): 443-455.

Michael, D. J. and R. M. Wightman (1999). "Electrochemical monitoring of biogenic amine neurotransmission in real time." Journal of Pharmaceutical and Biomedical Analysis **19**(1-2): 33-46.

Michel, B., A. Bernard, et al. (2001). "Printing meets lithography: soft approaches to high-resolution patterning." IBM J. Res. Dev. **45**(5): 697-719.

Mihailov, S. and S. Lazare (1993). "Fabrication of refractive microlens arrays by excimer laser ablation of amorphous Teflon." Appl. Opt. **32**(31): 6211-6218.

Mittler, R. (2002). "Oxidative stress, antioxidants and stress tolerance." Trends in Plant Science **7**(9): 405-410.

Miyake, H., S. Ye, et al. (2002). "Electroless deposition of gold thin films on silicon for surface-enhanced infrared spectroelectrochemistry." Electrochemistry Communications **4**(12): 973-977.

Monck, J. R., A. F. Oberhauser, et al. (1995). "The exocytotic fusion pore interface: a model of the site of neurotransmitter release." Molecular Membrane Biology **12**(1): 151-156.

Mosharov, E. V. (2008). "Analysis of single-vesicle exocytotic events recorded by amperometry." Methods Mol Biol **440**: 315-327.

Mosharov, E. V. and D. Sulzer (2005). "Analysis of exocytotic events recorded by amperometry." Nat Methods **2**(9): 651-658.

Müller, R. H., K. Mäder, et al. (2000). "Solid lipid nanoparticles (SLN) for controlled drug delivery - a review of the state of the art." European Journal of Pharmaceutics and Biopharmaceutics **50**(1): 161-177.

Musil, J., J. Lestina, et al. (2001). "Pulsed dc magnetron discharge for high-rate sputtering of thin films." Journal of Vacuum Science & Technology A: Vacuum, Surfaces, and Films **19**(2): 420-424.

Nagaoka, T. and T. Yoshino (1986). "Surface properties of electrochemically pretreated glassy carbon." Analytical Chemistry **58**(6): 1037-1042.

Neher, E. (1992). "Ion channels for communication between and within cells." Bioscience Reports **12**(1): 1-14.

Nicholson, R. S. (1965). "Theory and Application of Cyclic Voltammetry for Measurement of Electrode Reaction Kinetics." Analytical Chemistry **37**(11): 1351-1355.

O'Dea, J. J. and J. G. Osteryoung (1993). "Characterization of quasi-reversible surface processes by square-wave voltammetry." Analytical Chemistry **65**(21): 3090-3097.

O'Donnell, V. B., J. P. Eiserich, et al. (1998). "Nitration of Unsaturated Fatty Acids by Nitric Oxide-Derived Reactive Nitrogen Species Peroxynitrite, Nitrous Acid, Nitrogen Dioxide, and Nitronium Ion." Chemical Research in Toxicology **12**(1): 83-92.

Olanow, C. W. (1993). "A radical hypothesis for neurodegeneration." Trends in Neurosciences **16**(11): 439-444.

Oni, J., A. Pailleret, et al. (2004). "Functionalised electrode array for the detection of nitric oxide released by endothelial cells using different NO-sensing chemistries." Analytical and Bioanalytical Chemistry **378**(6): 1594-1600.

Paciotti, G. F., D. G. I. Kingston, et al. (2006). "Colloidal gold nanoparticles: a novel nanoparticle platform for developing multifunctional tumor-targeted drug delivery vectors." Drug Development Research **67**(1): 47-54.

Palshin, V., E. I. Meletis, et al. (1995). "Characterization of ion-beam-deposited diamond-like carbon films." Thin Solid Films **270**(1-2): 165-172.

Panyam, J. and V. Labhasetwar (2003). "Biodegradable nanoparticles for drug and gene delivery to cells and tissue." Advanced Drug Delivery Reviews **55**(3): 329-347.

Park, S., Y. Xie, et al. (2002). "Electrocatalytic Pathways on Carbon-Supported Platinum Nanoparticles: Comparison of Particle-Size-Dependent Rates of Methanol, Formic Acid, and Formaldehyde Electrooxidation." Langmuir **18**(15): 5792-5798.

Park, T. H. and M. L. Shuler (2003). "Integration of Cell Culture and Microfabrication Technology." Biotechnology Progress **19**(2): 243-253.

Patel, R. P., J. McAndrew, et al. (1999). "Biological aspects of reactive nitrogen species." Biochimica et Biophysica Acta (BBA) - Bioenergetics **1411**(2-3): 385-400.

Patwell, D. M., A. McArdle, et al. (2004). "Release of reactive oxygen and nitrogen species from contracting skeletal muscle cells." Free Radical Biology and Medicine **37**(7): 1064-1072.

Paul, S., C. Pearson, et al. (2003). "Langmuir−Blodgett Film Deposition of Metallic Nanoparticles and Their Application to Electronic Memory Structures." Nano Letters **3**(4): 533-536.

Pethig, R. and G. H. Markx (1997). "Applications of dielectrophoresis in biotechnology." Trends in Biotechnology **15**(10): 426-432.

Pihel, K., S. Hsieh, et al. (1995). "Electrochemical detection of histamine and 5-hydroxytryptamine at isolated mast cells." Analytical Chemistry **67**(24): 4514-4521.

Pihel, K., Q. D. Walker, et al. (1996). "Overoxidized Polypyrrole-Coated Carbon Fiber Microelectrodes for Dopamine Measurements with Fast-Scan Cyclic Voltammetry." Analytical Chemistry **68**(13): 2084-2089.

Pizziconi, V. B. and D. L. Page (1997). "A cell-based immunobiosensor with engineered molecular recognition--Part I: design feasibility." Biosensors and Bioelectronics **12**(4): 287-299.

Reiter, R., D.-x. Tan, et al. (2001). "Biochemical reactivity of melatonin with reactive oxygen and nitrogen species." Cell Biochemistry and Biophysics **34**(2): 237-256.

Resnick, P. and W. Buck (2002). Teflon® AF: A Family of Amorphous Fluoropolymers with Extraordinary Properties**:** 25-33.

Resnick, P. R. (1989). "The preparation and properties of a new family of amorphous fluoropolymers: teflon® AF." Journal of Fluorine Chemistry **45**(1): 100-100.

Rettig, J. and E. Neher (2002). "Emerging Roles of Presynaptic Proteins in Ca++-Triggered Exocytosis." Science **298**(5594): 781-785.

Robertson, J. (1993). "Deposition mechanisms for promoting sp3 bonding in diamond-like carbon." Diamond and Related Materials **2**(5-7): 984-989.

Robertson, J. (2002). "Diamond-like amorphous carbon." Materials Science and Engineering: R: Reports **37**(4-6): 129-281.

Ruske, F., V. Sittinger, et al. (2005). "Hydrogen doping of DC sputtered ZnO:Al films from novel target material." Surface and Coatings Technology **200**(1-4): 236-240.

Sarada, B. V., T. N. Rao, et al. (2000). "Electrochemical Oxidation of Histamine and Serotonin at Highly Boron-Doped Diamond Electrodes." Analytical Chemistry **72**(7): 1632-1638.

Sarro, P. M. (2000). "Silicon carbide as a new MEMS technology." Sensors and Actuators A: Physical **82**(1-3): 210-218.

Scharf, T. W., R. D. Ott, et al. (1999). "Structural and tribological characterization of protective amorphous diamond-like carbon and amorphous CN[sub x] overcoats for next generation hard disks." Journal of Applied Physics **85**(6): 3142-3154.

Schiller, S., G. Beister, et al. (1984). "Reactive high rate D.C. sputtering: Deposition rate, stoichiometry and features of TiOx and TiNx films with respect to the target mode." Thin Solid Films **111**(3): 259-268.

Segura, F., M. A. Brioso, et al. (2000). "Automatic analysis for amperometrical recordings of exocytosis." Journal of Neuroscience Methods **103**(2): 151-156.

Sen, A., S. Barizuddin, et al. (2009). "Preferential cell attachment to nitrogen-doped diamond-like carbon (DLC:N) for the measurement of quantal exocytosis." Biomaterials **30**(8): 1604-1612.

Shawgo, R. S., A. C. Richards Grayson, et al. (2002). "BioMEMS for drug delivery." Current Opinion in Solid State and Materials Science **6**(4): 329-334.

Sies, H. (1997). "Oxidative stress: oxidants and antioxidants." Experimental Physiology **82**(2): 291-295.

Sies, H. (1997). "Oxidative stress: oxidants and antioxidants." Exp Physiol **82**(2): 291-295.

Sigmund, P. (1969). "Theory of Sputtering. I. Sputtering Yield of Amorphous and Polycrystalline Targets." Physical Review **184**(Copyright (C) 2010 The American Physical Society): 383.

Silva, S. R. P. and G. A. J. Amaratunga (1995). "Doping of rf plasma deposited diamond-like carbon films." Thin Solid Films **270**(1-2): 194-199.

Smith, K. J., R. Kapoor, et al. (1999). "Demyelination: The Role of Reactive Oxygen and Nitrogen Species." Brain Pathology **9**(1): 69-92.

Sombers, L. A., H. J. Hanchar, et al. (2004). "The Effects of Vesicular Volume on Secretion through the Fusion Pore in Exocytotic Release from PC12 Cells." J. Neurosci. **24**(2): 303-309.

Spégel, C., A. Heiskanen, et al. (2007). "On-Chip Determination of Dopamine Exocytosis Using Mercaptopropionic Acid Modified Microelectrodes." Electroanalysis **19**(2-3): 263-271.

Spegel, C., A. Heiskanen, et al. (2008). "Fully automated microchip system for the detection of quantal exocytosis from single and small ensembles of cells." Lab Chip **8**(2): 323-329.

Spegel, C., A. Heiskanen, et al. (2008). "Chip Based Electroanalytical Systems for Cell Analysis." Electroanalysis **20**(6): 680-702.

Squires, T. M. and S. R. Quake (2005). "Microfluidics: Fluid physics at the nanoliter scale." Reviews of Modern Physics **77**(3): 977.

Sreenivas, K., M. Sayer, et al. (1989). "Properties of D.C. magnetron-sputtered lead zirconate titanate thin films." Thin Solid Films **172**(2): 251-267.

Stevens, C. F. and J. H. Williams (2000). "“Kiss and run” exocytosis at hippocampal synapses." Proceedings of the National Academy of Sciences of the United States of America **97**(23): 12828-12833.

Subramanian, V., E. E. Wolf, et al. (2003). "Green Emission to Probe Photoinduced Charging Events in ZnO−Au Nanoparticles. Charge Distribution and Fermi-Level Equilibration†." The Journal of Physical Chemistry B **107**(30): 7479-7485.

Sugimoto, W., K. Yokoshima, et al. (2006). "Charge storage mechanism of nanostructured anhydrous and hydrous ruthenium-based oxides." Electrochimica Acta **52**(4): 1742-1748.

Sun, X. and K. D. Gillis (2006). "On-Chip Amperometric Measurement of Quantal Catecholamine Release Using Transparent Indium Tin Oxide Electrodes." Analytical Chemistry **78**(8): 2521-2525.

Sun, X. and K. D. Gillis (2006). "On-chip amperometric measurement of quantal catecholamine release using transparent indium tin oxide electrodes." Anal Chem **78**(8): 2521-2525.

Tadanaga, K., J. Morinaga, et al. (2000). "Superhydrophobicâ^'Superhydrophilic Micropatterning on Flowerlike Alumina Coating Film by the Solâ^'Gel Method." Chemistry of Materials **12**(3): 590-592.

Tak, Y.-H., K.-B. Kim, et al. (2002). "Criteria for ITO (indium-tin-oxide) thin film as the bottom electrode of an organic light emitting diode." Thin Solid Films **411**(1): 12-16.

Tanaka, Y., K. Sato, et al. (2007). "Biological cells on microchips: New technologies and applications." Biosensors and Bioelectronics **23**(4): 449-458.

Tarpey, M. M. and I. Fridovich (2001). "Methods of Detection of Vascular Reactive Species: Nitric Oxide, Superoxide, Hydrogen Peroxide, and Peroxynitrite." Circ Res **89**(3): 224-236.

Tasche, C., E. Meyhofer, et al. (1999). "A force transducer for measuring mechanical properties of single cardiac myocytes." Am J Physiol Heart Circ Physiol **277**(6): H2400-2408.

Teixeira, V., H. N. Cui, et al. (2002). "Amorphous ITO thin films prepared by DC sputtering for electrochromic applications." Thin Solid Films **420-421**: 70-75.

Thomas, C. H., J.-B. Lhoest, et al. (1999). "Surfaces Designed to Control the Projected Area and Shape of Individual Cells." Journal of Biomechanical Engineering **121**(1): 40-48.

Thompson, R. Q., M. Porter, et al. (1993). "Zeptomole detection limit for alkaline phosphatase using 4-aminophenylphosphate, amperometric detection, and an optimal buffer system." Analytica Chimica Acta **271**(2): 223-229.

Thornton, J. A. (1974). "Influence of apparatus geometry and deposition conditions on the structure and topography of thick sputtered coatings." Journal of Vacuum Science and Technology **11**(4): 666-670.

Tian, Y., L. Mao, et al. (2005). "A carbon fiber microelectrode-based third-generation biosensor for superoxide anion." Biosensors and Bioelectronics **21**(4): 557-564.

Tolias, C. M., C. J. McNeil, et al. (1999). "Superoxide generation from constitutive nitric oxide synthase in astrocytes in vitro regulates extracellular nitric oxide availability." Free Radical Biology and Medicine **26**(1-2): 99-106.

Travis, E. R. and R. M. Wightman (1998). "SPATIO-TEMPORAL RESOLUTION OF EXOCYTOSIS FROM INDIVIDUAL CELLS." Annual Review of Biophysics and Biomolecular Structure **27**(1): 77-103.

Tse, D. C. S., R. L. McCreery, et al. (1976). "Potential oxidative pathways of brain catecholamines." Journal of Medicinal Chemistry **19**(1): 37-40.

Tsuboi, T., H. T. McMahon, et al. (2004). "Mechanisms of Dense Core Vesicle Recapture following “Kiss and Run” (“Cavicapture”) Exocytosis in Insulin-secreting Cells." Journal of Biological Chemistry **279**(45): 47115-47124.

Varma, S., J. McLachlan, et al. (2010). "Positionally controlled growth of cells using a cytophobic fluorinated polymer." Analytical and Bioanalytical Chemistry **396**(3): 1159-1165.

Voskerician, G., M. S. Shive, et al. (2003). "Biocompatibility and biofouling of MEMS drug delivery devices." Biomaterials **24**(11): 1959-1967.

Wei, E. P., C. W. Christman, et al. (1985). "Effects of oxygen radicals on cerebral arterioles." Am J Physiol Heart Circ Physiol **248**(2): H157-162.

Wen-Fa, W. and et al. (1994). "Effect of sputtering power on the structural and optical properties of RF magnetron sputtered ITO films." Semiconductor Science and Technology **9**(6): 1242.

Whitesides, G. M., E. Ostuni, et al. (2001). "SOFT LITHOGRAPHY IN BIOLOGY AND BIOCHEMISTRY." Annual Review of Biomedical Engineering **3**(1): 335-373.

Wightman, R. M., J. A. Jankowski, et al. (1991). "Temporally resolved catecholamine spikes correspond to single vesicle release from individual chromaffin cells." Proceedings of the National Academy of Sciences of the United States of America **88**(23): 10754-10758.

Wightman, R. M., T. J. Schroeder, et al. (1995). "Time course of release of catecholamines from individual vesicles during exocytosis at adrenal medullary cells." Biophysical Journal **68**(1): 383-390.

Williams, P. (1979). "The sputtering process and sputtered ion emission." Surface Science **90**(2): 588-634.

Xu, J. and F. W. Tse (1999). "Brefeldin A Increases the Quantal Size and Alters the Kinetics of Catecholamine Release from Rat Adrenal Chromaffin Cells." Journal of Biological Chemistry **274**(27): 19095-19102.

Yang, C.-Y., S. E. Babcock, et al. (1998). "Microstructure of electron-beam-evaporated epitaxial yttria-stabilized zirconia/CeO2 bilayers on biaxially textured Ni tape." Physica C: Superconductivity **307**(1-2): 87-98.

Yi, C., C.-W. Li, et al. (2006). "Microfluidics technology for manipulation and analysis of biological cells." Analytica Chimica Acta **560**(1-2): 1-23.

Yuanfang, G. and et al. (2009). "A microfluidic cell trap device for automated measurement of quantal catecholamine release from cells." Lab on a Chip **9**(23): 3442.

Zhou, Z., S. Misler, et al. (1996). "Rapid fluctuations in transmitter release from single vesicles in bovine adrenal chromaffin cells." Biophysical Journal **70**(3): 1543-1552.

Ziaie, B., A. Baldi, et al. (2004). "Hard and soft micromachining for BioMEMS: review of techniques and examples of applications in microfluidics and drug delivery." Advanced Drug Delivery Reviews **56**(2): 145-172.

LIST OF PUBLICATIONS

JOURNALS

I. **Syed Barizuddin**, Xin Liu, Joseph C. Mathai, Maruf Hossain, Kevin D. Gillis,and Shubhra Gangopadhyay, Self-aligned Microchip Device for Automated Measurement of Quantal Exocytosis (ACS Chemical Neuroscience, replying to reviewers comments).

II. Atanu Sen, **Syed Barizuddin**, Maruf Hossain, Louis Polo-Parada,Kevin D. Gillis, Shubhra Gangopadhyay, Preferential cell attachment to Nitrogen-doped diamond-like carbon (DLC:N) for measurement of quantal exocytosis, Biomaterials,30(2009)1604-1612.

III. Yuanfang Gao, Shantanu Bhattacharya, Xiaohui Chen, **Syed Barizuddin**, Shubhra Gangopadhyay, and Kevin D. Gillis, A microfluidic cell trap device for automated measurement of quantal catecholamine release from cells, Lab on a chip, 2009, 9, 3442-3446.

IV. Xin Liu, **Syed Barizuddin**, Cherian J. Mathai, Shubhra Gangopadhyay and kevin D. Gillis, Capturing single cells on lab-on-a-chip electrochemical electrode arrays for higher-throughput amperometric detection of quantal exocytosis (Manuscript ready to be sent to Lab on a chip).

V. Andrey Bezmelnitsyn, Rajagopalan Thiruvengadathan, **Syed Barizuddin**, Daniel Tappmeyer, Steven Apperson,Keshab Gangopadhyay, Shubhra Gangopadhyay, Modified Nanoenergetic Composites with Tunable Combustion Characteristics for Propellant Applications, Propellants Pyrotech. 2010, 00, 1 – 11.

PROFESSIONAL PRESENTATIONS

January 1, 2010 – Present

Poster Presentations:

Syed Barizuddin, Xin Liu, Kevin Gillis and Shubhra Gangopadhyay – "Self-aligned microchip device for automated measurement of quantal exocytosis" - Poster *presented at the Missouri regional life sciences summit, Kansas city, MO. March 2010.*

January 1, 2009 – December 31, 2009

Poster Presentations:

Syed Barizuddin, Shubhra Gangopadhyay, Kevin Gillis – "Faster and more efficient alternate to current technologies for electrophysiological studies at single cell level" - *Poster presented at the MU life sciences week, Columbia, MO. April 2009.*

January 1 – December 31, 2008

Invention Disclosure:

Syed Barizuddin, Shubhra Gangopadhyay, Kevin Gillis "Automated targeting of single cells on a micro electrode device by surface modification to achieve extremely high throughput"- Submitted invention disclosure to the University of Missouri, Columbia, MO. *February 2008.*

Poster Presentations:

Syed Barizuddin, Atanu Sen, Maruf Hossain, Shubhra Gangopadhyay, Kevin Gillis-"High throughput single cell targeting microchip device for neuroscience research and drug discovery"- *Poster presented at the MU life sciences week, Columbia, MO. April 2008.*

January 1 – December 31, 2007

Poster Presentations:

Syed Barizuddin, Atanu Sen, Maruf Hossain, Korampally Venumadhav,Yuanfang Gao, Kevin Gillis, Shubhra Gangopadhyay "Development of cytophobic films and silicon micro channel devices for patterning cells over electrochemical electrodes to measure quantal exocytosis" - *Poster presented at the "2nd annual nanotechnology and life science symposium" Wash-U, St. Louis, MO . March 2007.*

Syed Barizuddin, Atanu Sen, Maruf Hossain, Korampally Venumadhav,Yuanfang Gao, Kevin Gillis, Shubhra Gangopadhyay "Development of cytophobic films and silicon micro channel devices for patterning cells over electrochemical electrodes to measure quantal exocytosis" - *Poster presented at the MU life sciences week, Columbia, MO*. *April 2007.*

VITA

Syed Barizuddin was born in Hyderabad, Andhra Pradesh, India. He obtained his Bachelor of Engineering degree in Electronics and Communications Engineering from Gulbarga University, Karnataka, India in1996. After working as a testing and commissioning engineer in the low and medium voltage power distribution for a few years he started his higher education. He obtained his Master of Science degree in Electrical Engineering in 2006 and his Doctor of Philosophy degree in Electrical and Computer Engineering in 2010 from University of Missouri-Columbia. His research interests include bio-medical devices, biomaterials and nanomaterials.